

University of Alberta

Determination of Oligomeric State and Role of the Acidic C Terminal Tail of
Vaccinia Virus I3 Single Stranded DNA Binding Protein

by

Melissa Lynn Harrison

A thesis submitted to the Faculty of Graduate Studies and Research
in partial fulfillment of the requirements for the degree of

Master of Science

in

Virology

Medical Microbiology and Immunology

©Melissa Lynn Harrison

Fall 2013

Edmonton, Alberta

Permission is hereby granted to the University of Alberta Libraries to reproduce single copies of this thesis and to lend or sell such copies for private, scholarly or scientific research purposes only. Where the thesis is converted to, or otherwise made available in digital form, the University of Alberta will advise potential users of the thesis of these terms.

The author reserves all other publication and other rights in association with the copyright in the thesis and, except as herein before provided, neither the thesis nor any substantial portion thereof may be printed or otherwise reproduced in any material form whatsoever without the author's prior written permission.

DEDICATION

To my parents, Christina and Dave Harrison and my siblings Timothy and Kimberly for all their love, support and believing in me no matter what.

For Sonya Odsen, the best kind of friend anyone could ask for. This would have never been finished without her.

ABSTRACT

Single-stranded DNA (ssDNA) binding proteins (SSB) play a major role in DNA replication, recombination, and repair, by protecting ssDNA from nuclease attack and removing inhibitory secondary structure. Poxviruses are large double stranded DNA viruses that replicate within the cytoplasm of cells, and must encode their own DNA replication proteins. Previous work has identified the Vaccinia I3 protein as the virally encoded SSB. The structure of I3 has not been solved and the amino acid sequence lacks conservation to other SSB proteins, excepting an acidic C terminus. Our work has shown that I3 can form dimeric and tetrameric complexes. Removal of the C terminus prevents tetramer formation and increases the affinity for ssDNA. We have demonstrated that the C terminus is surface exposed and can compete with ssDNA for SSB binding. The C terminus plays a role in virus infection, as its obstruction decreases the amount of viral DNA replication.

ACKNOWLEDGEMENTS

I would like to thank my supervisor Dr. Evans for accepting me into his lab and for this very interesting project. I'd like to thank members of the Evans lab for helpful discussions: Megan Desaulniers, Nicole Favis, Li Qin, Wondim Teferi, and Branawan Gowrishankar. I'd especially like to thank Dr. Wendy Magee for all her help with experiments, helpful discussions, editing and moral support.

I'd like to thank my committee members Dr. Maya Shmulevitz and Dr. Mark Glover for helpful discussions and advice. Dr. Mary Hitt and Dr. Maya Shmulevitz and their labs for helpful discussions during lab meetings. Dr. Bart Hazes for help with protein crystallography and getting me started as an undergraduate student. Dr. Ross Edwards and Sheraz Khan for help with the MALLS experiments. Mark Burrell and the Agri-Food Discovery Place for growing fermenter cultures of two of my proteins. Dr. Steven Ogg for help with microscopy and the microinjection experiments. I'd like to thank Dr. Paula Traktman and Dr. Robert Ingham for kindly providing proteins and peptides respectively.

Most importantly I'd like to thank my family and friends for all their love, support and for believing in me. This work would have never been finished without all of their hard work, and for that I am eternally grateful.

TABLE OF CONTENTS

ACKNOWLEDGEMENTS	i
LIST OF TABLES	viii
LIST OF FIGURES	ix
LIST OF SYMBOLS AND ABBREVIATIONS	xi
CHAPTER 1: INTRODUCTION	1
1. SINGLE-STRANDED DNA-BINDING PROTEINS.....	2
General Characteristics	2
Oligosaccharide/Oligonucleotide Binding Fold Structure	3
T4 Bacteriophage GP32.....	5
T7 Bacteriophage GP2.5.....	8
Eukaryotic RPA	10
<i>Escherichia coli</i> SSB	13
2. POXVIRUSES	16
Virus Biology.....	16
Vaccinia	18
Molluscum Contagiosum.....	18
Orf.....	19
Fowlpox	19
Replication Cycle.....	20
DNA Replication Model.....	21
DNA Replication Proteins	25

DNA Polymerase (E9)	26
Thymidine Kinase (J2).....	26
Ribonucleotide Reductase (F4, I4)	27
Topoisomerase (H6).....	27
Single Stranded DNA Binding Protein (I3)	28
CHAPTER 2: MATERIALS AND METHODS	31
2.1 CLONING.....	33
2.1.1 Construction of Recombinant Plasmids.....	33
2.1.1.1 C-Terminal His6 Tagged VacI3 ₁₅₋₂₄₄	33
2.1.1.2 C-Terminal His6 Tagged VacI3 ₁₋₂₇₀	33
2.1.1.3 C-Terminal His6 Tagged FPVO88 ₂₅₋₂₄₁	33
2.1.1.4 C-Terminal His6 Tagged OrfO32 ₂₈₋₂₄₄ , MCVO46 ₃₀₋₂₂₇ and MCVO32 ₁₋₂₈₈ SSB Proteins	35
2.1.1.5 N Terminal His6 Tagged Non-Oligomerizing Vaccinia I3 Mutants	36
2.1.1.6 Untagged VacI3 ₁₋₂₄₄ and VacI3 ₁₋₂₇₀ SSBs.....	36
2.1.1.7 Untagged MCVO46 ₁₋₂₆₅ and MCVO46 ₁₋₂₈₈ SSBs	37
2.1.1.8 Vaccinia I3 Negative Charge Point Mutants	39
2.1.1.9 N-Terminal Flag Tagged I3	40
2.2 PROTEIN PURIFICATION.....	44
2.2.1 Expression and Purification of His6-Tagged Proteins.....	44
2.2.2 Expression and Purification of Untagged Proteins	45

2.3 ASSAYS	50
2.3.1 Crystallization Screens.....	50
2.3.2 Large Scale Crystallization	50
2.3.3 Immunoprecipitations of VacI3 ₁₋₂₇₀ (H6) Protein Complexes.....	51
2.3.4 Electrophoretic Mobility Shift Assays.....	52
2.3.5 Electrophoretic Mobility Shift Assays, Peptide Competition.....	52
2.3.6 Electrophoretic Mobility Shift Assays, Antibody Supershift	53
2.3.7 ssDNA Cellulose Elution Assay	53
2.3.8 Multi Angle Laser Light Scattering (MALLS)	54
2.3.9 Determination of Amount of I3 in Infected BSC40 Cells	55
2.3.10 Immunoprecipitations of I3 to Search for Binding Partners	55
2.4 MICROINJECTIONS.....	57
2.4.1 Cell Culture.....	57
2.4.2 Microinjection of Antibodies.....	57
2.4.3 Microinjection of Peptides.....	58
CHAPTER 3: RESULTS	60
MULTIMERIC ORGANIZATION OF POXVIRUS SINGLE-STRANDED DNA-BINDING PROTEINS.....	60
3.1 INTRODUCTION	60
3.2 RESULTS	63
3.2.1 Cloning and Purification of C-Terminal His6 Tagged Poxvirus Single Stranded DNA Binding Proteins.....	63

3.2.2 Crystallization of His6 Tagged Poxvirus SSBs.	64
3.2.3 Crystallization of VacI3 ₁₋₂₇₀ (H6) with Anti-I3 Fab Fragments	70
3.2.4 Crystallization of VacI3 ₁₅₋₂₄₄ (H6) with C-Terminal Tail Peptides	70
3.2.5 Crystallization of Non-Oligomerizing Vaccinia I3 Mutants	71
3.2.6 Co-crystallization of VacI3 ₁₅₋₂₄₄ (H6) with MCVO46 ₃₀₋₂₂₇ (H6)	71
3.2.7 Immunoprecipitations of VacI3 ₁₋₂₇₀ (H6) to Complex Other Poxviral SSBs.....	72
3.2.8 Multi Angle Laser Light Scattering to Determine the Complex Formed by VacI3 ₁₋₂₇₀ and VacI3 ₁₋₂₄₄ Untagged Proteins.....	77
3.3 DISCUSSION.....	80
CHAPTER 4: RESULTS	90
ROLE OF THE N and C TERMINI IN ssDNA BINDING	90
4.1 INTRODUCTION	90
4.2 RESULTS	93
4.2.1 Electrophoretic Mobility Shift Assays of His6 Tagged SSBs.	93
4.2.2 ssDNA Affinity Measured for His6 Tagged Poxviral SSBs.....	96
4.2.3 Cloning and Purification of Untagged Poxvirus SSBs.	99
4.2.4 Electrophoretic Mobility Shift Assays for Untagged Vaccinia and MCV SSBs.....	100
4.2.5 ssDNA Affinity Measured for Untagged Poxvirus SSBs.	101

4.2.6 Electrophoretic Mobility Shift Assays with Peptide Competition for ssDNA Binding	109
4.2.7 Anti-I3 Antibody Epitope Mapping	111
4.2.8 Using the 10D11 Anti-I3 Antibody to Supershift the ssDNA in EMSA.	112
4.2.9 Microinjection of 10D11 Anti-I3 Antibody into BSC40 Cells to Disrupt Virus Factories.....	114
4.2.10 Microinjection of C Terminal Tail Peptide into BSC40 Cells to Compete for ssDNA Binding.	118
4.2.11 Determining the Amount of I3 in a Vaccinia Infected Cell.....	122
4.2.12 Immunoprecipitations to Search for Binding Partners.....	122
4.3 DISCUSSION	127
CHAPTER 5 CONCLUSIONS AND FUTURE WORK.....	134
5.1 CONCLUSIONS.....	134
5.1.1 Multimerization Model	134
5.1.2 ssDNA Binding Model	135
5.1.3 C-Terminal Tail of I3 in Protein-Protein Interactions	136
5.2 FUTURE WORK.....	139
5.2.1 Crystal Structure	139
5.2.2 I3-ssDNA Complexes	139
5.2.3 Location of ssDNA and C-Terminal Tail Binding to the SSB	140

BIBLIOGRAPHY.....	141
APPENDIX 1: BUFFER COMPOSITIONS	165

LIST OF TABLES

Table 1: Proteins encoded by Vaccinia virus for DNA replication (Moss 2007).	25
Table 2: Poxvirus SSBs cloned and used in the experiments	42
Table 3: PCR primer sequences used to amplify poxvirus SSB genes	43
Table 4: Summary of VacI3 ₁₅₋₂₄₄ (H6) crystals	69
Table 5: Molecular weight (kDa) predictions of potential VacI3 ₁₋₂₇₀ :30-mer polyT complexes.	87
Table 6: Molecular weight (kDa) predictions of potential VacI3 ₁₋₂₄₄ :30-mer polyT complexes	88
Table 7: EC ₅₀ values from ssDNA elution of His6 tagged SSBs.....	97
Table 8: EC ₅₀ values from ssDNA elution of untagged SSBs	102
Table 9: P values from student's t tests of quantification of virus factory size from peptide microinjections	119

LIST OF FIGURES

Figure 1-1: Crystal Structure of OB Fold.	4
Figure 1-2: Structure of T4 bacteriophage GP32.	7
Figure 1-3: Structure of T7 bacteriophage GP2.5 dimer.	10
Figure 1-4: Structure of human replication protein A.	12
Figure 1-5: Structures of SSB proteins from <i>Escherichia coli</i> and <i>Deinococcus radiodurans</i>	15
Figure 1-6: Phylogenetic tree of poxvirus single-stranded DNA-binding proteins.	17
Figure 1-7: Poxvirus replication cycle.	23
Figure 1-8: Model for poxvirus DNA replication.	24
Figure 2-1: Amino acid sequence alignment of the SSBs used in the experiments.	32
Figure 2-2: SDS PAGE gels and HPLC tracings from the purification of VacI3 ₁₅₋₂₄₄ (H6).	46
Figure 2-3: SDS PAGE gels and HPLC tracings from the purification of VacI3 ₁₋₂₇₀	49
Figure 3-1: Purified C-terminal His6-tagged SSBs.	64
Figure 3-2: Crystals of VacI3 ₁₅₋₂₄₄ (H6)	66
Figure 3-3: Crystals of VacI3 ₁₅₋₂₄₄ (H6) optimized for ssDNA and protease cleavage.	67
Figure 3-4: Crystals of VacI3 ₁₅₋₂₄₄ (H6) with altered ssDNA.	68
Figure 3-5: Co-crystallization of VacI3 ₁₅₋₂₄₄ (H6) with MCVO46 ₃₀₋₂₂₇ (H6).	73
Figure 3-6: Anti-I3 10D11 antibody reactivity to Vaccinia and MCV SSBs.	74
Figure 3-7: Anti-I3 10D11 antibody reactivity to Orf and Fowlpox SSBs.	75
Figure 3-8: Immunoprecipitations using I3 ₁₋₂₇₀ (H6) to complex other poxviral SSBs.	76
Figure 3-9: Multi angle laser light scattering of VacI3 ₁₋₂₇₀	78
Figure 3-10: Multi angle laser light scattering of VacI3 ₁₋₂₄₄	79
Figure 3-11: Model of ssDNA:I3 complexes.	89
Figure 4-1: Electrophoretic mobility shift assay for VacI3 ₁₋₂₇₀ (H6) and VacI3 ₁₅₋₂₄₄ (H6).	94
Figure 4-2: Electrophoretic mobility shift assay for MCVO46 ₁₋₂₈₈ (H6) and MCVO46 ₃₀₋₂₂₇ (H6).	95
Figure 4-3: Electrophoretic mobility shift assay for OrfO32 ₂₈₋₂₄₄ (H6).	96
Figure 4-4: ssDNA cellulose elution curves for His6 tagged poxvirus SSBs.	98
Figure 4-5: Purified untagged poxvirus SSBs.	100
Figure 4-6: Electrophoretic mobility shift assay for VacI3 ₁₋₂₇₀ and VacI3 ₁₋₂₄₄	103
Figure 4-7: Electrophoretic mobility shift assay for MCVO46 ₁₋₂₈₈ and MCVO46 ₁₋₂₆₅	104
Figure 4-8: Electrophoretic mobility shift assay of I3 charge mutant proteins. .	105
Figure 4-9: ssDNA cellulose elution curves for VacI3 ₁₋₂₇₀ and VacI3 ₁₋₂₄₄	106
Figure 4-10: ssDNA cellulose elution curves for I3 charge mutant proteins.	107

Figure 4-11: ssDNA cellulose elution curves for MCVO46 ₁₋₂₈₈ and MCVO46 ₁₋₂₆₅	108
Figure 4-12: Electrophoretic mobility shift assay of C-terminal tail peptides competition with ssDNA.....	110
Figure 4-13: 10D11 anti-I3 antibody epitope determination.	111
Figure 4-14: Electrophoretic mobility shift assay of antibody supershift.....	113
Figure 4-15: Microinjection of 10D11 anti-I3 antibodies into Vaccinia infected cells.	116
Figure 4-16: Quantification of virus factory area from antibody microinjected cells.	117
Figure 4-17: Microinjection of C-terminal tail peptides into Vaccinia infected cells.	120
Figure 4-18: Quantification of virus factory area after microinjection with peptides.	121
Figure 4-19: Determination of how much I3 is in an infected cell.	123
Figure 4-20: Immunoprecipitation to determine if I3 can form a complex with cellular or viral proteins.	126
Figure 5-1: Model of I3 in complex with ssDNA.	138

LIST OF SYMBOLS AND ABBREVIATIONS

A + T: adenine and thymine
BSA: bovine serum albumin
ddH₂O: double distilled water
dNDP: deoxyribonucleotide diphosphate
dNTP: deoxyribonucleotide triphosphate
dsDNA: double stranded DNA
DTT: dithiothreitol
*Eco*SSB: *E. coli* SSB protein
EC₅₀: effective concentration for 50% elution
EMSA: electrophoretic mobility shift assay
G + C: guanine and cytosine
GLB: glycerol loading buffer
GP: gene product
HPLC: high performance liquid chromatography
IBE: imidazole boric acid EDTA buffer
IP: immunoprecipitation
IPTG: isopropyl β-D-1-thiogalactopyranoside
LB: Luria broth
MALLS: multi angle laser light scattering
MCV: Molluscum contagiosum virus
MEM: modified Eagle's medium
MOI: multiplicity of infection
mRNA: messenger RNA
NMR: nuclear magnetic resonance
OB fold: oligosaccharide/oligonucleotide binding fold
PBS: phosphate buffered saline
PBS-T: phosphate buffered saline with Tween
PCR: polymerase chain reaction
rNDP: ribonucleotide diphosphate
REV: reticuloendotheliosis virus
ROI: region of interest
RPA: replication protein A
RR: ribonucleotide reductase
R1: large subunit of ribonucleotide reductase
R2: small subunit of ribonucleotide reductase
rpm: revolutions per minute
SDS PAGE: sodium dodecyl sulfate polyacrylamide gel electrophoresis
siRNA: small interfering RNA
SSB: single-stranded DNA-binding protein
ssDNA: single stranded DNA
SV40: simian virus 40
TAE: tris acetic acid EDTA buffer
xg: times gravity
YFP: yellow fluorescent protein

CHAPTER 1: INTRODUCTION

This thesis is concerned with determining the multimeric structure of the Vaccinia single-stranded DNA-binding protein I3, as well as the role of the acidic C terminus.

This document will cover general characteristics of single-stranded DNA-binding proteins, and information about the common oligosaccharide/oligonucleotide binding fold. Biochemical and structural characteristics of four well studied single-stranded DNA-binding proteins; T4 bacteriophage GP32, T7 bacteriophage GP2.5, eukaryotic Replication Protein A, and *Escherichia coli* SSB, will follow.

A survey of the different poxviruses used in the experiments will be discussed, followed by an overview of poxvirus replication. An in-depth look at poxvirus DNA replication and the proteins involved in this process will be examined. The introduction will conclude with a review of the current literature on Vaccinia I3, and the objectives and rationale for the experiments conducted.

1. SINGLE-STRANDED DNA-BINDING PROTEINS

General Characteristics

Single-stranded DNA binding (SSB) proteins are essential proteins found throughout all kingdoms of life (Shereda *et al.* 2008). When these proteins were first characterized they were described as DNA-unwinding proteins, DNA-melting proteins or helix-destabilizing proteins (Alberts and Frey 1970, Molineux and Gefter 1975, Jensen *et al.* 1976). There are several characteristics that SSBs share; they bind preferentially and specifically to single stranded DNA (ssDNA) with no sequence specificity, they bind to ssDNA with varying degrees of cooperativity, and are required in stoichiometric rather than catalytic amounts (Prasad and Chiu 1987, Suck 1997). SSBs play an important role in DNA replication, recombination and repair by protecting transiently formed ssDNA from nuclease degradation and removing and preventing the formation of inhibitory secondary structures (Suck 1997). By preventing secondary structure formation, SSBs allow other enzymes access to the ssDNA, displacing the SSB (Suck 1997). Enzymes involved in DNA replication, recombination and repair can sometimes also directly bind to SSB proteins, usually mediated by the exposed acidic C terminus on the SSB (Chase and Williams 1986, Pestryakov and Lavrik 2008). These protein-protein interactions allow the SSBs to not only bind to and recruit replication, recombination and repair enzymes to the ssDNA, but SSBs can also stimulate the enzymatic activities of these other proteins (Chase and Williams 1986, Pestryakov and Lavrik 2008). The acidic C terminus of the SSBs is

conserved amongst the SSBs, and is the only region where sequence is conserved between the SSBs from different organisms.

Oligosaccharide/Oligonucleotide Binding Fold Structure

Although there is very little sequence homology between the SSBs, they all share similar functional groups that play a role in ssDNA binding (Prasad and Chiu 1987). Aromatic residues stabilize interactions between the ssDNA and SSB by intercalating between the ssDNA bases, and basic residues are involved in electrostatic interactions with the negatively charged phosphates on the ssDNA backbone (Prasad and Chiu 1987). With the elucidation of the crystal structures of SSBs from different organisms, it was demonstrated that most of the SSBs bind to ssDNA with a common structure, the oligosaccharide/oligonucleotide binding (OB) fold (Murzin 1993). OB folds have a Greek key formation, consisting of a five strand β sheet coiled to form a closed β barrel that is capped between the third and fourth strands by an α helix (Figure 1-1) (Murzin 1993). Proteins with very different sequences can fold into this same structure. This allows for the ssDNA ligand to bind based on the fold architecture and topology rather than the sequence of the SSB (Murzin 1993). Based on the solved structures of the SSBs from different organisms, SSBs can be classified into four groups based on their oligomeric organization: monomeric, dimeric, heterotrimeric, and homotetrameric (Suck 1997).

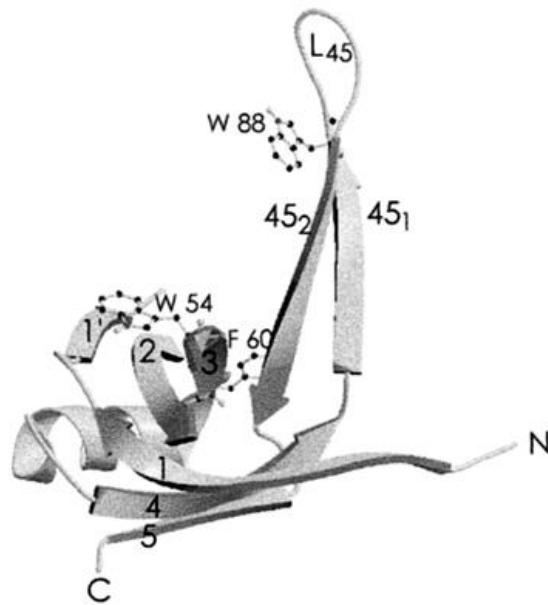


Figure 1-1: Crystal Structure of OB Fold.

Despite sequence divergence, most of the SSBs with solved structures use this fold to bind ssDNA.

T4 Bacteriophage GP32

One of the first SSBs to be characterized was gene product (GP) 32 from T4 bacteriophage. GP32 binds tightly and cooperatively to ssDNA and is required for *in vitro* replication of the T4 bacteriophage (Alberts *et al.* 1968, Alberts 1970, Alberts and Frey 1970). Early experiments determined that GP32 was produced in large quantities and was required in stoichiometric rather than catalytic amounts; therefore most likely playing a structural role in T4 bacteriophage replication (Snustad 1968, Alberts 1970, Alberts and Frey 1970, Liu *et al.* 1978). The initial role of GP32 was described as a helix destabilizer that could open up regions of DNA and was rapidly displaced as the double-helical structure reformed (Alberts and Frey 1970, Huberman *et al.* 1971, Liu *et al.* 1978). GP32 is an essential protein for DNA replication and acts by binding to and stimulating the T4 DNA polymerase (Huberman *et al.* 1971, Burke *et al.* 1980). It has been demonstrated that the protein-protein interactions between GP32 and other T4 proteins are through the negatively-charged C-terminal tail of GP32 (Breschkin and Mosig 1977b). Further work demonstrated that GP32 also interacts with T4 ligase, recombination nucleases and membrane proteins during recombination (Breschkin and Mosig 1977b, Mosig *et al.* 1977, Mosig *et al.* 1978). GP32 also functions in DNA replication by interacting directly with thymidylate synthase in the deoxyribonucleoside triphosphate biosynthesis enzyme complex (Wheeler *et al.* 1996).

Two different binding modes for GP32 have been described, an oligonucleotide binding mode and a polynucleotide binding mode

(Kowalczykowski *et al.* 1980). In the oligonucleotide binding model, there are two binding sites for non-electrostatic interactions with ssDNA at the N terminus of GP32 (Kowalczykowski *et al.* 1980, Kowalczykowski *et al.* 1981). At the C terminal end of GP32, the negatively charged C-terminal tail is bound back onto the GP32 protein by charged interactions with positive residues within GP32 (Kowalczykowski *et al.* 1980, Kowalczykowski *et al.* 1981). In the polynucleotide binding mode the C-terminal tail is removed to allow the positive charges to bind to ssDNA, increasing the length of ssDNA bound by GP32 to seven nucleotides (Kowalczykowski *et al.* 1980, Kowalczykowski *et al.* 1981). Cooperative binding occurs in this binding mode and several molecules of GP32 cluster along the ssDNA (Kowalczykowski *et al.* 1980, Kowalczykowski *et al.* 1981). This exposure of the C-terminal tail explains earlier experiments where it was observed that cooperative binding lead to an increase in tryptic cleavage of the C terminus, while the protein core resisted this cleavage (Williams and Konigsberg 1978, Wu *et al.* 1999).

Early mutational analysis identified the N terminal region of GP32 as the location for ssDNA binding and interaction with proteins that initiate DNA replication and recombination (Breschkin and Mosig 1977a, Williams *et al.* 1981). The C-terminal domain was identified as the region that interacted with recombination nucleases (Breschkin and Mosig 1977a, Williams *et al.* 1981). These experiments also attempted to predict the structure of GP32; based on amino acid sequence it was determined that the N and C termini were most likely α helical and the central core region contained mostly β sheets (Williams *et al.*

1981). The crystal structure of the ssDNA binding domain of GP32 has been solved and has identified the important subdomains within this region (Figure 1-2) (Shamoo *et al.* 1995). The first subdomain coordinates a zinc ion for conformational stability of GP32 (Shamoo *et al.* 1995). A small connecting region connects this zinc binding domain to the N terminus of the protein, a five stranded β sheet (Shamoo *et al.* 1995). ssDNA contacts a positively charged surface running parallel to a hydrophobic pocket on all three of the subdomains (Shamoo *et al.* 1995). These contacts prevent ssDNA from rotating and prevent the formation of any secondary structure that would impede the action of DNA metabolic enzymes (Shamoo *et al.* 1995).

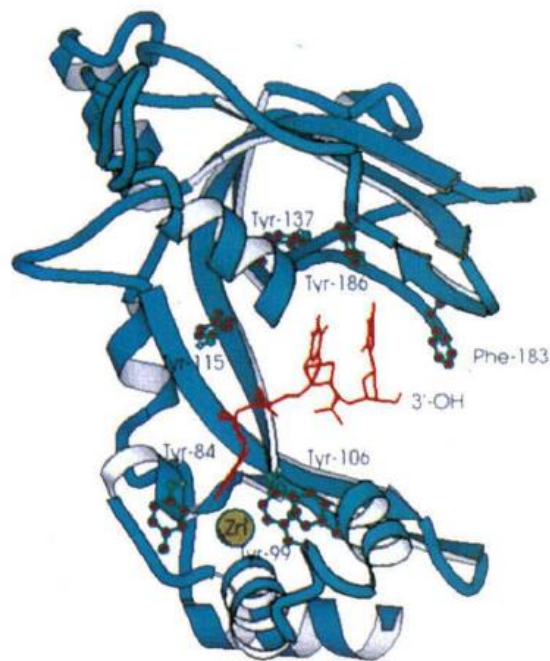


Figure 1-2: Structure of T4 bacteriophage GP32. The core ssDNA binding region utilizes an OB fold to bind ssDNA (red sticks) and a zinc ion for stability. GP32 forms a monomer in solution.

Shamoo *et al.* 1995. Nature. 376: 362-366.

T7 Bacteriophage GP2.5

T7 bacteriophage encodes its own DNA polymerase and it was believed to also encode its own DNA unwinding protein, similar to T4 GP32 (Reuben and Gefter 1973). Using single stranded DNA cellulose chromatography, a 31 kDa induced bacteriophage protein was purified from bacteriophage infected *E. coli* (Reuben and Gefter 1973, Reuben and Gefter 1974). This T7 encoded protein had similar properties to T4 GP32; it bound preferentially and strongly to ssDNA, could lower the melting temperature of dsDNA, and could remove inhibitory secondary structures and stimulate the bacteriophage encoded DNA polymerase (Reuben and Gefter 1973, Scherzinger *et al.* 1973, Reuben and Gefter 1974).

A T7 amber mutant defective in this SSB mapped the gene to between genes 2 and 3, location 2.5 (Araki and Ogawa 1981). Amber mutant bacteriophage can only grow on specific strains of bacteria that contain their own mutation that allows for the read-through of the mutant stop codon present in the bacteriophage (Epstein *et al.* 2012). These mutants had suppressed DNA synthesis, indicating that GP2.5 has a role in DNA replication (Araki and Ogawa 1981). These mutants were also extremely UV sensitive, indicating that GP2.5 also functions in DNA repair (Araki and Ogawa 1981). A role for GP2.5 in recombination was later elucidated. It was found that GP2.5 could promote the formation of joint molecules and homologous DNA pairing (Kong and Richardson 1996). Like other SSBs, GP2.5 is essential to bacteriophage T7 (Kim and Richardson 1993).

Like T4 bacteriophage GP32, GP2.5 directly interacts with proteins involved in DNA replication. Several reports have demonstrated that there is a direct interaction with T7 encoded DNA polymerase (Nakai and Richardson 1988, Kim *et al.* 1992b, Hamdan *et al.* 2005). GP2.5 has also been shown to interact with the helicase to promote strand exchange during recombination (Kim *et al.* 1992b, Kong and Richardson 1996). Deletion analysis has shown that these protein-protein interactions are mediated through the C terminus of GP2.5 (Kim and Richardson 1994, Hollis *et al.* 2001, Hyland *et al.* 2003, Hamdan *et al.* 2005, Marintcheva *et al.* 2006).

Gel filtration experiments demonstrated that GP2.5 forms a dimer along the ssDNA (Kim *et al.* 1992a). When the structure was solved, it was shown that the C terminus was required for dimer formation and likely stabilized the dimer interface through a domain swap with the second monomer in the dimer (Figure 1-3) (Hollis *et al.* 2001, Rezende *et al.* 2002). The C terminus is highly negatively charged, with fifteen of the last twenty one amino acids being acidic residues (Kim and Richardson 1994). Deletion experiments demonstrated that mutant GP2.5 proteins missing the C terminal twenty one or twenty six amino acids could no longer dimerize, no longer stimulate DNA synthesis, and had a higher affinity for ssDNA than the full length GP2.5 (Kim and Richardson 1994, He *et al.* 2003, Hyland *et al.* 2003, Shokri *et al.* 2006). More recent experiments have shown that the C terminus acts as an ssDNA mimic, and can bind to the ssDNA binding core of the SSB protein (Marintcheva *et al.* 2008).

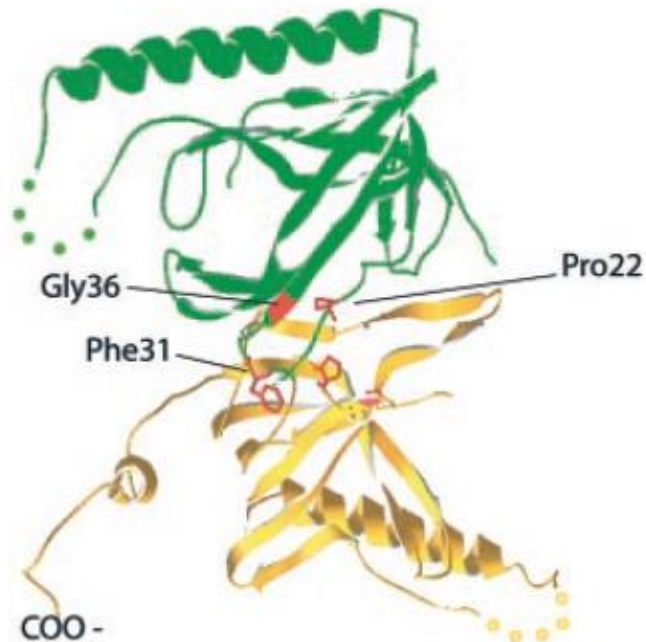


Figure 1-3: Structure of T7 bacteriophage GP2.5 dimer. Each monomer within the dimer has an OB fold.

Rezende *et al.* 2002. *Journal of Biological Chemistry*. 277: 50643-50653.

Eukaryotic RPA

In studies of eukaryotic DNA replication, virus genomes, such as SV40 were used to study cellular replication factors. One of the cellular proteins that have been identified from these studies was replication protein A (RPA) (Wobbe *et al.* 1987, Fairman and Stillman 1988, Wold and Kelly 1988, Wold *et al.* 1989). RPA is a multi-subunit DNA binding protein, essential for replication of the SV40 genome with a high and specific affinity for ssDNA (Fairman and Stillman 1988, Wold and Kelly 1988, Wold *et al.* 1989). RPA is also required for large T antigen

mediated unwinding of DNA containing the SV40 origin of replication (Wold and Kelly 1988).

RPA is a trimeric protein consisting of three polypeptides of 70, 32 and 14 kDa (Wold and Kelly 1988). Early experiments demonstrated that all three of the subunits are required for viability, but only the 70 kDa subunit directly bound to ssDNA (Wold *et al.* 1989, Brill and Stillman 1991, Erdile *et al.* 1991, Gomes and Wold 1995, Gomes and Wold 1996). The 70 kDa subunit requires the other subunits in order to be stably expressed, but the 32 and 14 kDa subunits can form a stable complex together and most likely play more of a structural role (Henricksen *et al.* 1994).

Like other SSBs, RPA directly interacts with several proteins involved in DNA replication, including the DNA polymerase alpha-primase complex and DNA polymerase delta (Longhese *et al.* 1994). RPA also has a role in DNA repair and interacts with several proteins involved in nucleotide excision repair (Coverley *et al.* 1991). Though the sequence of RPA is unrelated to GP32 T4 bacteriophage, it also contains a zinc finger motif (Erdile *et al.* 1991). RPA also uses the conserved OB fold structure to bind ssDNA (Bochkareva *et al.* 2002). In the final trimeric structure, six OB folds come together and all three of the subunits contain OB folds (Figure 1-4) (Bochkareva *et al.* 2002). Four of the OB folds are located in the 70 kDa subunit and one OB fold is present in each of the 32 and 14 kDa subunits (Bochkareva *et al.* 2002).

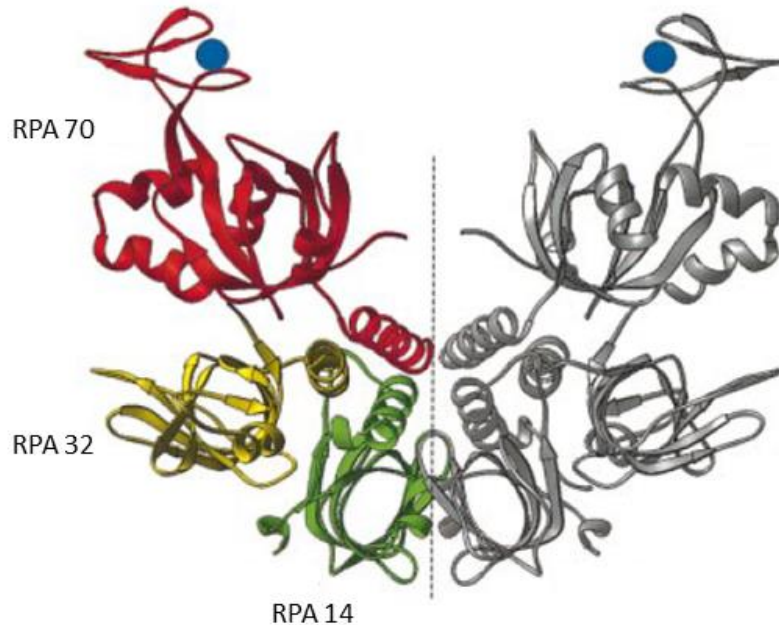


Figure 1-4: Structure of human replication protein A.

Subunits RPA70, RPA32 and RPA14 form a trimer, and two trimers dimerize to bring four OB folds together for ssDNA binding.

Adapted from: Bochkareva *et al.* 2002. The EMBO Journal. 21: 1855-1863.

RPA also has two binding modes dependent on the number of oligonucleotides bound. The first binding mode is non-cooperative and has a small binding site size of 8-10 nucleotides (Kim *et al.* 1992, Blackwell and Borowicz 1994, Pfuetzner *et al.* 1997). In this mode, the ssDNA binds two of the OB folds in the 70kDa subunit (Bochkarev *et al.* 1997, Bochkareva *et al.* 2002). In the second binding mode, 30 nucleotides are bound by four OB folds in a

cooperative manner, three in the 70 kDa subunits and the fourth from the 32 kDa subunit (Blackwell and Boroweic 1994, Iftode *et al.* 1999, Bochkareva *et al.* 2002). The switch between the binding modes results in a large conformational change and is mediated by the recruitment of ssDNA to the third and fourth OB fold within the trimerization core (Bochkareva *et al.* 2002, Fan and Pavletich 2012).

***Escherichia coli* SSB**

The SSB from *E. coli* was originally called an unwinding- protein for its first described function of unwinding duplex-DNA into ssDNA (Sigal *et al.* 1972). This protein has the same characteristics as other SSBs, such as binding specifically and with high affinity to ssDNA, and stimulating the action of the *E. coli* DNA polymerases (Sigal 1972, Molineux *et al.* 1974, Molineux and Gefter 1974, Molineux *et al.* 1975). This SSB has also been implicated in DNA repair and recombination by interacting with several proteins involved in these processes (Carlini *et al.* 1993).

E. coli SSB forms a tetramer along the ssDNA and all four monomers are capable of binding ssDNA (Weiner *et al.* 1975, Krauss *et al.* 1981, Griffith *et al.* 1984). This SSB forms octameric nucleosome like complexes along the ssDNA that consist of two tetramers wrapped with ssDNA (Bujalowski and Lohman 1987). This arrangement reflects one of three stable binding modes that have been described depending upon the number of nucleotides bound and the salt concentration (Figure 1-5) (Bujalowski and Lohman 1986).

In the SSB₃₅ mode, 35 nucleotides are bound to two of the monomers within the tetramer in low salt and low protein density (Lohman and Overman 1985, Lohman and Bujalowski 1988, Lohman *et al.* 1988, Bujalowski and Lohman 1989a). SSB₅₆ is a transitional binding mode where 56 nucleotides bind the tetramer, and an increase in ssDNA binding is observed when longer nucleotides contact the tetramer (Ruyechan and Wetmur 1975, Lohman *et al.* 1988). In the SSB₆₅ mode, 65 nucleotides wrap around all four monomers within the tetramer with a low level of positive cooperativity at high salt concentrations (Lohman and Overman 1985, Lohman *et al.* 1986, Bujalowski and Lohman 1987, Lohman *et al.* 1988, Bujalowski and Lohman 1989a). There is negative cooperativity between binding sites within the tetramer and positive cooperativity between tetramers along the ssDNA (Lohman and Bujalowski 1988, Bujalowski and Lohman 1989b).

Similar to other SSBs, the C terminus is negatively charged and influences the way ssDNA binds to the SSB (Sancar *et al.* 1981, Curth *et al.* 1996, Roy *et al.* 2007). The C terminus is the location of protein-protein interactions and upon other proteins binding to the C terminus, there is a shift to the SSB₃₅ mode to make the ssDNA more accessible to other proteins (Roy *et al.* 2007). Removal of the C terminus not only disrupts protein-protein interactions, but increases the affinity of the SSB for ssDNA (Williams *et al.* 1983).

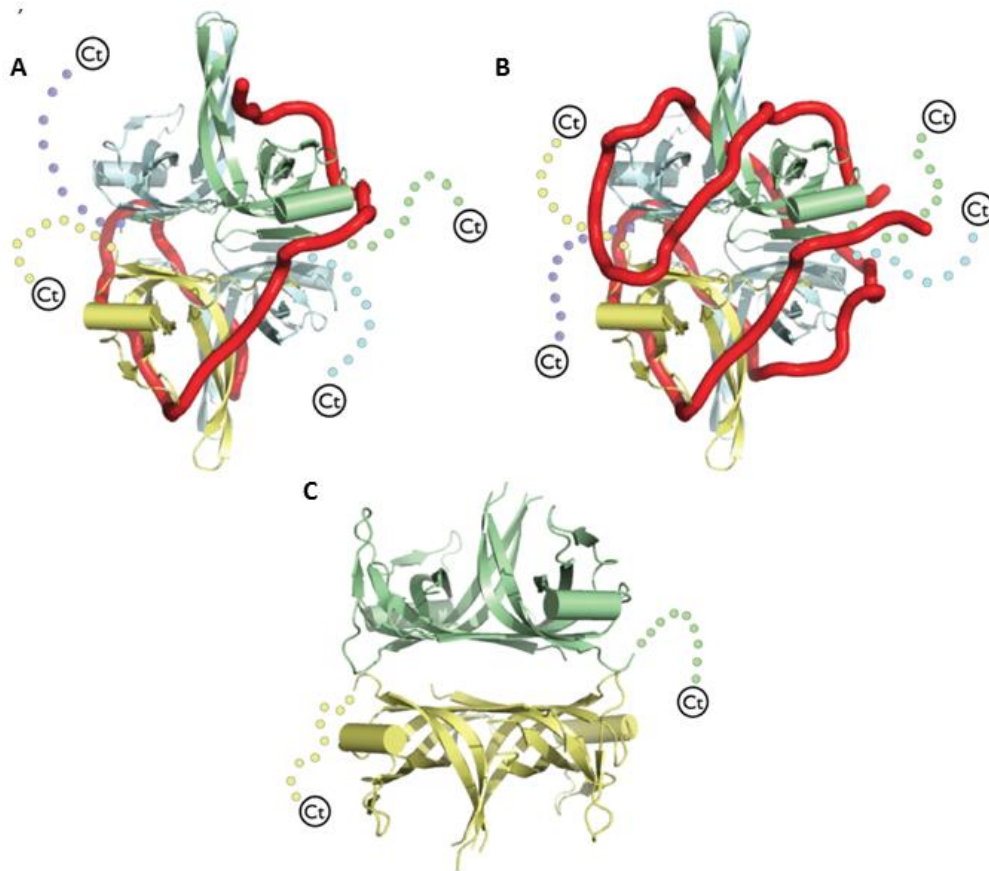


Figure 1-5: Structures of SSB proteins from *Escherichia coli* and *Deinococcus radiodurans*.

A) Structure of *E. coli* SSB₃₅ binding mode where the ssDNA (red) contacts two of the monomers in the homotetramer. B) Structure of *E. coli* SSB₆₅ binding mode where the ssDNA contacts all four of the monomers.

ssDNA is represented by the red ribbon. Flexible C terminal tail is represented by the dotted lines ending in Ct. C) Structure of *Deinococcus radiodurans* SSB protein, forming a dimer to bring together four OB folds.

Shereda *et al.* 2008. Critical Reviews in Biochemistry and Molecular Biology. 43:289-318

2. POXVIRUSES

Virus Biology

Two poxviruses infect humans, Variola virus and Molluscum Contagiosum virus (MCV), while others can become zoonoses infecting humans (Moss 2007). Variola, the most notorious of the poxviruses, is the causative agent of smallpox and was eradicated in 1977 through vaccination efforts led by the World Health Organization (Fenner *et al.* 1988).

Poxviruses virions have a characteristic morphology. They are brick shaped, are surrounded by a lipid membrane and contain a dumbbell shaped core (Dales and Siminovitch 1961, Easterbrook 1966, Cyrklaff *et al.* 2005). Within this core is the DNA genome complexed with proteins (Peters and Muller 1963, Cyrklaff *et al.* 2005).

Poxviruses are divided into two groups based on host range, the *Chordopoxvirinae* and *Entomopoxvirinae*, infecting vertebrate and insect hosts, respectively (McFadden 2005, Moss 2007). The *Chordopoxvirinae* can be further broken up into eight genera: *Orthopoxvirus*, *Parapoxvirus*, *Avipoxvirus*, *Capripoxvirus*, *Leporipoxvirus*, *Suipoxvirus*, *Molluscipoxvirus* and *Yatapoxvirus* (Moss 2007). Viruses from these families are genetically closely related (Figure 1-6).

My studies concerned SSBs cloned from a subset of these chordopoxviruses. These were Vaccinia virus (an orthopoxvirus), Fowlpox (an avipoxvirus), Orf (a parapoxvirus), and MCV (a molluscipoxvirus). A brief review of the biology of these viruses follows.

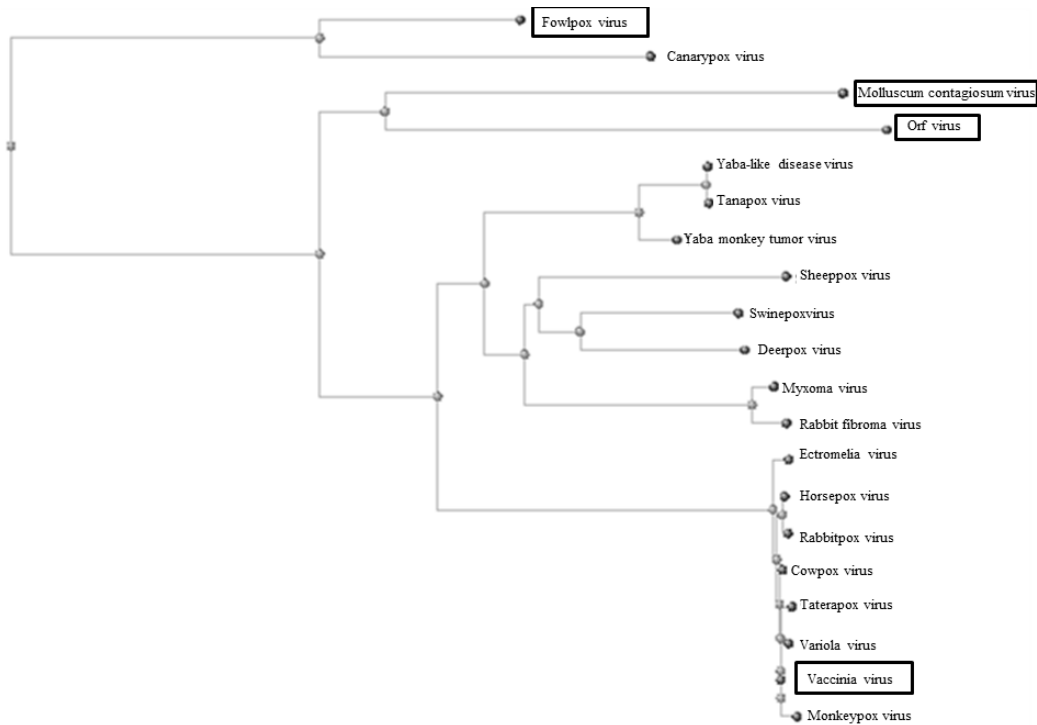


Figure 1-6: Phylogenetic tree of poxvirus single-stranded DNA-binding proteins. Tree was created using BLAST search against Vaccinia I3 protein sequence, followed by a pairwise sequence alignment based on the Kimura method (Kimura 1980). Entomopoxviruses were not picked up by this method, due to their divergent sequences. Viruses whose SSBs were used in the experiments are boxed.

Vaccinia

Vaccinia virus is an orthopoxvirus that infects humans but has an unknown natural history with no known natural host (Smith 2007). Vaccinia is most well known as the vaccine used in the eradication of smallpox by the World Health Organization (Fenner *et al.* 1988). Vaccinia has a linear A + T rich genome of 200 kbp with 263 potential genes (Goebel *et al.* 1990). The large genome allows researchers to genetically engineer Vaccinia for research purposes and to be used as a vaccine against other diseases (Smith 2007). It is the prototypical poxvirus that is most commonly studied in the laboratory.

Molluscum Contagiosum

Molluscum contagiosum (MCV) is the only member of the molluscipox virus family (Senkevich *et al.* 1996, Birthistle and Carrington 1997). MCV only causes infections in humans, and is responsible for skin infections mainly occurring in children (Gottlieb and Myskowski 1994, Senkevich *et al.* 1996, Senkevich *et al.* 1997, Shores 2009). However, it is becoming more prevalent as a sexually transmitted disease and in patients infected with HIV (Gottlieb and Myskowski 1994, Meadows *et al.* 1997, Tyring 2003, Wetzel and Wollenberg 2004). MCV infections are normally self-limiting, but in 5-10% of HIV patients the MCV infection causes extensive lesions that are often unresponsive to therapy (Gottlieb and Myskowski 1994, Meadows *et al.* 1997, Calista *et al.* 1999, Tyring 2003, Wetzel and Wollenberg 2004). However, these MCV infections are now being effectively controlled by cidofovir and highly active anti-retroviral therapy (HAART) (Meadows *et al.* 1997, Calista *et al.* 1999).

Orf

Orf virus is a member of the parapoxvirus family that causes cutaneous infections mainly in ungulates such as sheep and goats, but can cause infections in humans (Damon 2007). Orf virus particles are more ellipsoid and slightly smaller and more slender than Vaccinia particles (Hiramatsu *et al.* 1999). At 140 kbp, the genome of Orf is one of the smallest of the poxviruses (Fleming and Mercer 2007). The genome contains a high G + C content compared with other poxviruses and 88 open reading frames that are conserved with other poxviruses (Wittek *et al.* 1979, Damon 2007, Fleming and Mercer 2007). Interestingly, Orf lacks the genes involved in nucleotide metabolism that are present in other poxviruses (Fleming and Mercer 2007). Instead, Orf alters the cell cycle using a protein called PACR (Mo *et al.* 2009). PACR (poxvirus APC/cyclosome regulator) acts to deregulate the cell cycle by mimicking APC11 and is incorporated into the APC/C complex by binding APC2 (Mo *et al.* 2009, Mo *et al.* 2010). This prevents APC11 from binding APC2, and APC11 can now be readily degraded by the 26S proteasome (Ohta *et al.* 1999, Mo *et al.* 2010). This manipulates the cell into a state of replication that is sufficient to support virus genome replication (Mo *et al.* 2009, Mo *et al.* 2010).

Fowlpox

Fowlpox virus is a member of the avipoxviruses that infects poultry, either causing a cutaneous infection of the comb and wattle or a respiratory infection (Damon 2007). Fowlpox is an important disease in domesticated poultry and is spread by mechanical transmission via mosquitos (Damon 2007). Of the

poxviruses, Fowlpox has the largest poxvirus genome of around 300 kbp (Damon 2007). Integrated into the genome of vaccine and field strains of Fowlpox is an avian retrovirus, reticuloendotheliosis virus (REV) (Hertig *et al.* 1997). REV integration is probably not a recent phenomenon, and more Fowlpox strains are being shown to carry this integrated sequence (Kim and Tripathy 2001). The REV sequence has been mapped to a previously uncharacterized region in the right one third of the Fowlpox genome (Hertig *et al.* 1997). Most Fowlpox strains contain a near full length REV provirus that produces infectious REV upon Fowlpox infection, but some contain a rearranged remnant of the long terminal repeat of REV integrated into the same region of the Fowlpox genome (Hertig *et al.* 1997).

Replication Cycle

Replication of poxviruses occurs within discrete cytoplasmic foci known as virus factories (Dales 1963, Joklik and Becker 1964, Harford *et al.* 1966). Virus replication begins with the attachment of the virion membrane to the host cell membrane. After attachment, the virion membrane fuses with the host cell membrane and the virion core is transported into the cytoplasm of the infected cell (Dales 1963, Moss 2007). Within the virion core, early mRNAs are synthesized by proteins packaged within the virion core (Moss 1990, Shuman 1992). These early mRNAs encode for proteins involved in immune evasion, growth factors and enzymes and other factors required for DNA replication and intermediate gene transcription (Moss 2007). The core undergoes an uncoating process and the linear dsDNA genome is replicated as a concatemeric molecule (Traktman 1996, Moss 2007). Intermediate and late genes are subsequently transcribed and

translated into virion structural proteins, enzymes and early transcription factors (Vos and Stunnenberg 1988, Keck *et al.* 1990). Discrete membrane structures form and the concatemeric DNA genomes are resolved (Moyer and Graves 1981). Only one third of the replicated DNA is packaged into the immature virions (Joklik and Becker 1964). These virions mature, and the mature virions are wrapped with matrices derived from the trans-Golgi or endosomal membranes (Sodeik *et al.* 1993, Traktman 1996). The wrapped virions are transported to the cell surface along microtubules and are released from the host cell membrane (Schmelz *et al.* 1994, Traktman 1996). (Figure 1-7).

DNA Replication Model

The genomes of poxviruses are organized so that the central region contains conserved genes that are essential for DNA replication and virion formation, and the termini contain non-essential genes involved in host range, virulence and immune evasion, that diverge amongst the different families (Goelbel *et al.* 1990, Gubser *et al.* 2004). The original model for poxvirus DNA replication proposed by Moyer and Graves reflected a rolling hairpin model using terminal inverted repeats present at the end of the virus genome (Garon *et al.* 1978, Moyer and Graves 1981, Baroudy *et al.* 1982, Traktman 1996). This model proposed that poxvirus DNA replication is initiated when one of the termini is nicked to expose a 3'-OH (Figure 1-8 top panel) (Moyer and Graves 1981, Traktman 1996). This 3'-OH end can be extended by the DNA polymerase/processivity factor complex in a strand displacement primer extension DNA synthesis (Figure 1-8 top panel) (Moyer and Graves 1981, Traktman 1996).

The newly created priming hairpin is further extended to yield a complete copy of the DNA genome in a tail-tail dimeric molecule (Figure 1-8 top panel) (Moyer and Graves 1981, Traktman 1996). Genome replication would continue, yielding a series of concatemeric genomes alternating tail-tail and head-head (Moyer and Graves 1981, Traktman 1996).

However, recent data has indicated that this model is most likely incorrect. The D5 protein encoded by Vaccinia has been demonstrated to contain primase activity (DeSilva *et al.* 2007). D5 has been shown to be required for virus genome replication and can synthesize oligoribonucleotides *in vitro* (DeSilva *et al.* 2007). This suggests that poxviruses use a discontinuous DNA replication strategy, with leading and lagging strand synthesis, primed with Okazaki fragments (Figure 1-8 bottom panel). This model also reconciles early studies showing poxvirus DNA covalently linked to RNA, and the existence of short segments of DNA resembling Okazaki fragments (Olgiati *et al.* 1976, Esteban *et al.* 1977).

This model is further strengthened by the discovery of the G5 protein encoding a FEN 1-like flap endonuclease (Senkevich *et al.* 2009). Flap endonucleases function in DNA replication as nucleases to excise DNA/RNA primers that are displaced by the DNA polymerase when they collide with old primers (Figure 1-8 bottom panel) (Senkevich *et al.* 2009).

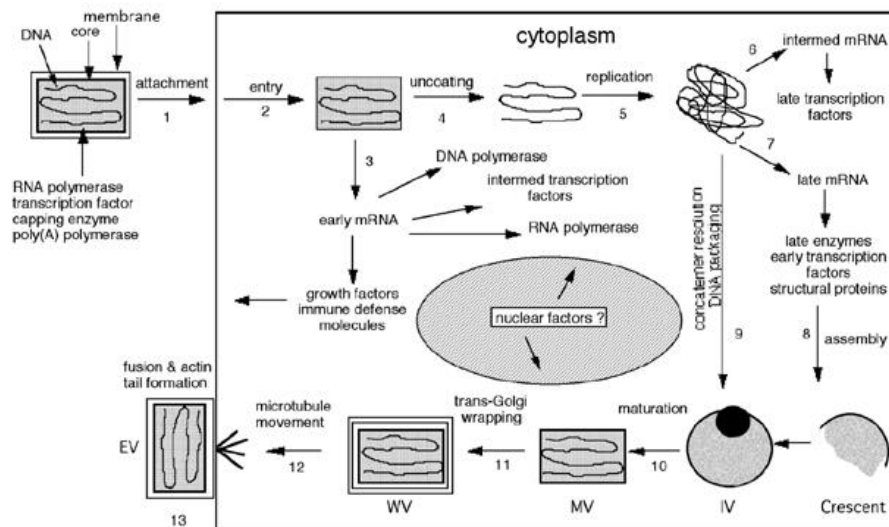


Figure 1-7: Poxvirus replication cycle.

Virions containing the dsDNA genome, enzymes and transcription factors attach to a cell. The membranes fuse and the core moves into the cytoplasm. Early mRNA is transcribed into factors for immune evasion, growth factors and enzymes for DNA replication and intermediate gene transcription. The core uncoats and the DNA is replicated as concatemers. Intermediate and late genes are transcribed and translated into virion structural proteins, enzymes and early transcription factors. Discrete membrane structures form and the concatemeric DNA is resolved and packaged into immature virions. The virions undergo a maturation process and are wrapped with membranes from the trans-Golgi and endosomal network. The mature, wrapped virions are transported to the cell surface along microtubules and are released from the cell membrane.

Moss, B. Chapter 74: *Poxviridae*: The viruses and their replication. In *Fields Virology*. 5th Edition. 2007. Wolters Kluwer Lippincott Williams and Wilkins. Philadelphia, USA.

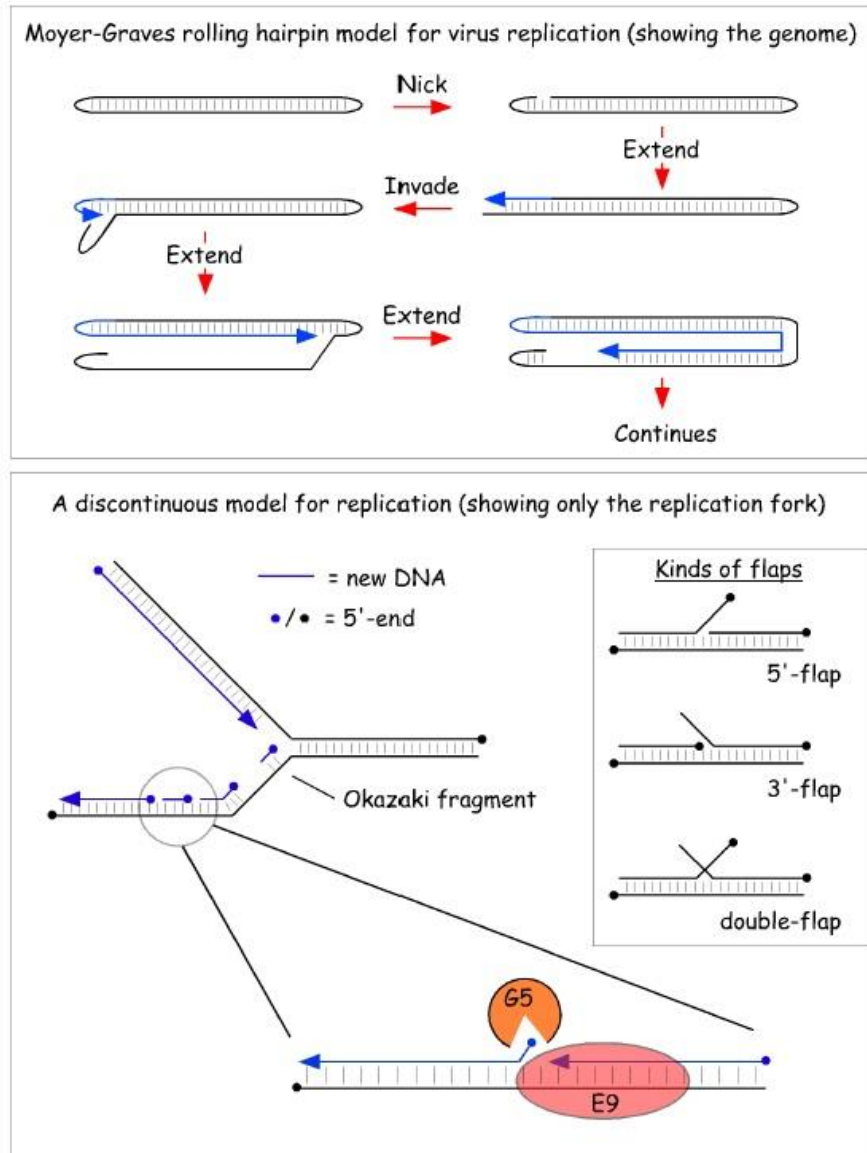


Figure 1-8: Model for poxvirus DNA replication.

The Moyer-Graves rolling hairpin model allows for the continuous synthesis of DNA, forming concatemers (upper panel). The discontinuous model for DNA replication takes into account the recent discoveries of poxviral encoded primase and FEN 1 flap endonuclease (G5). This model shows that poxviruses use Okazaki fragments to prime the DNA for replication of both leading and lagging strands. Vaccinia encoded G5 works with Vaccinia encoded DNA polymerase (E9) to remove the RNA primers.

Evans, D.H. Personal Communication.

DNA Replication Proteins

Due to replicating within the cytoplasm, poxviruses must encode their own proteins required for DNA replication. Many of these proteins have been well documented (Table 1). The following contains a description of several of the important proteins required for DNA replication in Vaccinia.

Table 1: Proteins encoded by Vaccinia virus for DNA replication (Moss 2007)

Function	Nomenclature from Vaccinia Virus	Properties
DNA polymerase	E9	3' exonuclease activity, DNA polymerase
Processivity factor	A20	Interacts with D4 to complex with DNA polymerase for increased processivity
NTPase (Primase)	D5	Nucleic acid independent nucleoside triphosphate activity, primase/helicase
Protein kinase	B1	Serine/threonine kinase
DNA ligase	A50	ATP dependent DNA ligase
Thymidine kinase	J2	phosphorylation of thymidine to thymidine 5' monophosphate
Thymidylate kinase	A48	phosphorylation of thymidine 5'-monophosphate to form thymidine 5'-diphosphate
Ribonucleotide reductase	F4/I4	formation of deoxyribonucleotides from ribonucleotides
Topoisomerase I	H6	Type 1 topoisomerase
Uracil DNA glycosylase	D4	removes uracil from DNA
dUTPase	F2	hydrolysis of dUTP to dUMP
Single-stranded DNA-binding protein	I3	binds ssDNA

DNA Polymerase (E9)

Vaccinia virus encodes its own DNA dependent DNA polymerase that is expressed early after infection (Berns *et al.* 1969, Citarella *et al.* 1972, Traktman *et al.* 1984). The DNA polymerase is a 110 kDa polypeptide that has been mapped to the E *Hind*III fragment (Challberg and Englund 1979, Traktman *et al.* 1984). The polymerase contains a strong 3' to 5' exonuclease activity that degrades ssDNA more rapidly than dsDNA and releases 5' mononucleotides (Citarella *et al.* 1972, Challberg and Englund 1979). A mixture of all four of the dNTPs is needed for maximal activity and the polymerase requires a divalent cation (Citarella *et al.* 1972).

Thymidine Kinase (J2)

Thymidine kinases are part of the pyrimidine salvage pathway and catalyze the phosphorylation of thymidine to thymidine 5' monophosphate. Among other proteins in the nucleotide biosynthesis pathways, Vaccinia encodes a thymidine kinase that has been mapped to the J *Hind*III fragment (Hruby and Ball 1982, Weir *et al.* 1982, Hruby *et al.* 1983). Vaccinia thymidine kinase has been shown to form a homotetrameric complex, the form of the protein active in phosphorylating thymidine to dTMP (Black and Hruby 1990, McCraith *et al.* 2000). Vaccinia thymidine kinase is regulated by a feedback loop, where accumulating levels of dTDP and dTTP decrease the enzymatic activity of the thymidine kinase as the infection progresses (Hruby 1985).

Ribonucleotide Reductase (F4, I4)

Vaccinia virus replicates within the cytoplasm of cells and must encode its own enzymes for nucleotide biosynthesis. One of the enzymes that Vaccinia encodes is a ribonucleotide reductase, an enzyme that catalyzes the conversion of rNDPs to dNDPs. Ribonucleotide reductase is a heterotetrameric protein, containing a large subunit (R1) and a small subunit (R2) that are encoded by two separate genes, I4L and F4L respectively (Slabaugh *et al.* 1988, Tengelsen *et al.* 1988, McCraith *et al.* 2000). The R2 subunit has been shown to be required for virus replication and virulence, while the R1 subunit can be replaced by the cellular R1 (Gammon *et al.* 2010).

Topoisomerase (H6)

Cells contain several enzymes that alter the topology of DNA. One such enzyme is the topoisomerase, which can be divided into two types. Type II topoisomerases break and rejoin dsDNA molecules using ATP (Lodish *et al.* 2000). This either changes a positive supercoil to a negative supercoil, or increases the number of negative supercoils by two (Lodish *et al.* 2000). Type I relax DNA by nicking and closing one strand of duplex DNA independently from ATP (Lodish *et al.* 2000). The type I topoisomerase becomes chemically bonded to the free 5' phosphate and becomes released when the nicked end is sealed (Lodish *et al.* 2000). This removes one supercoil (Lodish *et al.* 2000). Vaccinia encodes a type I topoisomerase that is encapsidated within the virion (Shuman and Moss 1987). Like cellular topoisomerases, the Vaccinia topoisomerase cleaves a single strand of duplex DNA, becomes covalently bound to the free end,

and is released upon sealing of the nicked strand to relax the supercoiled DNA (Shaffer and Traktman 1987).

Single Stranded DNA Binding Protein (I3)

The SSB protein from Vaccinia is located at the I3L gene locus. Like SSBs from other organisms, I3 protein binds specifically and strongly to ssDNA (Rochester and Traktman 1998). I3 is synthesized at early and intermediate times in the virus infection cycle and localizes to the virus factories during DNA replication (Rochester and Traktman 1998). Like other SSBs, I3 is essential to the virus; attempts to make an I3 knockout virus have been unsuccessful and siRNA knockdown experiments have shown that when I3 levels are decreased the level of virus replication and the number of virus progeny decrease (Rochester and Traktman 1998, Gammon and Evans 2009, Greseth *et al.* 2012).

There is little sequence conservation between I3 and other SSBs except for a shared property of negative charges within the C-terminal tail. Due to the similarities between this region in I3 and this region in other SSBs, there is the potential for I3 to bind to other proteins involved in DNA replication, recombination and repair in a similar manner as other SSBs. There have been a few reports in the literature on potential protein-protein interactions between I3 and other proteins. One report describes the use of anti-idiotypic antibodies directed against the small subunit of ribonucleotide reductase, to demonstrate an interaction with I3 (Davis and Mathews). Though not demonstrating a direct interaction, these experiments provide a logical binding partner for I3. A more recent report described the interaction between I3 and eIF4G, a cellular translation

initiation factor (Zaborowska *et al.* 2012). These are interesting data that requires further experimentation to determine if this interaction would occur in a virus infection and what the benefit to the virus is.

The ssDNA binding characteristics have previously been explored. Electrophoretic mobility shift assays demonstrated a discontinuity at approximately thirty two nucleotides per I3 monomer (Tseng *et al.* 1999). Beyond this breakpoint in the retardation curves, there was a disproportionately larger retardation of the complex than was expected with greater quantities of protein (Tseng *et al.* 1999). These data suggested that I3 was able to bind ssDNA in two binding modes. This hypothesis was confirmed using electron microscopy. Electron micrographs showed that at low nucleotide to I3 ratios, high protein densities, the ssDNA was thinly coated with small spheres (Tseng *et al.* 1999). At high nucleotide to I3 ratios, low protein densities, the ssDNA was more compacted and took on a beads-on-a-string appearance (Tseng *et al.* 1999). This model is similar to what is seen with other SSB proteins.

There is also a report of limited proteolysis experiments looking in to the different domains of I3. These experiments showed that the full length (270 amino acid) protein is converted by trypsin into five predominant protein fragments were formed: a 28.7kDa fragment corresponding to amino acids 1-259, a very stable 26.7kDa fragment corresponding to amino acids 21-259, a 17.0kDa fragment corresponding to amino acids 108-259, a 15.5kDa fragment corresponding to amino acids 108-246, and a 9.7kDa fragment corresponding to amino acids 21-107 (M. Tseng M.Sc. Thesis 1999). EMSA experiments demonstrated that the

ssDNA binding region is located in the fragment containing amino acids 7-93 (M. Tseng M.Sc. Thesis 1999). EMSA experiments also showed that the fragment containing amino acids 1-245 had the same breakpoint in retardation as the full length protein (M. Tseng M.Sc. Thesis 1999).

To build on these experiments our objectives are three fold. The first is to determine the structure of the poxvirus SSBs. Poxvirus SSBs are very highly conserved even amongst divergent viruses (Figure 1-9). To see how well the structure of these proteins is conserved between the poxvirus families, we attempt to solve the structure from several divergent poxviruses. We also use the information from the limited proteolysis studies to create truncated proteins that may crystallize easier.

The EMSA data from the proteolysis experiments suggest that the C-terminal tail is not required for the formation of either binding mode, because the same breakpoint in retardation was observed with full length and C terminal truncated I3 (M. Tseng M.Sc. Thesis 1999). The second objective is to determine what the role of the C-terminus is for ssDNA binding, and in the context of a virus infection.

Previous attempts to create an I3 knockout virus have been unsuccessful. However, using siRNAs to knockdown the expression of I3 decreases virus replication but progeny virus can still form (Gammon and Evans 2009, Greseth *et al.* 2012). The third objective is to determine if I3 is truly an essential protein to Vaccinia virus in an infection.

CHAPTER 2: MATERIALS AND METHODS

The compositions of all solutions are provided in Appendix 1

The sequences of the primers used in the PCR reactions can be found in Table 3

The first part of this thesis deals with attempts to determine the crystal structure of single-stranded DNA-binding proteins from several different poxviruses. This was accomplished by cloning N and C terminal truncated SSBs from Vaccinia, Molluscum Contagiosum, Orf and Fowlpox viruses, as well as full length Vaccinia and Molluscum Contagiosum SSB proteins, into plasmids for expression in *Escherichia coli*. Purified proteins underwent crystallization trials. Co-crystallization and immunoprecipitations were performed to determine if chimeric SSB complexes could occur. Multi angle laser light scattering was used to determine the oligomeric state of Vaccinia I3.

The second part of this thesis looks at the role of the negatively-charged C terminus of the poxvirus SSBs in ssDNA binding. To do this, we used electrophoretic mobility shift assays and ssDNA cellulose elution experiments with both His6 tagged and untagged poxvirus SSB proteins. We also used an anti-I3 antibody and peptides corresponding to the C terminus of Vaccinia I3 to look more closely at the C terminus in EMSA and ssDNA elution experiments. We used the antibody and peptides in microinjection experiments to look at the role of the C terminus in the context of a virus infection. An alignment of the amino acid sequences used is found in Figure 2-1. A summary of the features of these proteins is found in Table 2.

```

032 -----MKRAVSKTTVA-SNRAPQQE--DAAPARRFGENQAMSCDAINFAKSLSSSQTKAIDAVTLTPSQ
I3 -----MSKVIKK-----RVETS-----PRPTAS-SDSLQTCAGVIEYAKSISKNAKIEYVTLNASQ
088 MKNNLYEEKMNS-----KKQVKT-----QSKCENNASRFTCLDAVQYAKALCTKDTKIVKSVKLTPSH
046 -----MRKAVPGKQQTVLLRQKDP-ARPTSVSSPEEAPSRLTPVSVVEFARSLSPSSAKLIEHVTLTQSQ

032 YPSCSNINVCLVESLASKLVSPLIVVKGEFKIYPSKKTDMQRQN----DNGYFGRLKPVASPLLYQLLEN
I3 YANCSSISIKLTDLSLSSQMTSTFIMLEGETKLYKNKSKQ-DRS-----DGYFLKIKVTAASPMLYQLLEA
088 HNLCSNISVTLPEKYNEKLVSPFILVEGEGKIYQTRSDNFSRE-----ESYFLKIRPSVISPIHQMMEC
046 YPSCANIHITLVETLASKMVSPDIVVEGEAKVFRNKAKA-AEAFNKKGADAFFLRVRSVASPMLYQLLEC

032 IYENIKTGVRVPPSLRNFN-TETSIDNTFKSGCLYLN--RLTGALLEFTSDDDAQPICPLIREIENLATR
I3 VYGNIKHKERIPNSLHLSL-VETITEKTFKDESIFIN--KLNAMVEYVST-GESSILRSIEGELESLSKR
088 IYSDLGYLDP-----ENTMDEKTFKDGYYIYINKNKMSTIIEYTRNNKEVAGRKTLSSSEVEHLSKK
046 IYTNLRGGTRAPASM-CLSTLDTMEERTFKNCHLYINGNRIMSADVEYTGSDCVPRVVAMLRLETLAAR

032 DAQMATLILAPVVFYRSGGEGKVTFAVKKITMPRECSLTVLGLLEGEQTCVRMSETQPTFTEEQDVRGLGVV
I3 ERQLAKAIITPIVFYRSGTETKITFALKKLIIDREVVANVIGLSGDSERVSMTEN----VEEDLARNLGLV
088 DPQMVKAVLVASIFFENAVMCKISFSLKKLIMEKVCRKTLIDTNGE--VISIVTS----GETDTEDDS-DT
046 EPQMAKVVLAPIVLYRGSGEYKVTFALKRISMESMVHATVVVDASGEHVRLVMTESA---DDDERLAALGVM

032 DPGT-----GFEDEE-LEAP-FNI-HHHHHH
I3 DIDD-----EYDESD-KEKPIFNV-HHHHHH
088 ETDIDGVSGILEERSDGNRRGGYKIKETDEYDERSLFNVNHHHHHH
046 DTAL-----ELEDELA-DQDPLFNV-HHHHHH

```

Figure 2-1: Amino acid sequence alignment of the SSBs used in the experiments.

O32 from Orf, I3 from Vaccinia, O88 from Fowlpox, and O46 from *Molluscum contagiosum* were N- and C-terminally truncated (shown in grey). All N- and C-terminally truncated proteins contained a six histidine tag for purification (shown in green). We removed the N-terminal portion based on a large N-terminal truncation found in the sequence of the crocodilepox SSB. We truncated the C-terminal portion based on the prediction that the C terminus of the poxviral SSBs will be flexible and flexible regions interfere with crystal formation.

2.1 CLONING

2.1.1 Construction of Recombinant Plasmids

2.1.1.1 C-Terminal His6 Tagged VacI3₁₅₋₂₄₄

Plasmid containing N- and C-terminal truncated, C-terminal His6 tagged VacI3₁₅₋₂₄₄(H6), pVSSB_{p15-244}, was obtained from lab freezer stocks. This plasmid had been cloned into DHE142 (BL21 DE3 *recA pLysS*) (Zhang and Evans 1995) *E. coli* and was constructed by Dr. Xiao-Dan Yao (Evans Lab, unpublished data).

2.1.1.2 C-Terminal His6 Tagged VacI3₁₋₂₇₀

Plasmid containing full length VacI3₁₋₂₇₀, pNP205, was obtained from lab freezer stocks. This plasmid had been previously constructed by Dr. Nades Palaniyar (PhD. Thesis 1997). For expression in DHE143 *E. coli*, 1µg of plasmid was electroporated.

2.1.1.3 C-Terminal His6 Tagged FPVO88₂₅₋₂₄₁

The Fowlpox SSB gene FPVO88₂₅₋₂₄₁, was amplified by the polymerase chain reaction (PCR) from genomic DNA using the sense primer 5'-GGTACC-CATATGAA CGCATCTAGATTTACATGCC-3' and the antisense primer 5'-GAGCTCGCTGAGCTTATGGTGATGATGGTGATGGTCTCCGGAGGTTAC GACG-3'. The sense primer incorporated an *NdeI* site and the antisense primer incorporated a 6 histidine tag and a *BlnI* site. PCR was carried out using 1X *Taq* Buffer + KCl (Fermentas), 2.5mM MgCl₂ (Fermentas), 100µM of each dNTP, 150pmol of each primer, 25ng genomic DNA, and 1 unit of *Taq* DNA polymerase in a 50µL reaction. Amplification was carried out in the following steps: initial denaturation at 94°C for 2 minutes, then 30 cycles of denaturation at 94°C for 30

seconds, primer annealing at 52°C for 30 seconds, and primer extension at 72°C for 1 minute. The final cycle was followed by a 10 minute extension at 72°C.

10µL of the PCR reaction was electrophoresed on a 0.8% agarose gel stained with Sybr Safe (Invitrogen) to check for amplification. Following PCR, the PCR product was inserted into the pCR2.1-TOPO vector (Invitrogen). The PCR reaction (4µL), 1µL of ¼ diluted salt solution and 1µL of the pCR2.1-TOPO vector were combined and incubated at room temperature for 30 minutes then placed on ice. The TOPO reaction (1µL) was electroporated into 20µL of DH10B (*F mcrA Δ(mrr-hsdRMS-mcrBC) Φ80lacZΔM15 ΔlacX74 recA1 endA1 araD139Δ(ara, leu)7697 galUgalK λ rpsL nupG*) electrocompetent *E. coli*. Room temperature SOC media was added to the cells, and the cells were allowed to recover for 1 hour at 37°C in a horizontal shaker. The cells (5µL and 20µL) were spread onto LB plates containing kanamycin (50µg/mL) and X-Gal (40µg/mL), and incubated overnight at 37°C. White colonies were picked and analyzed by plasmid mini preparations. Plasmid DNA was digested using *NdeI* and *BlpI* to identify possible clones and positive clones were isolated. The positive clone (8µg) and pET11a vector were each digested using 1X Buffer O (Fermentas), 10units of *NdeI* and 10units of *BlpI* in a 20µL reaction at 37°C for 1 hour. Digests were run on 0.8% agarose gels and the DNA was gel purified using a GeneJet kit (Fermentas). Cut pET11a vector (100ng) was ligated to the O88₂₅₋₂₄₁ SSB insert in a 3:1 insert:vector ratio, and incubated at room temperature for 1.5 hours. The ligation reaction was electroporated into DH10B *E. coli* and spread onto LB plates containing ampicillin (100µg/mL).

Transformants were picked and analyzed by plasmid restriction digests. Plasmids were digested with *NdeI* and *BlpI* to identify possible clones, which were further confirmed by DNA sequencing using the T7 forward and T7 reverse primers (TAGC University of Alberta). Positive clones were electroporated into DHE142 *E. coli* and plated onto LB plates containing ampicillin (100µg/mL) and chloramphenicol (25µg/mL).

2.1.1.4 C-Terminal His6 Tagged OrfO32₂₈₋₂₄₄, MCVO46₃₀₋₂₂₇ and MCVO32₁₋₂₈₈ SSB Proteins

Plasmids containing C-terminal His6 tagged SSB proteins were obtained from GeneArt (optimized for expression in *E. coli*). These plasmids were electroporated into DH5α *E. coli* and cultured in LB with ampicillin (100µg/mL) for plasmid extraction. Plasmid DNA was digested with 1X Buffer O (Fermentas), 10 units *NdeI* and 10 units of *BamHI* in a 20µL reaction at 37°C for 1 hour. Reactions were electrophoresed on a 0.8% agarose gel, and the appropriate insert bands were purified using a GeneJet kit (Fermentas). *NdeI/BamHI* cut pET11a vector (100ng) was ligated with the insert SSB gene, at an insert:vector ratio of 3:1, at room temperature for 1.5 hours. The ligation reaction was electroporated into DH10B *E. coli* and spread onto LB plates containing ampicillin (100µg/mL), grown at 37°C overnight. Colonies were picked and analyzed by restriction digest. Plasmids were digested with *NdeI* and *BamHI* for the presence of the insert, and correct clones were verified by sequencing using the T7 forward and T7 reverse primers. Correct plasmids were electroporated into the expression strain DHE142

and spread onto LB plates containing ampicillin (100µg/mL) chloramphenicol (25µg/mL).

2.1.1.5 N Terminal His6 Tagged Non-Oligomerizing Vaccinia I3 Mutants

Recently, a paper has been published wherein the authors generated a series of clustered charge-to-alanine mutations in Vaccinia I3 as a structure/function analysis (Greseth *et al.* 2012). Three of these proteins were deficient in self-interaction and were unable to support a viable virus (Greseth *et al.* 2012). Of these three mutants, two were still able to bind to ssDNA, #4 (K182A, R183A, E184A, R185A) and #7 (E231A, R232A) (Greseth *et al.* 2012). I was fortunate to receive plasmids containing these N-terminal His6 tagged proteins from Dr. Paula Traktman. These plasmids were electroporated into the DHE142 *E. coli* strain for protein expression.

2.1.1.6 Untagged VacI3₁₋₂₄₄ and VacI3₁₋₂₇₀ SSBs.

Full length VacI3₁₋₂₇₀ and C-terminal truncated VacI3₁₋₂₄₄ were amplified using PCR with the following primers: VacI3₁₋₂₇₀ sense primer 5'-CTTTAAGAA-GGAGATATACATATGAGTAAGGTAATCAAGAAGAG-3' and antisense primer 5'-CTTTGTTAGCAGCCGGATCCTTATAGATTGAATATTGGCTTT-TCT-3'; I3₁₋₂₄₄ sense primer 5'-CTTTAAGAAGGAGATATACATATGAGTAA-GGTAATCAAGAAGAG -3' and antisense primer 5'-CTTTGTTAGCAGCCG-GATCCTTAAGCCAGATCTTCTTCTACAT-3'. Sense primers contain *NdeI* sites and antisense primers contain *BamHI* sites. All primers contain homology to pET11a at the 5' end for Infusion cloning. PCR was carried out using 1X *Taq* Buffer + KCl (Fermentas), 2.5mM MgCl₂ (Fermentas), 100µM of each dNTP,

150pmol of each primer, 25ng Vaccinia Copenhagen genomic DNA, and 1 unit of *Taq* DNA polymerase in a 50µL reaction. Amplification was carried out in the following steps: initial denaturation at 95°C for 2 minutes, then 30 cycles of denaturation at 95°C for 30 seconds, primer annealing at 53°C for 30 seconds, and primer extension at 72°C for 1 minute. The final cycle was followed by a 10 minute extension at 72°C. The PCR reaction was electrophoresed on a 0.8% agarose gel stained with Sybr Safe (Invitrogen). PCR product bands were gel purified using a GeneJet kit (Fermentas). *NdeI* and *BamHI* cut pET11a vector (137ng) was ligated to the purified PCR product in a 3:1 insert:vector ratio using Infusion cloning. The Infusion reaction contained 1X Polymerase Buffer, 0.1µg Vaccinia DNA polymerase, cut pET11a vector and PCR product in a 20µL reaction. The Infusion reaction was incubated at 37°C for 20 minutes before 1µL was electroporated into DH10B *E. coli* and spread onto LB plates supplemented with ampicillin (100µg/mL). Colonies were picked and plasmids were analyzed by restriction digest. Plasmids were digested with *NdeI* and *BamHI* for the presence of the insert, and correct clones were verified by sequencing using the T7 forward and T7 reverse primers. Correct plasmids were electroporated into the expression strain DHE142 and spread onto LB plates containing ampicillin (100µg/mL) and chloramphenicol (25µg/mL).

2.1.1.7 Untagged MCVO46₁₋₂₆₅ and MCVO46₁₋₂₈₈ SSBs

Full length MCVO46₁₋₂₈₈ and C-terminal truncated MCVO46₁₋₂₆₅ were amplified using PCR with the following primers: MCVO46₁₋₂₈₈ sense primer 5'-CTTTAAGAAGGAGATATACATATGCGTAAAGCAGTTCCGGGTAAAC-3'

and antisense primer 5'- CTTTGTTAGCAGCCGGATCCTTACACATTA AAC-AGCGGGTCCTGATC -3'; MCVO46₁₋₂₆₅ sense primer 5'-CTTTAAGAAGGAG-ATATACATATGCGTAAAGCAGTTCCGGGTAAAC -3' and antisense primer 5'- CTTTGTTAGCAGCCGGATCCTTACAGACGTTTCATCATCATCTGCGC-3'. Sense primers contain *NdeI* sites and antisense primers contain *BamHI* sites. All primers contain homology to pET11a at the 5' end for Infusion cloning. PCR was carried out using 1X *Taq* Buffer + KCl (Fermentas), 2.5mM MgCl₂ (Fermentas), 100μM of each dNTP, 150pmol of each primer, 25ng MCV 1-295 His6 GeneArt plasmid for template, and 1 unit of *Taq* DNA polymerase in a 50μL reaction. Amplification was carried out in the following steps: initial denaturation at 95°C for 2 minutes, then 30 cycles of denaturation at 95°C for 30 seconds, primer annealing at 53°C for 30 seconds, and primer extension at 72°C for 1 minute. The final cycle was followed by a 10 minute extension at 72°C. 10μL of the PCR reaction was electrophoresed on a 0.8% agarose gel stained with Sybr Safe (Invitrogen). PCR product bands were gel purified using a GeneJet kit (Fermentas). *NdeI* and *BamHI* cut pET11a vector (137ng) was ligated to the purified PCR product in a 3:1 insert:vector ratio using Infusion cloning. The Infusion reaction contained 1X Polymerase Buffer, 0.1μg Vaccinia DNA polymerase, cut pET11a vector and PCR product in a 20μL reaction. The Infusion reaction was incubated at 37°C for 20 minutes before 1μL was electroporated into DH10B *E. coli* and spread onto LB plates containing ampicillin (100μg/mL). Colonies were picked and plasmids were analyzed by restriction digest. Plasmids were digested with *NdeI* and *BamHI* for the presence of the insert, and correct

clones were verified by sequencing using the T7 forward and T7 reverse primers. Correct plasmids were electroporated into the expression strain DHE142 and spread onto LB plates supplemented with ampicillin (100µg/mL) and chloramphenicol (25µg/mL).

2.1.1.8 Vaccinia I3 Negative Charge Point Mutants

Mutations were introduced into negative charges within the C terminus of the full length Vaccinia I3 protein, and were created using the Quik Change II XL Site-Directed Mutagenesis Kit (Agilent Technologies). Three mutant proteins were created: 3 Neutral Charges, 6 Neutral Charges, and 3 Positive Charges. Mutations were done in a step wise manner, the order being as follows: 3 Neutral Charges E241A, D251A then D260A; 6 Neutral Charges E240AE241A, D251AE255A, then D260AE264A; 3 Positive Charges E241K, D251K, then D260K (Table 2 for primer sequences). All reactions were in a volume of 50µL, contained 10ng of Vaccinia full length untagged plasmid as template, and were completed as per the manufacturer's instructions using *Pfu* Ultra HF polymerase. Amplification was carried out with the following conditions: initial denaturation of 95°C for 1 minute followed by 18 cycles of denaturation at 95°C for 50 seconds, primer annealing at 60°C for 50 seconds, and primer extension at 68°C for 7 minutes. The last step consisted of a 68°C 7 minute final extension. Following amplification, the PCR reaction was treated with 1µL of *DpnI* restriction enzyme at 37°C for 1 hour. For transformation into XL-10 Gold Ultracompetent *E. coli* (Tet^r Δ(*mcrA*)183 Δ(*mcrCB-hsdSMR-mrr*)173 *endA1 supE44 thi-1 recA1 gyrA96 relA1 lac* Hte [F' *proAB lacI^q ZΔM15 Tn10* (Tet^r)

Amy Cam^r], 45µL of cells were transferred to a prechilled round bottom tube and treated with 2µL of β-mercaptoethanol before incubation on ice for 10 minutes. *DpnI* treated DNA was added to the cells and incubated on ice for 30 minutes. Cells were heat shocked for 30 seconds at 42°C and then incubated for 2 minutes on ice. Prewarmed NZY⁺ media was added to the cells before recovery incubation at 37°C for 1 hour. Cells was plated in duplicate onto LB plates containing ampicillin (100µg/mL) and incubated overnight. Colonies were analyzed by plasmid restriction digest and plasmids were sent for sequencing to verify that the point mutations were successful using the T7 forward and T7 reverse primers. Correct plasmids were electroporated into the expression strain DHE142 and the bacteria were spread onto LB plates containing ampicillin (100µg/mL) and chloramphenicol (25µg/mL).

2.1.1.9 N-Terminal Flag Tagged I3

An N-terminal Flag tagged Vaccinia I3 was amplified by the polymerase chain reaction (PCR) from genomic DNA using the sense primer 5'-GTCGACA-TGGACTACAAGGACGACGATGACAAGATGAGTAAGGTAATCAAGAAGAGAG -3' and the antisense primer 5'-GCGGCCGCTTATACATTGAATATTG-GCTTTTC -3'. The sense primer incorporated a *SalI* site and a Flag tag, and the antisense primer incorporated a *NotI* site. PCR was carried out using 1X *Taq* Buffer + KCl (Fermentas), 2.5mM MgCl₂ (Fermentas), 100µM of each dNTP, 150pmol of each primer, 25ng genomic DNA, and 1 unit of *Taq* DNA polymerase in a 50µL reaction. Amplification was carried out in the following steps: initial denaturation at 94°C for 2 minutes, then 30 cycles of denaturation at 94°C for 30

seconds, primer annealing at 52°C for 30 seconds, and primer extension at 72°C for 1 minute. The final cycle was followed by a 10 minute extension at 72°C.

10µL of the PCR reaction was electrophoresed on a 0.8% agarose gel stained with Sybr Safe (Invitrogen) to check for amplification. Following PCR, the PCR product was inserted into the pCR2.1-TOPO vector (Invitrogen). The PCR reaction (4µL), 1µL of ¼ diluted salt solution and 1µL of the pCR2.1-TOPO vector were combined and incubated at room temperature for 30 minutes then placed on ice. The TOPO reaction (1µL) was electroporated into 20µL of DH10B (*F mcrA Δ(mrr-hsdRMS-mcrBC) Φ80lacZΔM15 ΔlacX74 recA1 endA1 araD139Δ(ara, leu)7697 galUgalK λ rpsL nupG*) electrocompetent *E. coli*. Room temperature SOC media was added and the cells were allowed to recover for 1 hour at 37°C in a horizontal shaker. The cells (5µL and 20µL) were spread onto LB plates containing kanamycin (50µg/mL) and X-Gal (40µg/mL), and incubated overnight at 37°C. White colonies were picked and analyzed by plasmid mini preparations. Plasmid DNA was digested using *SalI* and *NotI* to identify possible clones and positive clones were isolated. The positive clone (8µg) and pET11a vector were each digested using 1X Green Buffer (Fermentas), 10units of *SalI* and 10units of *NotI* in a 20µL reaction at 37°C for 1 hour. Digests were run on 0.8% agarose gels and the DNA was gel purified using a GeneJet kit (Fermentas). Cut pSC66 vector (100ng) was ligated to the Flag tagged I3 insert in a 3:1 insert:vector ratio, and incubated at room temperature for 1.5 hours. pSC66 contains a poxvirus early/late promoter so proteins can be expressed during a poxvirus infection. The ligation reaction was electroporated

into DH10B *E. coli* and spread onto LB plates containing ampicillin (100µg/mL). Transformants were picked and analyzed by plasmid restriction digests. Plasmids were digested with *SaII* and *NotI* to identify possible clones.

Table 2: Poxvirus SSBs cloned and used in the experiments

Protein Name	Virus	Amino Acid Range	Tags	GenBand DNA ID	GenBank Protein ID
VacI3 ₁₋₂₇₀ (H6)	Vaccinia	1-270 (Full Length)	C Terminal His6	J03399.1	AAB59805.1
VacI3 ₁₅₋₂₄₄ (H6)	Vaccinia	15-244	C Terminal His6	J03399.1	AAB59805.1
VacI3 ₁₋₂₇₀	Vaccinia	1-270 (Full Length)	None	J03399.1	AAB59805.1
VacI3 ₁₋₂₄₄	Vaccinia	1-244	None	J03399.1	AAB59805.1
MCVO46 ₁₋₂₈₈ (H6)	MCV	1-288 (Full Length)	C Terminal His6	NC001731.1	NP043997.1
MCVO46 ₃₀₋₂₂₇ (H6)	MCV	30-227	C Terminal His6	NC001731.1	NP043997.1
MCVO46 ₁₋₂₈₈	MCV	1-288 (Full Length)	None	NC001731.1	NP043997.1
MCVO46 ₁₋₂₆₅	MCV	1-265	None	NC001731.1	NP043997.1
FPVO88 ₂₅₋₂₄₁ (H6)	Fowlpox	25-241	C Terminal His6	NC002188.1	NP039051.1
OrfO32 ₂₈₋₂₄₄ (H6)	Orf	28-244	C Terminal His6	DQ184476.1	ABA00549.1
N Flag I3	Vaccinia	1-270 (Full Length)	N Terminal Flag	J03399.1	AAB59805.1

Table 3: PCR primer sequences used to amplify poxvirus SSB genes

Primer	Sequence 5'-3'
FpxSSBFwd	GGTACCCATATGAACGCATCTAGATTTGCGTGCC
FpxSSBRev	GAGCTCGCTGAGCTTAATGGTGATGATGGTGATGGTCTCCGGAGGTTACGACG
Myx-fw-M28	GGTACCCATATGGAACCCGCGCAGCCAC
Myc-rc-C239	GAGCTCGGATCCTTACGATTCCACCATCGAAATC
VacInfsnFwd	CTTTAAGAAGGAGATATACATATGAGTAAGGTAATCAAGAAGAG
VacInfsn244Rev	CTTTGTTAGCAGCCGGATCCTTAAGCCAGATCTTCTTCTACAT
VacInfsnRev 270	CTTTGTTAGCAGCCGGATCCTTATAGATTGAATATTGGCTTTCT
MCVInfsnFwd	CTTTAAGAAGGAGATATACATATGCGTAAAGCAGTCCGGGTAAAC
MCVInfsnRev 265	CTTTGTTAGCAGCCGGATCCTTACAGACGTTTCATCATCATCTGCGC
MCVInfsnRev288	CTTTGTTAGCAGCCGGATCCTTACACATTAACAGCGGGTCTGATC
VacCTerm MutE241A Fwd	GAAAATGTAGAAGCAGATCTGGCTCGTAATCTGGGACTTG
VacCTerm MutE241A Rev	CAAGTCCCAGATTACGAGCCAGATCTGCTTCTACATTTTC
I3 CTerm D251A Fwd	CTGGCTCGTAATCTGGGACTTGTTGCTATTGATGATGAA
I3 CTerm D251A Rev	TTCATCATCAATAGCAACAAGTCCCAGATTACGAGCCAG
I3 CTerm D260A Fwd	ATTGATGATGAATATGATGAAGCTAGCGATAAAGAAAAGCCAATATTCAA
I3 CTerm D260A Rev	TG
VacCTerm MutE240AE241A Fwd	CATTGAATATTGGCTTTCTTTTATCGCTAGCTTCATCATATTTCATCAAT
VacCTerm MutE240AE241A Rev	CAATGACTGAAAATGTAGCAGCAGATCTGGCTCGTAATCTG
VacCTerm MutD251AE255A Fwd	CAGATTACGAGCCAGATCTGCTGCTACATTTTCAGTCATTG
VacCTerm MutD251AE255A Rev	CTGGGACTTGTGCTATTGATGATGCATATGATGAAGATAG
I3 CTerm D260A E264A Fwd	CTATCTTCCTCATATGCATCATCAATAGCAACAAGTCCCAG
I3 CTerm D260A E264A Rev	ATATGATGAAGCTAGCGATAAAGCAAAGCCAATATTCAATGTATAA
I3 CTerm E241K Fwd	TTATACATTGAATATTGGCTTTGCTTTTATCGCTAGCTTCATCATAT
I3 CTerm E241K Rev	GAAAATGTAGAAAAAGATCTGGCTCGTAATCTGGGACTTG
I3 CTerm D251K Fwd	CAAGTCCCAGATTACGAGCCAGATCTTTTCTACATTTTC
I3 CTerm D251K Rev	TTCATCATATTCATCATCAATTTAACAAGTCCCAGATTACGAGCCAG
VacCTerm MutD260K Fwd	CTGGCTCGTAATCTGGGACTTGTTAAAATTGATGATGAATATGATGAA
VacCTerm MutD260K Rev	ATTGATGATGAATATGATGAAAAAGCGATAAAGAAAAGCCAATATTCAA
N Flag I3 Fwd	TG
N Flag I3 Rev	CATTGATAATTGGCTTTTCTTTATCGCTTTTTCATCATATTTCATCAAT GTCGACATGGACTACAAGGACGACGATGACAAGATGAGTAAGGTAATCAA GAAGAGAG
	GCGGCCGCTTATACATTGAATATTGGCTTTTC

2.2 PROTEIN PURIFICATION

2.2.1 Expression and Purification of His6-Tagged Proteins

DHE142 colonies containing the His6-tagged SSB were picked and grown overnight in 100mL of LB, supplemented with 25µg/mL chloramphenicol and 100µg/mL ampicillin. Seven and a half litres of identical media were inoculated with 15ml of the overnight culture and grown to an OD₆₀₀ of 0.6 in a 37°C shaking incubator. Cultures were induced with 1mM IPTG and shaken for 30 minutes. Rifampicin was then added to 50µg/mL. Cultures were allowed to grow for an additional 2.5 hours at 37°C for a total of a 3 hour induction. Bacterial cells were harvested at 6000xg for 10 minutes at 4°C and resuspended in 35mL nickel binding buffer. Cells were stored at -20°C.

The cell pellet was thawed at 37°C before sonication with 10 second pulses for 2 minutes. Insoluble components were pelleted by centrifugation at 20,000xg for 30 minutes. The pellet was resuspended in 30mL nickel binding buffer, sonicated again and centrifuged. The supernatants were pooled and further clarified using Millipore SteriFlip 0.45µm Vacuum Filter units. Clarified supernatant was loaded onto a 1mL HisTrapFF column (GE Healthcare), using an AKTA HPLC. Protein was eluted using imidazole in a stepwise gradient mixed by the HPLC by combining the nickel binding and nickel elution buffers. The imidazole gradient was as follows: 10 column volumes without imidazole, 2 column volumes at 25mM imidazole, 2 column volumes at 50mM imidazole, 8 column volumes at 100mM imidazole, 6 column volumes at 200mM imidazole and 5 column volumes at 800mM imidazole. 1mL fractions were collected and fractions were

run on 10% SDS PAGE Coomassie stained gels. Fractions containing the highest amount of protein were pooled and dialyzed overnight at 4°C in 1L heparin binding buffer with 2 buffer changes. The dialyzed sample was run over a 5mL HiTrap Heparin HP column (GE Healthcare) using the AKTA HPLC. Protein was eluted using a stepwise gradient of increasing NaCl concentrations created by the HPLC mixing heparin binding and heparin elution buffers. The gradient was as follows: 5 column volumes at 50mM NaCl and 5 column volumes at 1M NaCl. Fractions were run on a 10% SDS PAGE Coomassie stained gel. Bradford assays were performed on the fractions containing protein. For experiments, proteins were either dialyzed against 1X Buffer A overnight or run through PD-Mini Trap G-25 spin columns (GE Healthcare) to exchange to low salt 1X Buffer A. Example SDS PAGE gels and AKTA traces from the purification of I3₁₅₋₂₄₄(H6) are shown in Figure 2-2.

2.2.2 Expression and Purification of Untagged Proteins

DHE142 colonies containing untagged SSB protein were picked and grown overnight in 100mL of LB with 25µg/mL chloramphenicol and 100µg/mL ampicillin. Seven and a half litres of identical media were inoculated with 15ml of the overnight culture and grown to an OD₆₀₀ of 0.6 in a 37°C shaking incubator. Cultures were induced with 1mM IPTG and shaken for 30 minutes. Rifampicin was then added to 50µg/mL. Cultures were allowed to grow for an additional 2.5 hours at 37°C for a total of a 3 hour induction. Bacterial cells were harvested at 6000xg for 10 minutes at 4°C and resuspended in 35mL 1X Buffer A. Cells were stored at -20°C.

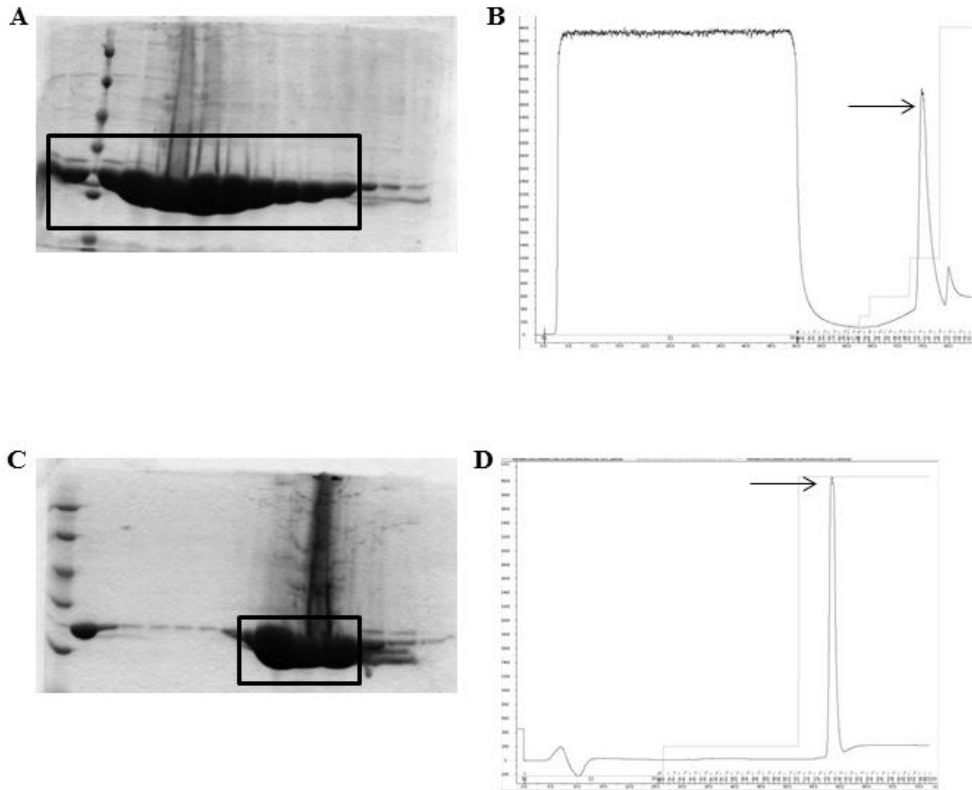


Figure 2-2: SDS PAGE gels and HPLC tracings from the purification of VacI₁₅₋₂₄₄(H6).

A) Coomassie stained gel of elution fractions from nickel column. Fractions pooled for dialysis are boxed. B) HPLC tracing of nickel purification of VacI₁₅₋₂₄₄(H6). The peak corresponding to the pooled fractions is indicated (arrow). C) Coomassie stained gel of elution fractions from heparin column purification of VacI₁₅₋₂₄₄(H6). Protein fractions used in dialysis for experimentation are boxed. D) HPLC tracing of heparin purification. Peak fraction corresponding to boxed lanes in SDS PAGE gel is indicated (arrow).

The cell pellet was thawed at 37°C before sonication with 10 second pulses for 2 minutes. Insoluble components were pelleted by centrifugation at 20,000xg for 30 minutes. The pellet was resuspended in 30mL 1X Buffer A, sonicated a second time and centrifuged. The supernatants were pooled and further clarified using Millipore SteriFlip 0.45µm Vacuum Filter units. Clarified supernatant was loaded onto a 5mL HiTrap Heparin HP column (GE Healthcare) using the AKTA HPLC. Untagged SSB proteins were eluted from the column in 1mL fractions by a gradient mixed by the AKTA using a mixture of heparin binding and heparin elution buffers. The gradient was as follows: 50mM NaCl for 2 column volumes, 100mM NaCl for 3 column volumes, 250mM NaCl for 5 column volumes, 500mM NaCl for 5 column volumes, 1M NaCl for 5 column volumes, 1.5M NaCl for 2 column volumes, 2M NaCl for 2 column volumes. Fractions were run on 10% SDS PAGE Coomassie stained gels and the fractions with the highest amount of SSB protein were pooled for dialysis at 4°C overnight in 1L 1X Buffer A with 2 buffer changes. The dialyzed sample was run over an ssDNA cellulose column at 4°C and eluted with ssDNA cellulose buffers in a step wise gradient in 1mL fractions. The gradient was as follows: 15mL 50mM Buffer A, 25mL 500mM Buffer A, 30mL 2M Buffer A. Fractions were run on 10% SDS PAGE Coomassie stained gels and the fractions with the highest amount of SSB protein were pooled for dialysis in 1L 1X Buffer A at 4°C overnight with 2 buffer changes. The dialyzed sample was run over a 5mL HiTrap Heparin HP column (GE Healthcare) using an AKTA HPLC. The column was washed with 5 column volumes of 50mM Buffer A and eluted with 5 column volumes of 1M Buffer A in

1mL fractions. Fractions were run on 10% SDS PAGE Coomassie stained gels, Bradford assays were performed on the fractions. For experiments, proteins were dialyzed against 1X Buffer A overnight. Example SDS PAGE gels and AKTA traces from the purification of I3₁₋₂₇₀ are shown in Figure 2-3.

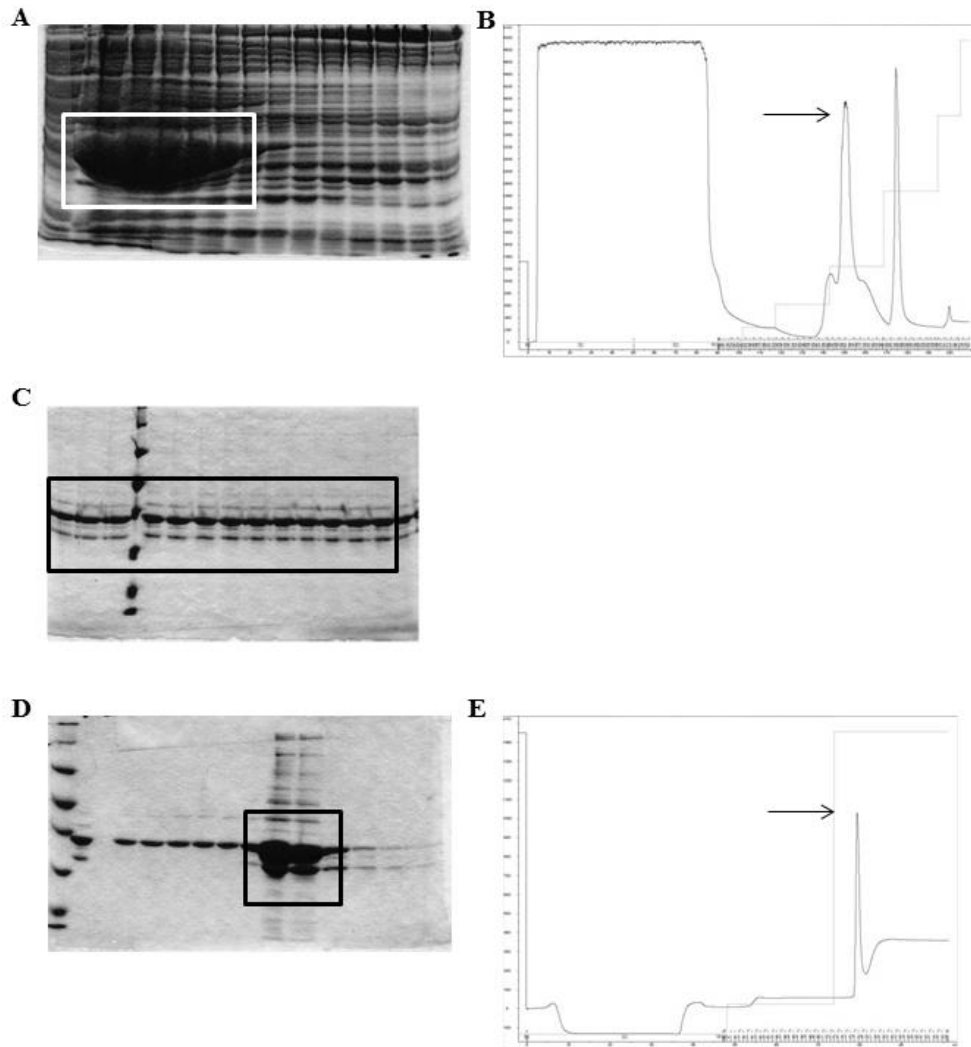


Figure 2-3: SDS PAGE gels and HPLC tracings from the purification of VacI3₁₋₂₇₀.

A) Coomassie stained gel of elution fractions from heparin column. Fractions pooled for dialysis are boxed. B) HPLC tracing of heparin purification of VacI3₁₋₂₇₀. The peak corresponding to the pooled fractions is indicated (arrow). C) Coomassie stained gel of elution fractions from ssDNA cellulose column purification. Protein fractions used in dialysis for experimentation are boxed. D) Coomassie stained gel of elution fractions from second heparin column purification of VacI3₁₋₂₇₀. E) HPLC tracing of heparin purification. Peak fraction corresponding to boxed lanes in SDS PAGE gel is indicated (arrow).

2.3 ASSAYS

2.3.1 Crystallization Screens

Proteins at 10mg/mL were bound to a 30-mer polyT oligonucleotide in a 1:1 molar ratio for 1 hour at 37°C. Crystallization screens were performed using a Honeybee crystallization robot (Genomic Solutions) against several commercial Nextall screens: Cryos, JCSG+, JCSG Core I, JCSG Core II, JCSG Core III, JCSG Core IV, MbClass, Nucleix, and PACT Suites (Qiagen). Protein was mixed with crystallization solution in equal volumes in a 0.2µL drop with 50µL in the buffer chamber. There were three samples per screen condition: SSB, SSB+30-mer polyT, buffer control (no protein). Plates were sealed and crystals were observed through a light microscope.

2.3.2 Large Scale Crystallization

Hits from the small scale screens were replicated in larger scale. Protein at 10mg/mL was mixed with crystallization solution in equal volumes in a 2µL drop on a hanging drop plate, with 1mL solution in the buffer chamber. There were three samples per condition: SSB, SSB+30-mer polyT, buffer control (no protein). Plates were sealed with vacuum grease and crystals were observed through a light microscope. For the protease screens, a 1:100, 1:1000 or 1:10,000 dilution of a protease stock solution (Proti-Ace Kit, Hampton Research) was added to the VacI3₁₅₋₂₄₄(H6) samples before mixing with the crystallization solution. For growing crystals with Fab fragments, a 1:1 ratio of 10D11 anti-I3 antibody Fab fragment was bound to the I3₁₋₂₇₀(H6) protein at 37°C for 1 hour before mixing with the crystallization solution. This antibody had previously been used in

Western blots and could detect the His6 tagged Vaccinia I3 protein. For co-crystals, a 1:1:1 molar ratio of each protein and 30-mer polyT oligonucleotide were mixed and incubated for 20 minutes at 37°C before mixing with the crystallization solution. For crystals with native C-terminus (N30mer) and scrambled C-terminus (S30mer) peptides, peptides were mixed in a 1:1 molar ratio with VacI3₁₅₋₂₄₄(H6) and incubated at 37°C for 1 hour before mixing with the crystallization solution. Crystals were mounted in cryoloops (Hampton Research) and flash frozen in liquid nitrogen for X-ray diffraction. Crystals were tested for diffraction using an in house Rigaku FRE SuperBright system.

2.3.3 Immunoprecipitations of VacI3₁₋₂₇₀(H6) Protein Complexes

Equimolar amounts of VacI3₁₋₂₇₀(H6) and either OrfO32₂₈₋₂₄₄(H6), MCVO46₃₀₋₂₂₇(H6), MCVO46₁₋₂₈₈(H6) or FPVO88₂₅₋₂₄₁(H6) proteins were combined in a total volume of 800µL. 10D11 anti-I3 mouse monoclonal antibody (15.3mg/mL) was added and the mixture was incubated at 4°C overnight on a rotator. Protein G Sepharose 4 Fast Flow beads (GE Healthcare) were prepared as follows: 300µL of bead slurry was pelleted at 3000rpm for 15 seconds, the supernatant was removed and the beads were washed 3 times with 1X Buffer A, finally the beads were resuspended in 1X Buffer A to a 50% slurry. The 50% bead slurry (100µL) was added to the protein mixture and incubated for 2 hours at 4°C. The beads were pelleted at 8000rpm for 15 seconds, the supernatant was removed and the beads were gently washed 5 times with 1mL 1X Buffer A. The final wash was discarded and 50µL of 4X SDS PAGE loading buffer was added to the sample. The sample was boiled for 5 minutes and centrifuged for 10 seconds at

18,000 xg. Samples were run on a 10% SDS PAGE Coomassie stained gel or transferred to ImmobilonFL membrane (Millipore) for Western blotting. For Western blotting, membranes were incubated with a 1 in 1000 dilution of anti-His6 mouse monoclonal primary antibody (Roche) in Western blot blocking buffer for 2 hours at room temperature. Membranes were washed with PBS-T for 15 minutes, and incubated with a 1 in 20,000 dilution of IR-Dye 800CW goat anti mouse secondary antibody (Li-cor) for 1 hour at room temperature. Membranes were washed for 20 minutes with PBS-T, 10 minutes with PBS, and scanned with a Li-cor Odyssey.

2.3.4 Electrophoretic Mobility Shift Assays

Varying amounts of SSBs were mixed in a 20 μ L reaction with 1X EMSA Buffer and 1 μ g Φ X174 ssDNA. Samples were incubated for 20 minutes at 37°C. 2 μ L of GLB loading dye was added to each sample and the samples were run on 0.8% SeaKem LE agarose (Lonza) gels at 30V for 17 hours at 4°C. His6 tagged proteins were run on gels prepared with IBE buffer, untagged proteins were run on gels prepared with TAE buffer. Gels were stained with Sybr Safe (Invitrogen) stain for 1 hour at room temperature and visualized with a GelDoc camera (BioRad).

2.3.5 Electrophoretic Mobility Shift Assays, Peptide Competition

Untagged VacI3₁₋₂₇₀ protein (30 μ g) was bound to increasing amounts of a 30-mer peptide corresponding to the native I3 C terminus (N30mer) (EEDLARNLGLVDIDDEYDESDSKEKPIFNV), or a scrambled version of this sequence (S30mer) (DNSDLDKYVYPRGELEVDIAEDNDKIFEDL) peptide in

1:1, 5:1, 10:1, 20:1 or 30:1 molar ratios in a 20 μ L reaction with 1X EMSA Buffer for 20 minutes at 37°C. Samples were incubated at 37°C for 20 minutes after the addition of 1 μ g of Φ X174 ssDNA. GLB loading dye was added to each sample and the samples were run on 0.8% SeaKem LE agarose (Lonza) gels at 30V for 17 hours at 4°C. Gels were stained with Sybr Safe (Invitrogen) stain for 1 hour at room temperature and visualized with a GelDoc camera (BioRad).

2.3.6 Electrophoretic Mobility Shift Assays, Antibody Supershift

Anti-I3 10D11 mouse monoclonal antibody or an isotype control anti-E9 4E5 mouse monoclonal antibody was added to 1, 5 or 10 μ g of VacI3₁₋₂₇₀ or VacI3₁₋₂₄₄ untagged proteins in 1:1, 2:1 and 5:1 molar ratios (antibody:SSB) in a 20 μ L reaction with 1X EMSA buffer and incubated at 37°C for 20 minutes. The reaction was incubated for another 20 minutes at 37°C after the addition of 1 μ g of Φ X174 ssDNA. GLB loading dye was added to each sample, and the samples were run on a 0.8% SeaKem LE agarose (Lonza) gel at 30V for 17 hours at 4°C. Gels were stained with Sybr Safe (Invitrogen) for 1 hour at room temperature prior to imaging.

2.3.7 ssDNA Cellulose Elution Assay

ssDNA cellulose from calf thymus DNA (Sigma) was prepared as follows: 10g ssDNA cellulose was resuspended in 10mL ddH₂O to make a 50% slurry. 500 μ L of the 50% slurry was transferred to a microfuge tube and centrifuged at 1000xg for 60 seconds. The supernatant was removed and the cellulose was resuspended in 1mL ddH₂O. The ssDNA cellulose was washed twice with 1X Buffer A before the final supernatant was removed. SSB protein (20nmol) in

500 μ L was bound to the ssDNA cellulose at room temperature for 1 hour on a rotator. After 1 hour incubation, the sample was centrifuged at 1000xg for 60 seconds and the flow through supernatant was removed. The cellulose was gently resuspended in 50mM NaCl Buffer A and rotated for 5 minutes at room temperature. The sample was centrifuged at 1000xg for 60 seconds and the 50mM supernatant was removed. The cellulose was gently resuspended in 300mM NaCl Buffer A and rotated at room temperature for 5 minutes. The sample was centrifuged at 1000xg for 60 seconds and the 300mM supernatant was removed. This process was repeated using Buffer A with 600mM, 900mM, 1.2M, 1.5M, 1.8M, 2.1M, 2.4M, 2.7M and 3.0M NaCl. Supernatants were run on a 10% SDS PAGE Blue Silver Coomassie stained gel. Gels were imaged using the BioRad Gel Doc gel camera system and the band intensity was measured relative to the flow through using the BioRad Image Lab Software. Total protein was calculated as an additive effect of the band intensities and converted to percent total protein, which was graphed against NaCl concentration.

2.3.8 Multi Angle Laser Light Scattering (MALLS)

Bovine serum albumin (BSA) or SSB protein were loaded onto a Superdex 200 10/300 GL column (GE Healthcare) and eluted with an isocratic elution with 150mM Buffer A in 500 μ L fractions using an AKTA HPLC (Amersham). Fractions were run on a 10% SDS PAGE Coomassie stained gel and peak fractions were pooled and concentrated to 100 μ L using Amicon Ultra 0.5mL 10K Ultracel centrifugal filters (Millipore). 100 μ L of 200 μ M of BSA or SSB protein was loaded onto a Superose 6 column that is in line with a Wyatt Systems REX

and DAWN MALLS. Elution was detected as changes in the refractive index. Data was analyzed using the ASTRA software to determine the molecular weight of the sample, and BSA was used to normalize the detectors. For samples with ssDNA, SSB was collected off the MALLS, bound with 30mer polyT oligonucleotide in a 1:1 molar ratio, reloaded onto the column and analyzed again by MALLS.

2.3.9 Determination of Amount of I3 in Infected BSC40 Cells

A confluent 150mm dish of BSC40 cells was infected with Vaccinia strain WR at an MOI of 5 for 6 hours. Cells were harvested and counted using Trypan blue (Invitrogen). Samples with known numbers of cells, as counted using a Countess Automated Cell Counter (Invitrogen), were prepared with 4X SDS PAGE loading dye and run on an SDS PAGE gel along with VacI3₁₋₂₇₀ dilutions of known concentrations in order to prepare a standard curve. Proteins were transferred to an Immobilon FL membrane for Western blotting as described above. Anti-I3 10D11 mouse monoclonal antibody (1:10,000 dilution) and a goat anti-mouse (1:20,000 dilution, IR-Dye 800CW, Li-cor) were used to detect I3. The membrane was scanned with a Li-cor Odyssey and the band intensities were quantified using the Odyssey software (Version 3.0).

2.3.10 Immunoprecipitations of I3 to Search for Binding Partners

Confluent BSC40 cells on a 150mm dish were infected with Vaccinia virus strain WR at an MOI of 5 for 1 hour. Virus was removed and Opti-MEM (Gibco) was added. At 2 hours post infection, 8µg of N Flag I3 pSC66 plasmid was transfected into the cells using Lipofectamine (Invitrogen). The transfection

was allowed to proceed overnight at 37°C. The next day the cells were harvested, washed with 1X PBS A, and lysed with a 21.5 gauge needle in 0.5mL lysis buffer.

A 30-mer polyT oligonucleotide was added to the lysates and incubated on ice for 1 hour. Monoclonal mouse anti-Flag magnet beads (Sigma) were added to infected cell supernatants and incubated overnight at 4°C on a nutator. The beads were washed three times in TBS and boiled in 4X SDS PAGE loading buffer. Samples were fractionated on duplicate SDS PAGE gels for silver staining and Western blotting, as described above. The samples were blotted for Flag I3 (1° antibody: mouse anti-Flag M2, 1:1000, Sigma; 2° antibody: goat anti-mouse IR-Dye 800CW, 1:20,000, Li-cor), cellular R1 (1° antibody: mouse anti-cellular R1, 1:100, Chemicon International; 2° antibody: goat anti-mouse IR-Dye 800CW, 1:20,000, Li-cor), cellular R2 (1° antibody: goat anti-cellular R2 N-18, 1:100, Santa Cruz Biotechnologies; 2° antibody: donkey anti-goat IR-Dye 680, 1:20,000, Li-cor), Vaccinia R1 (1° antibody: rabbit anti-Vaccinia R1, 1:100, from Dr. Chris Mathews; 2° antibody: goat anti-rabbit IR-Dye 680, 1:20,000, Li-cor), and Vaccinia R2 (1° antibody: mouse anti-vaccinia R2 clone 4B3, 1:1000, Pro Sci; 2° antibody: goat anti-mouse IR-Dye 800CW, 1:20,000, Li-cor).

2.4 MICROINJECTIONS

2.4.1 Cell Culture

BSC40 cells were seeded onto sterile coverslips at a 1 in 12 split in 100mm dishes, and allowed to grow overnight in MEM. The next day, coverslips had a 50% confluent monolayer of cells. These coverslips were transferred to a new 100mm dish with MEM for injections.

2.4.2 Microinjection of Antibodies

10D11 anti-I3 and anti-His6 (isotype control) mouse monoclonal antibodies were adjusted to 5mg/ml, diluting with microinjection buffer. Samples were centrifuged at 14,000xg for 15 minutes to remove insolubles. Approximately 250 BSC40 cells per coverslip were microinjected using the Eppendorf FemtoJet system. Samples were done in duplicate. Following injections, coverslips were transferred to a 24 well plate and were infected with 0.5mL A5L-YFP Vaccinia virus (Katsafanas and Moss 2007) at an MOI of 5 for 6 hours. One hour post infection, 0.5mL MEM media was added to the coverslips. At 6 hours, virus was aspirated and cells were fixed with 4% paraformaldehyde on ice for 30 minutes, followed by 0.1M glycine for 20 minutes at room temperature. Coverslips were washed 3 times for 5 minutes with PBS-T and stored overnight at 4°C in 3% BSA. Cells were stained using Cy5 labelled goat anti mouse secondary antibody at a 1 in 2000 dilution in 3% BSA blocking solution for 1 hour at room temperature. Cells were counterstained using DAPI and rhodamine phalloidin for 15 minutes at room temperature. The coverslips were washed three times in PBS-T before mounting onto microscope slides using Mowoil. Slides were visualized

using a WaveFX (Olympus IX-81/Yokagawa CSUX1) spinning disc confocal microscope and the Volocity version 6.0.1 (PerkinElmer). The following filters were used for antibody injected cells: DAPI for DAPI, FITC for YFP, TRITC for rhodamine phalloidin, Cy5 for Cy5 labelled secondary antibody. Virus factory size was analyzed using Volocity version 6.0.1. ROI tools were used to draw around the factories and the computer algorithm calculated area. The factory areas were graphed and student t tests were performed to determine significant differences in mean factory area.

2.4.3 Microinjection of Peptides

N30mer (EEDLARNLGLVDIDDEYDESDKEKPIFNV), S30mer (DNSDLDKVYPRGELEVDAEDNDKIFEDL), c-Jun (Biotin-Acp-PQTVPEMPGE(pT)PPL(pS)PIDMESQERI) and JunB (Biotin-Acp-TVPEARSRDA(pT)PPV(pS)PINMEDQERI) peptides (N30mer and S30mer peptides were from the Institute for Biomolecular Design, University of Alberta, JunB and c-Jun peptides were a kind gift from Dr. Robert Ingham, University of Alberta) were adjusted to 5mg/ml, diluting with a 1mg/ml solution of Texas Red Dextran MW 70, 000, in a final volume of 10 μ l. Both the c-Jun and JunB peptides were biotinylated and contained two phosphorylated residues. Peptide samples were centrifuged for 15 minutes at 14,000xg to remove insoluble aggregates. Approximately 250 BSC40 cells per coverslip were microinjected using the Eppendorf FemtoJet system. Two coverslips were injected per sample. After injections, coverslips were transferred to a 24 well plate and were infected with A5L-YFP Vaccinia virus at an MOI of 5 in 0.5ml for 6 hours. At 1 hour post

infection, 0.5ml MEM media was added to the well of each coverslip. After 6 hours of infection, virus was aspirated and cells were fixed in a 4% paraformaldehyde solution on ice for 30 minutes, followed by 0.1M glycine for 20 minutes at room temperature. The coverslips were washed in PBS-T three times for 5 minutes and stored overnight at 4°C in 3% BSA. Cells were stained with DAPI and Alexa647 phalloidin for 15 minutes at room temperature. Coverslips were washed with PBS-T 3 times for 5 minutes before mounting onto microscope slides using Mowoil. Slides were visualized using a WaveFX (Olympus IX-81/Yokagawa CSUX1) spinning disc confocal microscope (PerkinElmer). The following filters were used for peptide injected cells: DAPI for DAPI, FITC for YFP, TRITC for Texas Red dextran, Cy5 for Alexa647 phalloidin. Virus factory size was analyzed using Volocity version 6.0.1 as described above.

CHAPTER 3: RESULTS

MULTIMERIC ORGANIZATION OF POXVIRUS SINGLE-STRANDED DNA-BINDING PROTEINS

3.1 INTRODUCTION

Oligosaccharide/oligonucleotide binding (OB) folds are used by different types of proteins to bind to ssDNA. The OB fold structure features a five stranded closed β barrel that is capped by an α helix between the third and fourth strands, commonly called a 'Greek key' formation (Murzin 1993). This common fold allows proteins with varying sequences to bind to ssDNA based on fold architecture and topology (Murzin 1993). Single stranded DNA binding (SSB) proteins use the OB fold to bind to ssDNA despite the divergence in amino acid sequence amongst these proteins (Suck 1997). As more SSB structures are being solved, there emerges differences in the oligomeric states used to bring different numbers of OB folds together (Suck 1997). Based on the number of OB folds brought together, one can divide the SSB proteins into four classes; monomeric (T4 bacteriophage GP32), dimeric (T7 bacteriophage GP2.5), heterotrimeric, (eukaryotic RPA), and homotetrameric, (*E. coli*) (Suck 1997).

There is little to no sequence conservation between SSBs from various organisms and Vaccinia I3 is no exception. Recently there has been a report searching for sequence homology between I3 and other proteins (Kazlauskas and Venclovas 2012). This report used various bioinformatics tools to search for homology between I3 and any other proteins present in the protein database. The authors found no homology between I3 and any OB fold containing SSB homolog

(Kazlauskas and Venclovas 2012). The authors did find some homology between the central region of I3 and small protein B (SmpB) from *Aquifex aeolicus* (Kazlauskas and Venclovas 2012). SmpB is a bacterial protein that binds to tmRNA; a hybrid RNA that acts as both transfer and messenger RNA (Karzai *et al.* 1999, Dong *et al.* 2002). However, the region of putative homology between I3 and SmpB spans sixty six amino acids, of which thirty three show a high degree of conservation (Kazlauskas and Venclovas 2012). Though far from definitive, this provides interesting information on the possible evolutionary history of I3.

The structure of I3 has not been solved, but recently there has been a paper published performing a structure/function analysis to gain insights into important residues in I3 (Greseth *et al.* 2012). This group used site directed mutagenesis to characterize charge-to-alanine mutant I3 proteins in self-interaction, ssDNA binding, and biological competence (Greseth *et al.* 2012). A yeast two-hybrid system has been used to previously show that I3 can self-interact (McCraith *et al.* 2000). Charge-to-alanine mutant I3 proteins were differentially tagged with either 3xFlag or His6 and tested for self-interaction. Three mutant proteins, #4 (K182A, R183A, E184A, R185A), 5 (K211A, K212A) and 7 (E231A, R232A), were unable to self-interact; the residues are hypothesized to form a common binding pocket due to their close proximity to each other (Greseth *et al.* 2012). Two of these three mutant I3 proteins, #4 and 7, retained their ssDNA binding function, indicating that the ability to bind to a 24-mer ssDNA does not require self-interaction (Greseth *et al.* 2012).

Wild type I3 and the charge-to-alanine mutant proteins were loaded through a gel filtration column to look further at the multimerization properties of I3. Wild type I3 eluted from the column in fractions that reflect monomer structures, as well as higher ordered structures that are at least tetrameric (Greseth *et al.* 2012). Mutant proteins #4 and 7 only eluted in fractions that correspond to monomers, they did not elute in the higher ordered fractions; an expected finding based on the lack of self-interaction (Greseth *et al.* 2012). Attempts to replace the wild type I3 sequence with the charge-to-alanine mutant sequences into the virus genomes were unsuccessful for both mutants #4 and 7 (Greseth *et al.* 2012). This suggests that the ability to form higher ordered structures likely plays a biological role in the virus infection. However, until the structure is solved, the nature of the higher ordered structures remains to be determined. The objectives of our experiments are to determine the crystal structure of SSBs from several different poxviruses, and to look more closely at the self-interaction and multimerization properties of Vaccinia I3.

3.2 RESULTS

3.2.1 Cloning and Purification of C-Terminal His6 Tagged Poxvirus Single Stranded DNA Binding Proteins.

SSBs from several distantly related chordopoxviruses were cloned into *E. coli* expression vectors and purified. Both full length VacI3₁₋₂₇₀ and an N and C terminal truncated VacI3₁₅₋₂₄₄ were obtained from lab freezer stocks. An N and C terminal truncated FPVO88₂₅₋₂₄₁ protein was cloned from the Fowlpox genome using PCR. DNA sequences of a full length MCVO46₁₋₂₈₈, an N and C terminal truncated MCVO46₂₀₋₂₂₇, and an N and C terminal truncated OrfO32₂₈₋₂₄₄ SSB were obtained from GeneArt. All proteins contained a C-terminal His6 tag, were expressed in DHE142 *E. coli* and purified using nickel and heparin affinity chromatography. Purified fractions were electrophoresed on Coomassie stained SDS PAGE gels. Based on these gels, it was determined that the purified proteins were >95% pure (Figure 3-1). MCVO46₁₋₂₈₈(H6) and FPVO88₂₅₋₂₄₁(H6) did not express very well in comparison with the other SSB proteins (Figure 3-1). These two proteins were grown as 100L fermenter cultures at the Agri-Food Discovery Place (University of Alberta) to try to improve yield, but the attempts were unsuccessful. VacI3₁₋₂₇₀(H6), VacI3₁₅₋₂₄₄(H6), MCVO46₃₀₋₂₂₇(H6) and OrfO32₂₈₋₂₄₄(H6) were expressed in high enough amounts to be used in subsequent experiments.

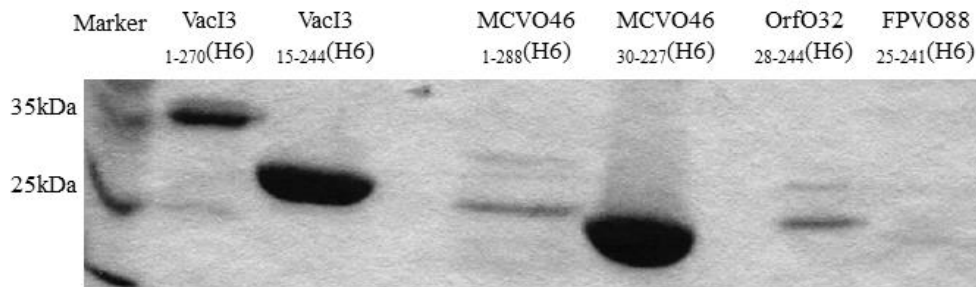


Figure 3-1: Purified C-terminal His6-tagged SSBs. Affinity purified proteins were run on a 10% SDS PAGE gel and visualized using Coomassie stain.

3.2.2 Crystallization of His6 Tagged Poxvirus SSBs.

Each SSB was screened against commercial Nextall crystallization screens either alone or bound to a 30-mer polyT oligonucleotide in a 1:1 molar ratio.

Crystals in the screen plates were grown using the sitting drop vapour diffusion method. VacI3₁₅₋₂₄₄(H6) produced crystals in nearly thirty of the conditions screened (Figure 3-2 A-D). The protein crystals grew in two different forms; hexagonal and rhombohedral (Table 4). The screening conditions that produced crystals were replicated in larger scale using the hanging-drop method. These conditions were also modified for slightly altered salt and pH to try to improve the crystals. Several of these conditions produced crystals of diffractable size, both with and without the 30-mer ssDNA (Figure 3-2 E-I). These crystals formed orthorhombic, rhombohedral and needle shaped crystals (Table 4). Of all the crystals tested, only one diffracted to a best resolution of only 10.5Å.

To try to improve the quality of the VacI3₁₅₋₂₄₄(H6) crystals for diffraction, several techniques were used. The first was a protease screen to use trace amounts of different proteases to remove any flexible portions of the protein that may be

interfering with crystal packing. Trace amounts of α -chymotrypsin, trypsin, elastase, papain, subtilisin and endoproteinase Glu-C were added to VacI3₁₅₋₂₄₄(H6) immediately before mixing with the crystallization conditions that produced the best crystals. Crystals formed of VacI3₁₅₋₂₄₄(H6) when exposed to 1:1000 α -chymotrypsin and to 1:10,000 papain (Figure 3-3). The crystals from this experiment grew as orthorhombic, rhombohedral and tetragonal crystals (Table 4). These crystals were also tested for diffraction but did not yield any results. The second method for improving crystal quality was to alter the ratio of ssDNA to protein. Initial experiments were performed by binding the SSB proteins in a 1:1 molar ratio with a 30-mer polyT oligonucleotide. In order to potentially stabilize the crystal structure, we grew VacI3₁₅₋₂₄₄(H6) crystals in a 1:1 molar ratio with a 100-mer polyT oligonucleotide (Figure 3-4 A). These crystals grew as hexagonal plates and were not large enough for diffraction testing. We also grew VacI3₁₅₋₂₄₄(H6) crystals with increasing molar ratios of 30-mer polyT oligonucleotide from 1:1 to 10:1 DNA:protein, in the large scale conditions that gave the best crystals. Crystals were observed in several of these conditions (Figure 3-4 B-D). Again, these crystals grew as hexagonal plates and were too small for diffraction testing.

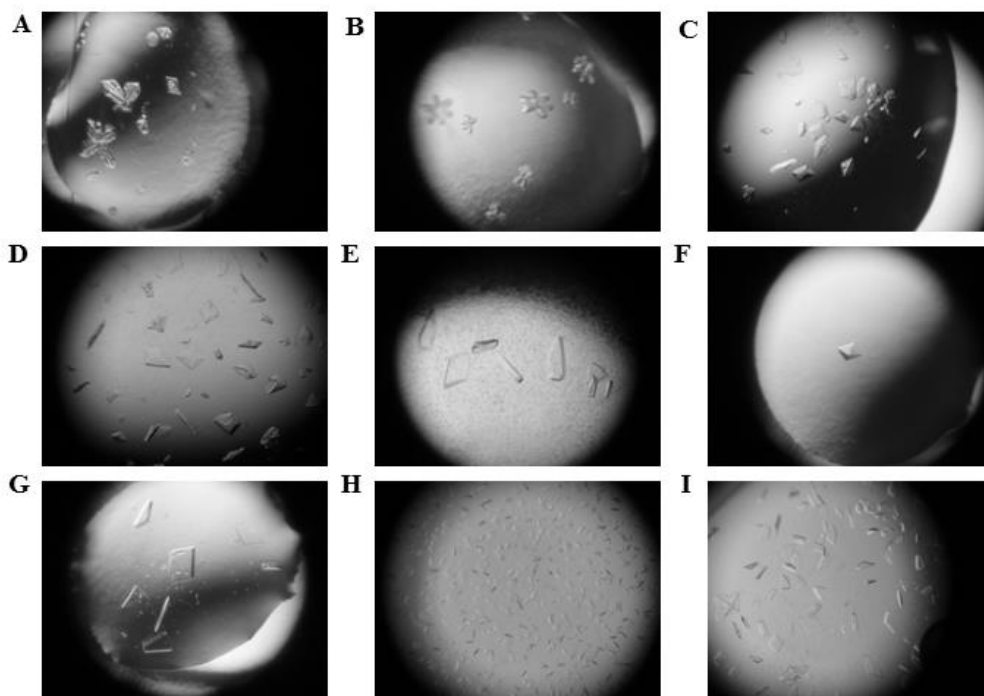


Figure 3-2: Crystals of VacI₃₁₅₋₂₄₄ (H6)
 SSB/ssDNA complexes were incubated for 20 minutes at 37°C.
 SSB protein was either crystallized by itself or in a 1:1 molar ratio
 with 30-mer poly T oligonucleotide, then mixed with an equal
 volume of crystallization solution. A-D) Crystals from condition
 screening plates grown using the sitting-drop method. A) Crystals
 of VacI₃₁₅₋₂₄₄(H6). B-D) Crystals of VacI₃₁₅₋₂₄₄(H6) with 30-mer poly
 T oligonucleotide. E-I) Crystals of VacI₃₁₅₋₂₄₄(H6) with 30-mer poly
 T oligonucleotide from large scale plates, grown using the hanging
 drop method.

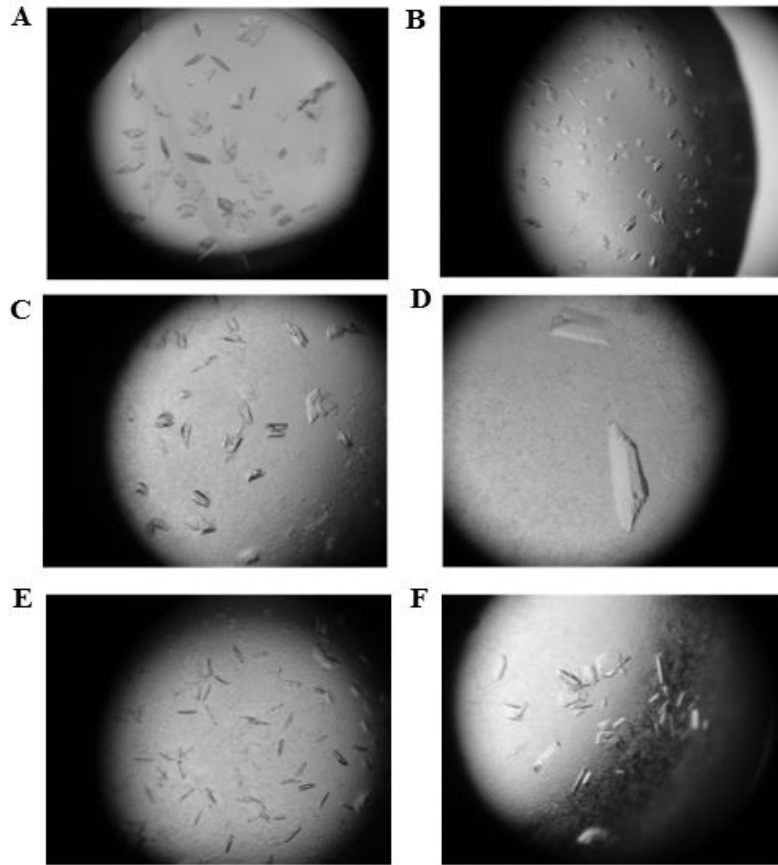


Figure 3-3: Crystals of VacI₃₁₅₋₂₄₄ (H6) optimized for ssDNA and protease cleavage. SSB/ssDNA complexes were incubated for 20 minutes at 37°C and subsequently mixed with protease. The protein solution was mixed with an equal volume of crystallization solution. Crystals were grown using the hanging-drop method. A) SSB/ssDNA complex incubated with 1:1000 α chymotrypsin. B-F) SSB/ssDNA complex mixed and incubated with 1:10,000 papain.

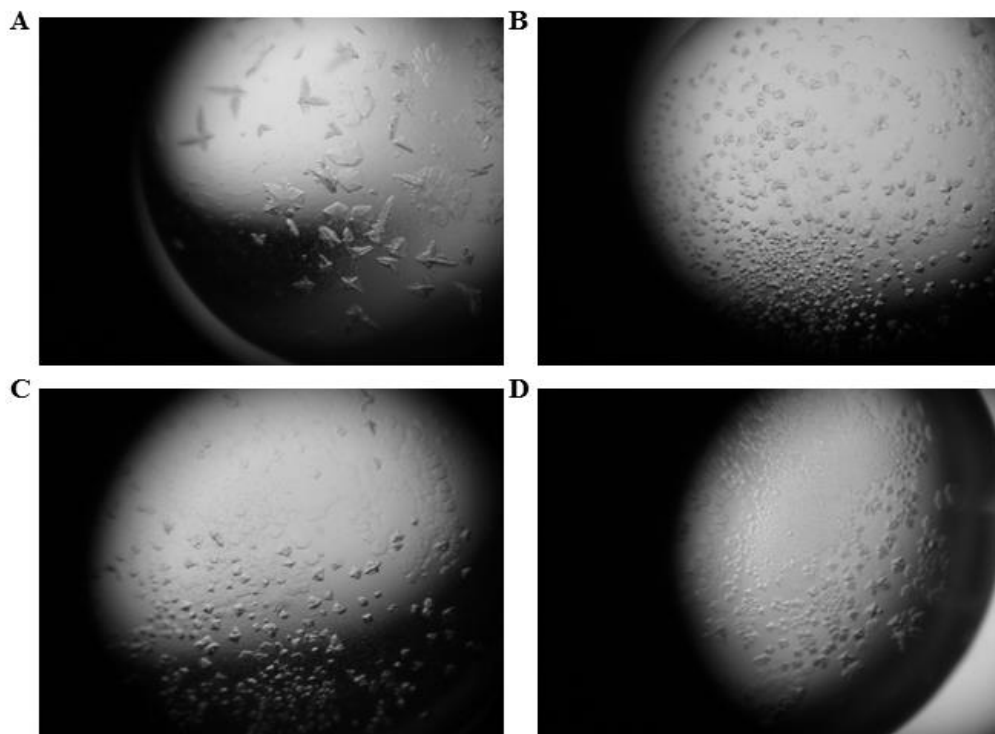


Figure 3-4: Crystals of VacI₁₅₋₂₄₄ (H6) with altered ssDNA.

VacI₁₅₋₂₄₄(H6) and ssDNA were incubated for 20 minutes at 37°C. A) VacI₁₅₋₂₄₄(H6) protein was mixed in a 1:1 molar ratio with a 100-mer poly T oligonucleotide. SSB/ssDNA complex was mixed with equal volumes of crystallization solution and crystals were grown using the hanging-drop method. B-D) VacI₁₅₋₂₄₄(H6) protein was mixed with 30-mer poly T oligonucleotide in a 9:1 ssDNA:SSB ratio. SSB/ssDNA complexes were mixed in equal volumes with crystallization solution; crystals were grown using the hanging drop method.

Table 4: Summary of VacI₁₅₋₂₄₄(H6) crystals

Figure	Crystallization Conditions	PolyT Oligonucleotide	Proteases Present	Crystal Morphology
3-2 A	0.2M sodium sulfate 0.1M Bis Tris Propane pH 7.5 20% PEG 3350	NA	NA	Hexagonal
3-2 B	0.2M sodium citrate 0.1M Bis Tris Propane pH 6.5 20% PEG 3350	1:1 Molar Ratio 30-mer	NA	Hexagonal
3-2 C	0.2M sodium citrate 0.1M Bis Tris Propane pH 7.5 20% PEG 3350	1:1 Molar Ratio 30-mer	NA	Rhombohedral
3-2 D	0.2M sodium citrate 0.1M Bis Tris Propane pH 8.5 20% PEG 3350	1:1 Molar Ratio 30-mer	NA	Rhombohedral
3-2 E	0.2M sodium citrate 0.1M Bis Tris Propane pH 8.5 20% PEG 3350	1:1 Molar Ratio 30-mer	NA	Orthorhombic
3-2 F	0.35M sodium chloride 0.1M Tricine pH 8 28% PEG 1000, 10% glycerol	1:1 Molar Ratio 30-mer	NA	Rhombohedral
3-2 G	0.2M potassium/ sodium tartrate 20% PEG 3350	1:1 Molar Ratio 30-mer	NA	Orthorhombic
3-2 H	0.2M sodium citrate 0.1M Bis Tris Propane pH 7.5 20% PEG 3350	1:1 Molar Ratio 30-mer	NA	Needles
3-2 I	0.15 sodium citrate 0.1M Bis Tris Propane pH 8.5 20% PEG 3350	1:1 Molar Ratio 30-mer	NA	Orthorhombic Triclinic
3-3 A	0.2M sodium citrate 0.1M Bis Tris Propane pH 6.5 20% PEG 3350	1:1 Molar Ratio 30-mer	1:1000 α chymotrypsin	Orthorhombic
3-3 B	0.2M sodium citrate 0.1M Bis Tris Propane pH 8.5 20% PEG 3350	NA	1:10,000 papain	Rhombohedral
3-3 C	0.2M sodium citrate 0.1M Bis Tris Propane pH 8.5 20% PEG 3350	NA	1:10,000 papain	Tetragonal
3-3 D	0.2M sodium citrate 0.1M Bis Tris Propane pH 7.5 20% PEG 3350	NA	1:10,000 papain	Rhombohedral
3-3 E	0.2M sodium citrate 0.1M Bis Tris Propane pH 7.5 20% PEG 3350	NA	1:10,000 papain	Needles
3-3 F	0.2M sodium citrate 0.1M Bis Tris Propane pH 8.5 20% PEG 3350	NA	1:10,000 papain	Orthorhombic
3-4 A	0.2M sodium citrate 0.1M Bis Tris Propane pH 8.5 20% PEG 3350	1:1 Molar Ratio 100-mer	NA	Hexagonal
3-4 B	0.2M sodium citrate 0.1M Bis Tris Propane pH 7.5 20% PEG 3350	9:1 Molar Ratio 30-mer	NA	Hexagonal
3-4 C	0.2M sodium citrate 0.1M Bis Tris Propane pH 8.5 20% PEG 3350	1:1 Molar Ratio 100-mer	NA	Hexagonal
3-4 D	0.2M sodium citrate 0.1M Bis Tris Propane pH 8.5 20% PEG 3350	1:1 Molar Ratio 100-mer	NA	Hexagonal

3.2.3 Crystallization of VacI3₁₋₂₇₀(H6) with Anti-I3 Fab Fragments

Western blot experiments have demonstrated that the anti-I3 10D11 antibody is able to detect the His tagged VacI3₁₋₂₇₀ protein. Fab fragments of the anti-I3 10D11 mouse monoclonal antibody were created using a commercial kit (Pierce). Full length VacI3₁₋₂₇₀(H6) tagged I3 was mixed in a 1:1 molar ratio with these Fab fragments and some of the sample was incubated with a 1:1 molar ratio with 30-mer polyT oligonucleotide. The protein mixture was screened against all crystallization conditions in the commercial screens, as well as against the conditions that produced the best VacI3₁₅₋₂₄₄(H6) crystals in the large scale plates. These experiments were performed to see if by stabilizing the flexible C terminus, the epitope for the anti-I3 antibody, the crystal structure would become stabilized and pack more efficiently. No crystals were observed in any of the conditions in any of the plates.

3.2.4 Crystallization of VacI3₁₅₋₂₄₄(H6) with C-Terminal Tail Peptides

Peptides corresponding to the native C terminus (N30mer) or a scrambled version (S30mer) were mixed with VacI3₁₅₋₂₄₄(H6) in a 1:1 molar ratio some of the sample was incubated with a 1:1 molar ratio with 30-mer polyT oligonucleotide. The samples were crystallized against the conditions that produced the best VacI3₁₅₋₂₄₄(H6) crystals. We did this experiment to see if we could stabilize the crystals by binding the C-terminal tail sequence to I3. Control drops of I3-ssDNA complexes with no peptides were able to produce crystals as previously reported. However, drops containing I3-ssDNA and peptides were no

longer able to produce crystals, indicating that the peptides poisoned the crystal growth.

3.2.5 Crystallization of Non-Oligomerizing Vaccinia I3 Mutants

Full length N terminal His6 tagged Vaccinia I3 proteins #4 and #7 were obtained as a kind gift from Dr. Paula Traktman. These proteins have been shown to be non-oligomerizing but still are capable of binding to ssDNA and contain the following charge to alanine mutations: #4: K182A, R183A, E184A, R185A; #7: E132A, R232A (Greseth *et al.* 2012). These proteins were screened against all commercial crystallization screens, both with and without 30-mer polyT oligonucleotide. Both proteins were also co-crystallized with VacI3₁₅₋₂₄₄(H6) in a 1:1 molar ratio in the conditions that gave the best VacI3₁₅₋₂₄₄(H6) crystals. None of the screening plates grew any crystals. Interestingly, none of the large scale conditions in the co-crystallization plate grew any crystals. These mutants appear to poison crystal formation.

3.2.6 Co-crystallization of VacI3₁₅₋₂₄₄(H6) with MCVO46₃₀₋₂₂₇(H6)

In order to attempt to grow crystals of the other poxvirus SSBs, VacI3₁₅₋₂₄₄(H6) and MCVO46₃₀₋₂₂₇(H6) were mixed in a 1:1 molar ratio, both with and without 30-mer polyT oligonucleotide, and were mixed with the crystallization conditions that produced the best crystals of VacI3₁₅₋₂₄₄(H6). Crystals were observed in several of the conditions (Figure 3-5 A-B). To determine if the crystals were only of VacI3₁₅₋₂₄₄(H6) or contained both proteins, crystals from several different drops were removed with a cryoloop, washed twice in crystallization solution and mixed with 4X SDS PAGE loading buffer. Crystals

were run on a 10% SDS PAGE gel and silver stained. Two bands were observed in the crystal lanes, one corresponding to VacI3₁₅₋₂₄₄(H6) and the other corresponding to MCVO46₃₀₋₂₂₇(H6) (Figure 3-5 C). These results suggested that VacI3₁₅₋₂₄₄(H6) can interact with MCVO46₃₀₋₂₂₇(H6).

3.2.7 Immunoprecipitations of VacI3₁₋₂₇₀(H6) to Complex Other Poxviral SSBs.

To test whether Vaccinia I3 could interact with the SSBs from other poxviruses, we performed immunoprecipitations using full length VacI3₁₋₂₇₀(H6) to determine if VacI3₁₋₂₇₀(H6) could form a complex with any of the other poxvirus SSBs. Western blots were performed using the anti-I3 10D11 mouse monoclonal antibody to check if the antibody would recognize the other poxviral SSBs. Anti- I3 10D11 did not detect any of the other SSBs, and therefore was sufficient for use in the immunoprecipitations (Figure 3-6 B,D, 3-7 B,D). Anti-I3 10D11 antibodies also did not detect VacI3₁₅₋₂₄₄(H6) so VacI3₁₋₂₇₀(H6) was used in these experiments (Figure 3-6 A-B). Equi-molar amounts of VacI3₁₋₂₇₀(H6) was mixed with each MCVO46₃₀₋₂₂₇(H6), MCVO46₁₋₂₈₈(H6), OrfO32₂₈₋₂₄₄(H6) and FPVO88₂₅₋₂₄₁(H6), and mixed with 153µg of anti-I3 antibody (final volume 1 mL) overnight at 4°C. The antibody and any attached proteins were pulled out with Protein G Sepharose beads. Proteins were mixed with 4X SDS PAGE loading buffer and run on 10% SDS PAGE gels and visualized with Coomassie Blue-Silver stain. We observed bands on the gels for the immunoprecipitations of MCVO46₃₀₋₂₂₇(H6), MCVO46₁₋₂₈₈(H6) and OrfO32₂₈₋₂₄₄(H6), corresponding to both VacI3₁₋₂₇₀(H6) and the other SSB (arrows, Figure 3-8 A-C). However, in the

immunoprecipitation for FPVO88₂₅₋₂₄₁(H6), the Fowlpox SSB was not complexed by VacI3₁₋₂₇₀(H6) (Figure 3-8 D). These results confirmed that Vaccinia I3 is able to interact with MCV and Orf SSBs but cannot interact with Fowlpox SSB.

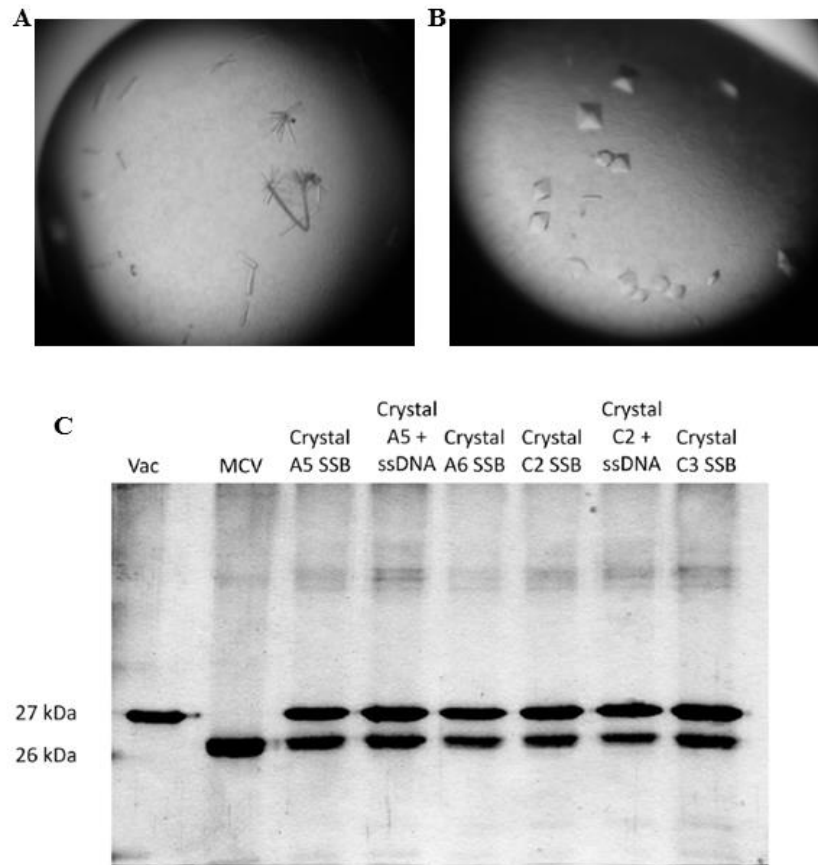


Figure 3-5: Co-crystallization of VacI3₁₅₋₂₄₄ (H6) with MCVO46₃₀₋₂₂₇ (H6).

A, B) VacI3₁₅₋₂₄₄(H6) protein was mixed in a 1:1:1 molar ratio with MCVO46₃₀₋₂₂₇(H6) and 30-mer poly T oligonucleotide and incubated for 20 minutes at 37°C. SSB/ssDNA complexes were mixed with equal volumes of crystallization solution; crystals were grown by the hanging-drop method. C) Silver stained SDS PAGE gel of co-crystals. Co-crystals were removed from the drop, washed with crystallization solution and boiled in 4X SDS PAGE loading buffer. Crystals were run on 10% SDS PAGE silver stained gel to check for the presence of both VacI3₁₅₋₂₄₄(H6) and MCVO46₃₀₋₂₂₇(H6) SSB proteins. A5, A6, C2, and C3 refer to the wells in which the crystals were removed.

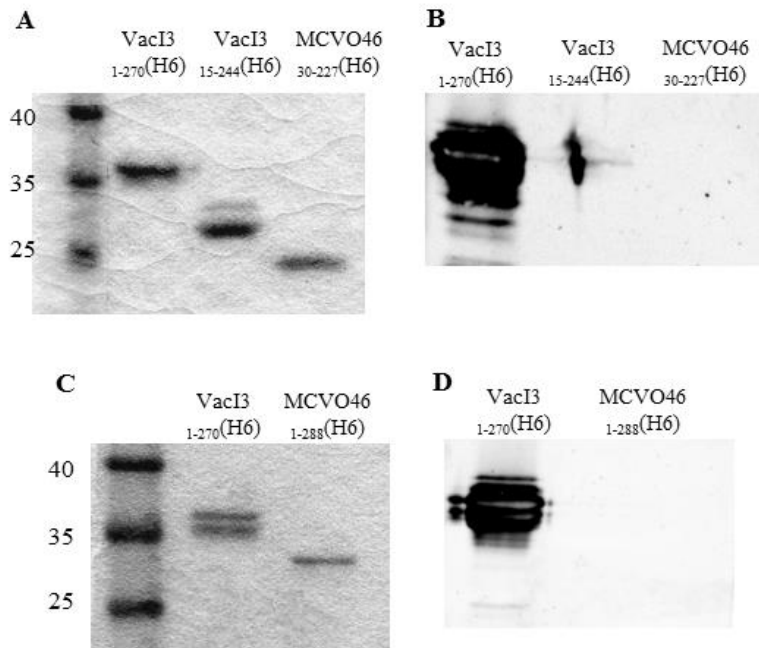


Figure 3-6: Anti-I3 10D11 antibody reactivity to Vaccinia and MCV SSBs.

Proteins were run on 10% SDS PAGE gels and visualized by Coomassie stain. Identical gels were used in Western blots to see if the poxviral SSB proteins could be detected by the anti-I3 10D11 antibody.

A) Coomassie stained gel showing VacI3₁₋₂₇₀(H6), VacI3₁₅₋₂₄₄(H6) and MCVO46₃₀₋₂₂₇(H6) proteins. B) Western blot using 10D11 anti-I3 antibody to detect SSBs. C) Coomassie gel showing VacI3₁₋₂₇₀(H6), and MCVO46₃₀₋₂₂₇(H6). D) Western blot using 10D11 anti-I3 antibody to detect the SSBs. The 10D11 anti-I3 antibody was only able to detect VacI3₁₋₂₇₀(H6), and not any of the other poxvirus SSBs.

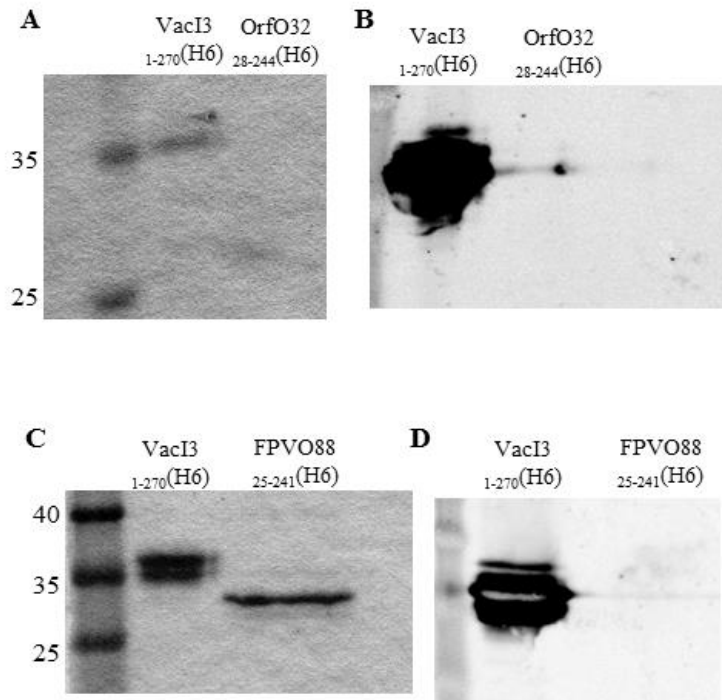


Figure 3-7: Anti-I3 10D11 antibody reactivity to Orf and Fowlpox SSBs.

Proteins were run on 10% SDS PAGE gels and visualized by Coomassie stain. Identical gels were used in Western blots to see if the poxviral SSB proteins could be detected by the 10D11 anti-I3 antibody.

A) Coomassie gel showing VacI3₁₋₂₇₀(H6) and OrfO32₂₈₋₂₄₄(H6) SSBs. B) Western blot using 10D11 anti-I3 antibody to detect SSBs. C) Coomassie gel showing VacI3₁₋₂₇₀(H6), and FPVO88₂₅₋₂₄₁(H6) SSB proteins. D) Western blot using anti-I3 antibody to detect SSB proteins. The 10D11 anti-I3 antibody was only able to detect VacI3₁₋₂₇₀(H6), and not any of the other poxvirus SSBs.

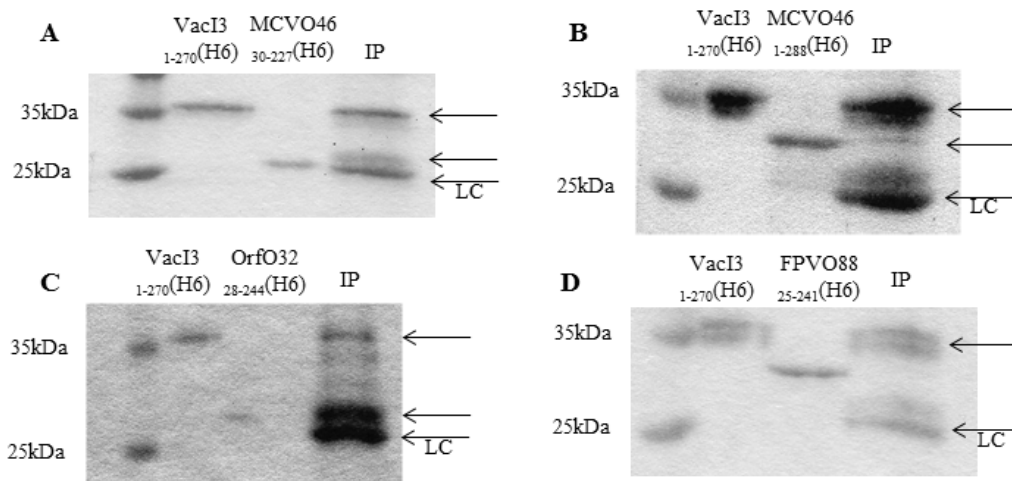


Figure 3-8: Immunoprecipitations using I3₁₋₂₇₀(H6) to complex other poxviral SSBs.

Equal moles of each SSB protein were mixed together in an 800 μ L reaction to which 153 μ g anti-I3 10D11 monoclonal antibody was added. Proteins were mixed overnight at 4°C. Antibodies were pulled down using Protein G Sepharose beads. Proteins were run on 10% SDS PAGE gels and visualized with Coomassie stain. Arrows indicate the presence of either I3₁₋₂₇₀(H6) and/or the other poxvirus SSB protein pulled down in the immunoprecipitation (IP lane). A) VacI3₁₋₂₇₀(H6) can complex with MCVO46₃₀₋₂₂₇(H6). B) VacI3₁₋₂₇₀(H6) can complex with MCVO46₁₋₂₈₈(H6). C) VacI3₁₋₂₇₀(H6) can complex with OrfO32₂₈₋₂₄₄(H6). D) VacI3₁₋₂₇₀(H6) cannot form a complex with FPVO88₂₅₋₂₄₁(H6).

LC=Light Chain

3.2.8 Multi Angle Laser Light Scattering to Determine the Complex Formed by VacI3₁₋₂₇₀ and VacI3₁₋₂₄₄ Untagged Proteins

In order to determine the complex that the Vaccinia I3 protein forms, and if the removal of the C terminal tail could alter the oligomeric state of the complex, purified untagged VacI3₁₋₂₇₀ and VacI3₁₋₂₄₄ were fractionated on a Superose 6 column in line with a Wyatt Systems REX and DAWN MALLS to detect light scattering by the protein complex. The data was analyzed with the ASTRA software and a bovine serum albumin standard was used to calibrate for the molecular weight predictions. Protein was collected, concentrated and bound to 30-mer polyT oligonucleotide in a 1:1 molar ratio before reloading through the Superose 6 column. In the sample containing protein alone, VacI3₁₋₂₇₀ produced a single peak at a molecular weight of 38kDa \pm 2kDa and VacI3₁₋₂₄₄ produced a single peak at a molecular weight of 31kDa \pm 7kDa (Figures 3-9, 3-10). When bound to the 30-mer polyT oligonucleotide, VacI3₁₋₂₇₀ produced two peaks; the first corresponding to a molecular weight of 135kDa \pm 5kDa and the second at a molecular weight of 61kDa \pm 5kDa (Figure 3-9). When bound to the 30-mer polyT oligonucleotide, VacI3₁₋₂₄₄ produced a single peak corresponding to a molecular weight of 118kDa \pm 2kDa (Figure 3-9).

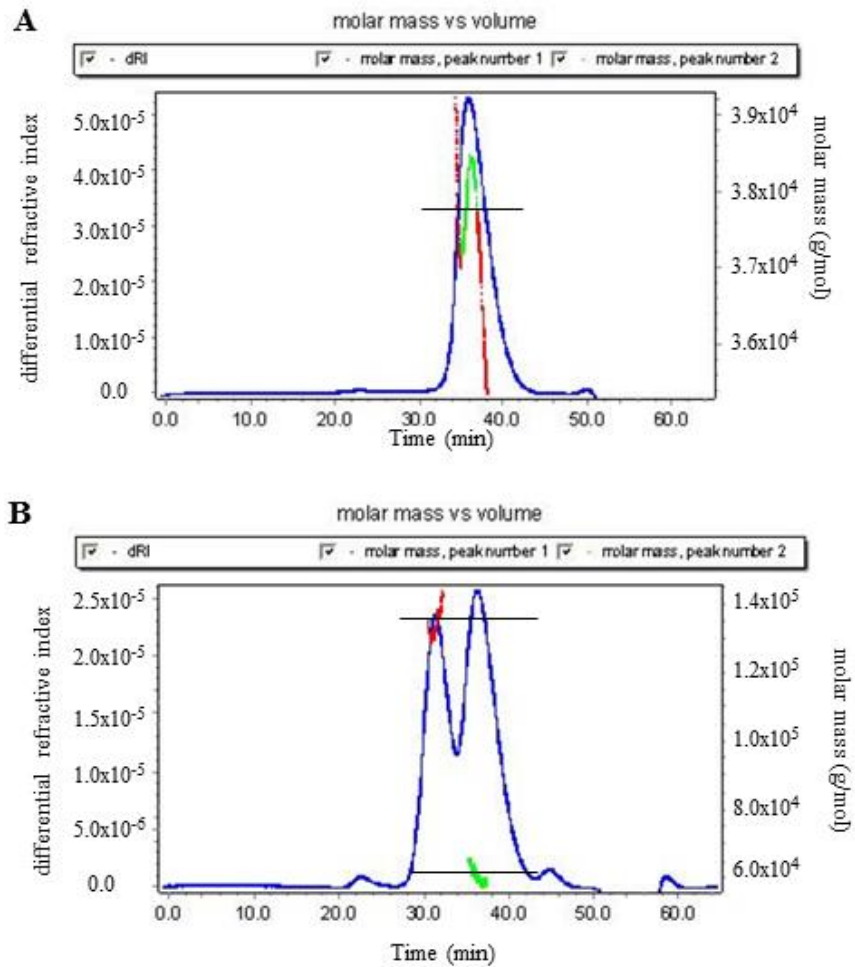


Figure 3-9: Multi angle laser light scattering of VacI3₁₋₂₇₀. Purified proteins were loaded through a Superose 6 column. Protein was detected by refractive index with a Wyatt Systems REX and a DAWN MALLS. Data was analyzed with ASTRA software. A) VacI3₁₋₂₇₀ protein shows a single peak at 38 ± 2 kDa. B) VacI3₁₋₂₇₀ plus 30-mer shows two peaks at 135 ± 5 kDa and 61 ± 5 kDa. Horizontal bars indicate approximation of molecular weight.

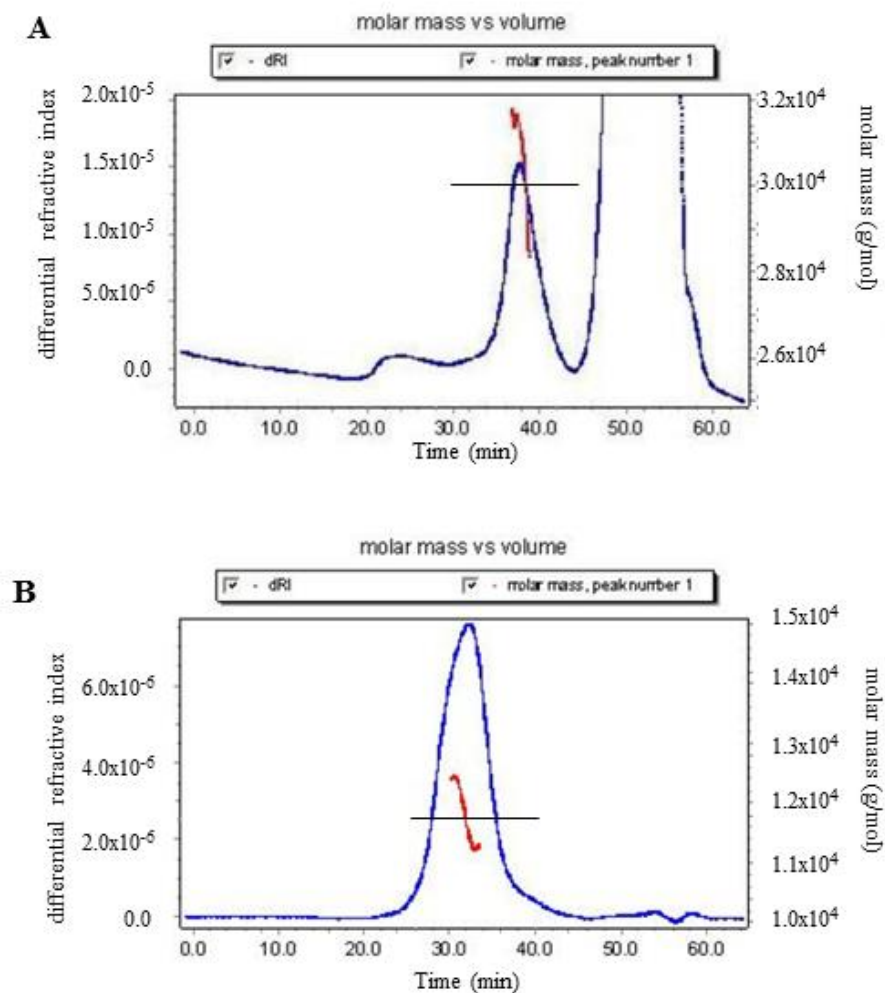


Figure 3-10: Multi angle laser light scattering of VacI3₁₋₂₄₄. Purified proteins were loaded through a Superose 6 column. Protein was detected by refractive index with a Wyatt Systems REX and a DAWN MALLS. Data was analyzed with ASTRA software. A) VacI3₁₋₂₄₄ showing a peak at 31 ± 7 kDa. B) VacI3₁₋₂₄₄ plus 30-mer showing a single peak at 118 ± 2 kDa. Horizontal bars indicate approximation of molecular weight.

3.3 DISCUSSION

The structures of many of the single stranded DNA binding proteins (SSB) have been solved. Despite little sequence similarity between these proteins, most SSBs bind to ssDNA through a common oligosaccharide/oligonucleotide binding (OB) fold (Murzin 1993). Although the SSBs use a common fold for DNA binding, they form different quaternary structures. T4 GP32 forms a monomer in solution and along the ssDNA (Alberts and Frey 1970) while the SSB protein from the related T7 bacteriophage, GP2.5 forms a dimer in solution (Kim *et al.* 1992a, Hollis *et al.* 2001). SSBs from bacteria can form several different structures along the ssDNA. The most widely studied of the SSBs is the SSB from *E. coli*. This protein forms a tetramer and can adopt two different binding modes depending on protein and salt concentration (Krauss *et al.* 1981, Lohman and Overman 1985). A variation on this structure is seen in the SSBs from the *Deinococcus* and *Thermus* genera. These SSBs form dimers and each dimer contains two OB folds, a total of four OB folds are brought together in the final structure (Eggington *et al.* 2004).

The sequences of the SSBs from poxviruses are very divergent from the other SSBs. However, there is structural homology between the SSBs, so it is tempting to hypothesize that the poxvirus SSBs use OB folds to bind to ssDNA. In order to try to determine the structure, the SSBs from several different poxviruses were cloned and expressed in *E. coli*. These proteins contained a C terminal His6 tag and were from several divergent poxviruses: full length Vac13₁₋₂₇₀(H6) and MCVO46₁₋₂₈₈(H6), and N and C terminally truncated versions of the

SSBs, VacI3₁₅₋₂₄₄(H6), MCVO46₃₀₋₂₂₇(H6), OrfO32₂₈₋₂₄₄(H6) and FPVO88₂₅₋₂₄₁(H6). The poxviral SSBs were truncated at both the N and C terminus for ease in crystallization studies. The N terminus was truncated based on the sequence from crocodilepox. Crocodilepox has a large deletion at the N terminus, so we inferred that the N terminus is not essential for function, and have deleted this region from the proteins. The C terminus of SSB proteins is flexible and based on a conservation of function and the characteristic pattern of negatively charged amino acids, the C terminus of the poxvirus SSBs is predicted to also be a flexible region. Since flexible regions impede crystallization, this region was also removed from our constructs (Dong *et al.* 2007). We chose to crystallize the SSB proteins from divergent poxviruses to see how the structures of the SSB are conserved across the poxviral genera and in the hope that at least one might crystallize.

After purification, the Vaccinia, MCV and Orf proteins were expressed in high enough concentrations that they could be used in crystallization trials. The proteins were crystallized both with and without a 30-mer polyT oligonucleotide, as the structure solved with ssDNA would be more informative in how the SSB binds ssDNA, and also to see if it favoured the formation of crystals. These proteins were screened against several commercial screens and VacI3₁₅₋₂₄₄(H6) produced crystals in several of the conditions (Figure 3-2). These were regrown in a larger scale and tested for x-ray diffraction. One of the crystals diffracted to best diffraction of 10.5Å, unfortunately still not enough resolution to solve the structure. To improve the quality of the crystals, we tried several different

methods. The first was *in situ* proteolysis with trace amounts of several different proteases (Figure 3-3). Crystals of VacI3₁₅₋₂₄₄(H6) were successfully grown in the presence of trace amounts of α -chymotrypsin and papain, but these crystals did not diffract when tested. The second method to improve crystal quality was to stabilize the crystal with longer pieces of ssDNA and with an increased amount of ssDNA per protein monomer (Figure 3-4). Large crystals of the VacI3₁₅₋₂₄₄(H6) protein with a 100-mer polyT oligonucleotide and with a 30-mer polyT oligonucleotide in ratios from 1:1 to 10:1 were grown. These crystals also did not diffract. The VacI3₁₅₋₂₄₄(H6) SSB was easy to crystallize but did not produce diffraction quality crystals. The crystals grew quickly and this may have produced a disordered internal structure, which does not produce good diffraction patterns upon x ray exposure. The solved crystal structure of the poxvirus SSBs will be useful for understanding how this protein binds to ssDNA, either with or without an OB fold, and if and how different monomers come together to bind the ssDNA.

We were given two full length mutant Vaccinia I3 proteins as a kind gift from Dr. Paula Traktman. These proteins, Vaccinia I3 #4 and Vaccinia I3 #7, have charge to alanine mutations that prevent them from oligomerizing, but these proteins retained the ability to bind to ssDNA (Greseth *et al.* 2012). Both of these mutants were used in the crystallization screens alone and were mixed in a 1:1 molar ratio with VacI3₁₅₋₂₄₄(H6) in the conditions that produced the best VacI3₁₅₋₂₄₄(H6) crystals. These mutants did not produce crystals on their own in any of the screening conditions, and they also prevented the formation of the VacI3₁₅₋₂₄₄(H6) crystals that normally would have formed. Proteins within crystals form a lattice

and this lattice requires protein-protein interactions. By creating mutants that can no longer form these protein-protein interactions, the formation of the lattice may be impeded and crystals do not form.

We were unable to grow crystals of any of the other poxvirus SSBs, and in an attempt to do so, mixed MCVO46₃₀₋₂₂₇(H6) with VacI3₁₅₋₂₄₄(H6) in the conditions that gave the best VacI3₁₅₋₂₄₄(H6) crystals. In several of the conditions we were able to grow crystals both with and without ssDNA (Figure 3-5 A-B). To determine the composition of the crystals, proteins were run on SDS PAGE gels and silver stained. Both VacI3₁₅₋₂₄₄(H6) and MCVO46₃₀₋₂₂₇(H6) proteins were observed to be in all the crystals tested (Figure 3-5 C). This suggested that Vaccinia I3 can interact with the MCV SSB and form hybrid crystals.

To test for interactions between SSBs from different poxviruses, we did a series of immunoprecipitations using VacI3₁₋₂₇₀(H6) to pull down the SSBs from the other poxviruses. We used the VacI3₁₋₂₇₀(H6) protein because the anti-I3 antibody did not recognize the truncated VacI3₁₅₋₂₄₄(H6) protein (Figure 3-6 A-B). We confirmed that we could use the 10D11 anti-I3 antibody for the immunoprecipitation experiments by performing a series of Western blots to ensure that the anti-I3 antibody did not cross react with the SSBs from the other poxviruses (Figure 3-6, 3-7). The immunoprecipitations showed that VacI3₁₋₂₇₀(H6) can able to complex with the SSBs from MCV and from Orf but not from Fowlpox (Figure 3-8). However, we did not pull down equi-molar amounts of each SSB, most likely because Vaccinia I3 would have a higher affinity for Vaccinia I3 over the SSBs from the other poxviruses, due to the sequence

divergence between the poxvirus SSBs. This confirmed the result obtained in the co-crystallization experiments, which showed that the SSBs from different species of poxviruses retain enough sequence similarity to form chimeric complexes. This also reflects the phylogeny of the different poxviruses. MCV and Orf are more closely related to Vaccinia virus, while Fowlpox is the most distantly related of the poxviruses used in these experiments (Figure 1-7). We were able to pull down a larger amount of the full length MCV₁₋₂₈₈(H6) protein, suggesting that the C terminus is important for this interaction. These data also show that the ability to oligomerize is sequence dependent. In order to definitively test this hypothesis further, reciprocal immunoprecipitations should be performed. We could not do this in the experiments described above because all of the proteins have the same C-terminal His6 tag and the Vaccinia SSB antibody is I3 specific.

Together, the co-crystallization, the crystallization of Vaccinia I3 #4 and Vaccinia I3 #7, and the immunoprecipitations indicate that self-interaction is an important property of I3. Previous electron microscopy experiments have suggested that Vaccinia I3 can form an octameric complex along the ssDNA (Tseng *et al.* 1999). This is far from definitive as the bead counting in electron micrographs can be subjective. In order to determine what oligomeric complex Vaccinia I3 forms, we used multi-angle laser light scattering on untagged VacI3₁₋₂₇₀ and VacI3₁₋₂₄₄ alone, and each protein bound to a 30-mer polyT oligonucleotide. When ssDNA was not present, VacI3₁₋₂₇₀ eluted as a single peak corresponding to a molecular weight of 38 ± 2 kDa (Figure 3-9). The predicted molecular weight of Vaccinia I3 based on amino acid sequence is 30kDa. This

molecular weight determination, coupled with the large hydrodynamic radius of the eluted protein, suggests that VacI3₁₋₂₇₀ exists as a monomer and dimer in rapid exchange; the potential VacI3₁₋₂₇₀ complexes are found in Table 5. When the 30-mer polyT oligonucleotide was added (9kDa), two peaks were observed, corresponding to molecular weights of 135 ± 5 kDa and 61 ± 5 kDa (Figure 3-9). The data from this plot suggest that the peak at 135kDa is most likely a tetramer bound to one molecule of 30-mer ssDNA and the peak at 61kDa most likely reflects a dimer bound to one molecule of 30-mer ssDNA. These estimations are based on the molecular weights of potential VacI3₁₋₂₇₀:30-mer polyT complexes (Table 5). Recently, it has been shown that Vaccinia I3 adopts a tetrameric structure in solution (Greseth *et al.* 2012). These researchers used gel filtration analysis on purified His6 recombinant proteins to determine the multimerization properties of I3. They observed elution profiles consistent with a monomer, as well as a higher ordered structure that was at least a tetramer (Greseth *et al.* 2012). These observations are consistent with what was observed in the above experiments for VacI3₁₋₂₇₀, where peaks corresponding to a monomer, dimer and tetramer were all observed. However, it should be noted that the higher order structures were only found with the presence of ssDNA in the above experiments and without ssDNA in the literature (Greseth *et al.* 2012). However, it is feasible that the structures found in this report are due to DNA contamination. If there was ssDNA contamination then only tetramers would be detected and the dimers could potentially be missed.

The data from VacI3₁₋₂₄₄ without ssDNA shows a single peak at a molecular weight of 31±7kDa; most likely this protein exists as a monomer in solution (Figure 3-10) (Table 6). When bound to 30-mer polyT oligonucleotide, VacI3₁₋₂₄₄ elutes as a single peak at 118±2kDa (Figure 3-10). This structure is most likely a tetramer bound to a single 30-mer ssDNA; an estimation based on molecular weights of the potential VacI3₁₋₂₄₄:30-mer polyT complexes (Table 6). The removal of the C terminus appears to stabilize the monomer form of I3 when not bound to ssDNA. In the presence of ssDNA, the C-terminal tail interferes with the formation of multimeric complexes and we observe both the dimer and tetramer. The removal of the C-terminal tail prevents this from occurring and stabilizes the tetramer. However, the MALLS experiments are an approximation of the molecular weight of the complexes and have an error ranging from 2-7kDa (Figures 3-9, 3-10). A more definitive determination of the multimeric state of Vaccinia I3 will come from the crystal structure.

These data suggest a model for ssDNA binding. Previous research has shown that the minimum binding site for DNA in I3 spans ~10 nucleotides (Rochester and Traktman 1998, Tseng *et al.* 1999). Therefore, the 30-mer polyT used in these experiments is long enough to potentially bind to at least two I3 monomers. We used the 30-mer polyT in our experiments based on previous data showing that the saturation point for I3 is ~30 nucleotides (Tseng *et al.* 1999). We suggest that the C-terminal tail could bind into the ssDNA binding cleft of another monomer and then recruit more I3 protein to the ssDNA (Figure 3-11). If the ssDNA was still exposed, then the recruited I3 molecule could bind to the ssDNA

since I3 most likely has a higher affinity for ssDNA than its C terminal tail. This model of self-recruitment allows for the rapid and cooperative coating of the SSB along the ssDNA. This model also allows for the formation of higher ordered structures that have been found in these and other experiments, since the C-terminal tail could bind to the ssDNA- binding cleft of other monomers (Tseng *et al.* 1999, Greseth *et al.* 2012).

Table 5: Molecular weight (kDa) predictions of potential VacI3₁₋₂₇₀:30-mer polyT complexes.

		VacI3 ₁₋₂₇₀			
		1	2	3	4
30-mer PolyT	0	30	60	90	120
	1	39	69	99	129
	2	48	78	108	138
	3	57	87	117	147
	4	66	96	126	
	5	75	105	135	
	6	84	114	144	
	7	93	123		
	8	102	132		
	9	111	141		
	10	120			
	11	129			

Table 6: Molecular weight (kDa) predictions of potential VacI3₁₋₂₄₄:30-mer polyT complexes

		VacI3 ₁₋₂₄₄			
		1	2	3	4
30-mer PolyT	0	27	54	81	108
	1	36	63	90	117
	2	45	72	99	126
	3	54	81	108	135
	4	63	90	117	
	5	72	99	126	
	6	81	108		
	7	90	117		
	8	99	126		
	9	108			
	10	117			
	11	126			

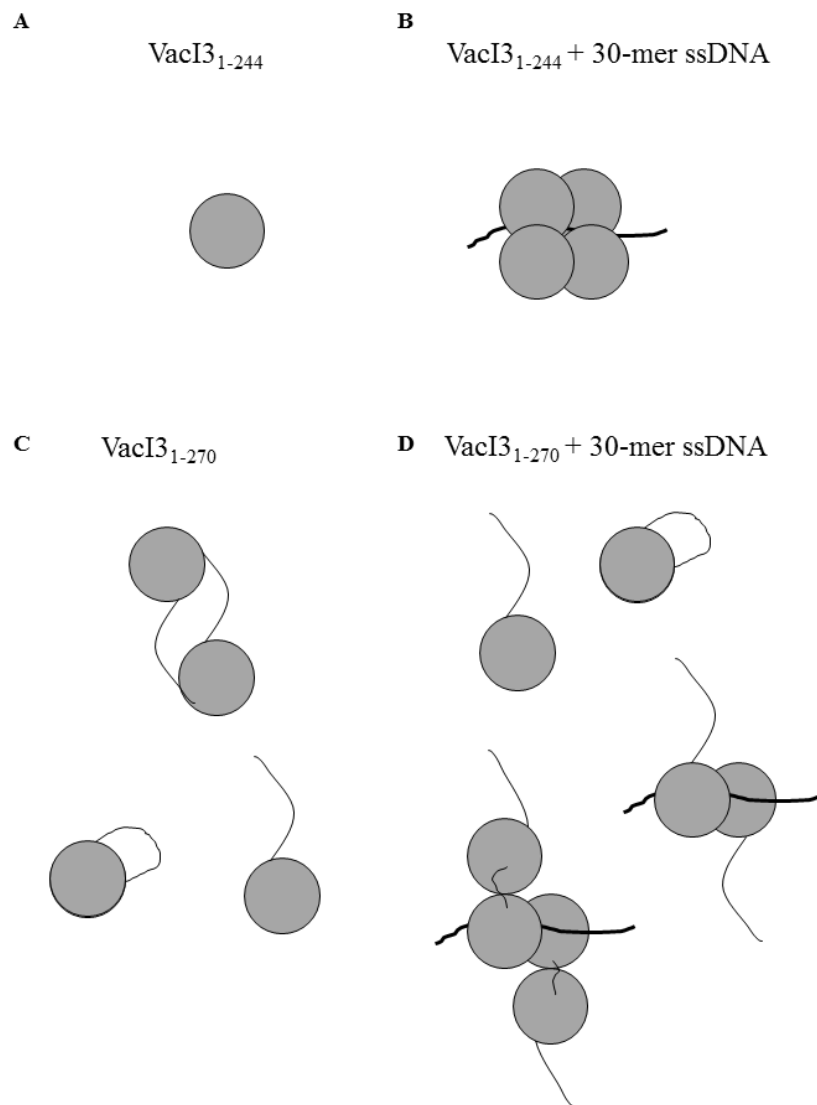


Figure 3-11: Model of ssDNA:I3 complexes.

A) C-terminal truncated VacI3_{1-244} forms a monomer in solution when ssDNA is not present. B) When ssDNA (thick black line) is present, VacI3_{1-244} forms a stable tetramer. C) In the absence of ssDNA, full length VacI3_{1-270} forms a monomer in rapid exchange with a dimer. The C-terminal tail can bind into the ssDNA binding pocket of I3. D) When a 30-mer polyT is present, the ssDNA displaces the C-terminal tail. The tail is now available to bind to a second I3 monomer, creating higher ordered structures.

CHAPTER 4: RESULTS

ROLE OF THE N and C TERMINI IN SSDNA BINDING

4.1 INTRODUCTION

Mutational studies on GP32 from T4 bacteriophage were performed to determine its role in DNA replication and recombination. These studies determined that GP32 interacts with the T4 DNA polymerase, DNA ligase and several recombination nucleases (Breschkin and Mosig 1977a, 1977b). Though these experiments did not determine how GP32 was interacting with the polymerase and the ligase, they did show that mutations that altered the C terminus prevented GP32 from interacting with recombination nucleases and that the mutant proteins were able to protect the ssDNA from degradation by these nucleases (Breschkin and Mosig 1977a, 1977b). Experiments using a C terminal truncated GP32 protein showed that by removing the sixty C terminal amino acids, the resulting protein was a stronger helix destabilizer (Hosoda and Moise 1978, Williams et al. 1981). However, this truncated protein lost the ability to interact with the T4 DNA polymerase (Moise and Hosoda 1976). Removal of these C terminal sixty amino acids also inhibited interactions with other proteins involved in DNA replication (Burke *et al.* 1980).

Studies on GP2.5 from bacteriophage T7 also demonstrated this feature. Mutational analyses using a C terminal truncated protein missing the C terminal twenty six amino acids, showed that the C terminus was essential for interactions

with the T7 DNA polymerase, and thioredoxin (Kim *et al.* 1992a, Kim and Richardson 1994, He *et al.* 2003, Hyland *et al.* 2003, Hamdan *et al.* 2005).

The C terminus of SSBs, being essential for protein-protein interactions, has also been extensively studied and described for the *E. coli* SSB (Reviewed in Lohman and Ferrari 1994, Shereda *et al.* 2008). The ability of the C-terminal domain to bind to several different proteins involved in the processes of DNA replication, recombination and repair bring all these different proteins to the ssDNA so they can perform their cellular functions.

One feature common to all the SSBs is that although there is very little sequence similarity, there is a high level of conservation of negative charges in the C terminus. Examples are found in the bacteriophage; the C terminal half of GP32 from T4 carries a net negative charge of -17 and of the last twenty one amino acids in T7 GP2.5, fifteen are acidic (Williams *et al.* 1981, Kim and Richardson 1994). These negative charges exist in a flexible region of the protein, as the C terminus is not present in the crystal structures, and are exposed on the surface, therefore available to make interactions with other proteins (Hosoda and Moise 1978). The presence of negative charges within a flexible region of the protein also raises the question if the C terminus may have an effect on the ssDNA binding ability of the SSB. This hypothesis has most thoroughly been explored with GP2.5 form T7 bacteriophage.

Mutagenesis experiments using C terminal truncated GP2.5 proteins, have demonstrated that not only do the truncated proteins lose their ability to bind to the T7 bacteriophage DNA polymerase, but there is an increase in affinity for

ssDNA (Rezende *et al.* 2002, He *et al.* 2003, Hyland *et al.* 2003, Shokri *et al.* 2006, Marintcheva *et al.* 2006). This increase in affinity led to the hypothesis that the negative charges present in the C-terminal tail could mimic the ssDNA and potentially bind in the SSBs' ssDNA binding pocket (Shokri *et al.* 2006). These suggestions had previously been hinted at in experiments with GP32 from T4 bacteriophage. Researchers had raised twelve hybridomas against GP32 and found that for all of the antibodies, the epitope was the C terminal tail, and that for at least six of the twelve, the antibodies could cross react with DNA (Krassa *et al.* 1991). This was supported by earlier experiments on GP2.5 that showed that the C terminally truncated proteins could no longer dimerize (Rezende *et al.* 2002, He *et al.* 2003). It was proposed that because the C terminus was flexible and was on the outside of GP2.5, that the C terminus stabilized the dimer through a domain swapping interaction to the ssDNA binding surface of the other monomer in the dimer (Hollis *et al.* 2001). This hypothesis was recently confirmed by NMR and crosslinking studies that demonstrated that the C terminus of GP2.5 bound to the same region of the SSB as ssDNA (Marintcheva *et al.* 2008).

While they have little sequence conservation with the other SSBs, the poxvirus SSB proteins do conserve the pattern of negatively charged amino acids within the C terminus. Of the last thirty amino acids in Vaccinia I3, thirteen are negatively charged. From this, we hypothesize that the C terminus of I3 might mimic ssDNA and compete with ssDNA for binding to the SSB. The objectives of the following experiments were to examine the role of the C-terminal tail in ssDNA binding.

4.2 RESULTS

4.2.1 Electrophoretic Mobility Shift Assays of His6 Tagged SSBs.

To test whether the truncated poxviral SSBs were still able to bind to ssDNA, each His6 tagged SSB was subjected to an electrophoretic mobility shift assay. 1-100µg of VacI3₁₋₂₇₀(H6), VacI3₁₅₋₂₄₄(H6), OrfO32₂₈₋₂₄₄(H6) and MCVO46₃₀₋₂₂₇(H6) were bound to 1µg of single stranded M13mp19 DNA for 20 minutes at 37°C. MCVO46₁₋₂₈₈(H6) was only expressed in low amounts so this experiment used 1-6µg of protein. The protein-ssDNA complexes were then fractionated on a 0.8% agarose gel run with imidazole running buffer. We used imidazole in the gel and running buffer to ensure that the His6 tag on the proteins did not affect how the proteins migrated in the gel. Gels were then stained with Sybr Safe (Invitrogen) and visualized with ultraviolet light. At high protein levels, all of the SSB proteins were able to shift the ssDNA within the gel (Figure 4-1, 4-2, 4-3). At equivalent amounts of protein, VacI3₁₅₋₂₄₄(H6) had reduced the mobility of the ssDNA within the gel more than VacI3₁₋₂₇₀(H6) (Figure 4-1 A-B). MCVO46₁₋₂₈₈(H6) produced a very small shift of the ssDNA within the gel but this was most likely due to the small amount of protein used in the experiment because this protein did not express very well (Figure 4-2 B). However, the other proteins shifted the ssDNA within the gel to a similar degree as MCVO46₁₋₂₈₈(H6) at comparable amounts of protein. MCVO46₃₀₋₂₂₇(H6) produced the greatest shift of the ssDNA within the gel, significantly retarding the mobility of the ssDNA right to the wells of the gel (Figure 4-2 A). MCVO46₃₀₋₂₂₇(H6) required the least amount of all the proteins to produce this shift. OrfO32₂₈₋₂₄₄(H6)

shifted the ssDNA to a similar level as VacI3₁₋₂₇₀(H6) at comparable amounts of protein (Figure 4-3). This was less of a reduction in mobility than what was seen with similar amounts of VacI3₁₅₋₂₄₄(H6) and MCVO46₃₀₋₂₂₇(H6).

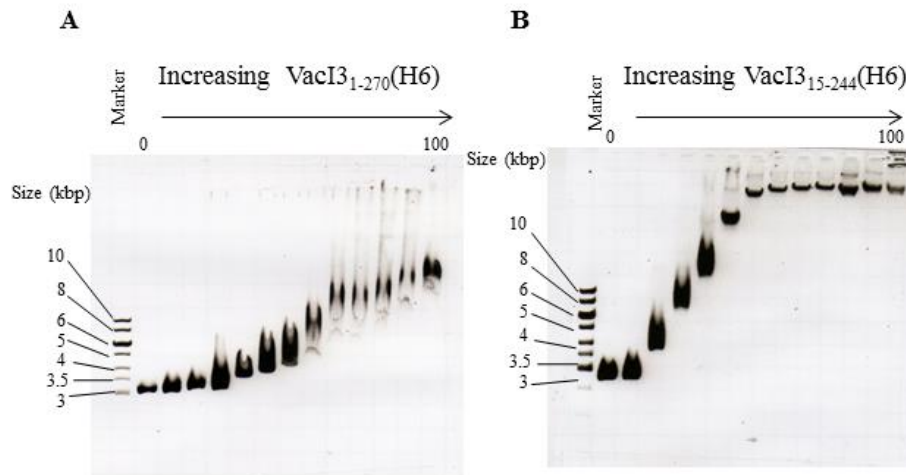


Figure 4-1: Electrophoretic mobility shift assay for VacI3₁₋₂₇₀(H6) and VacI3₁₅₋₂₄₄(H6).

Reactions contained 1 μg single stranded M13mp19 and increasing amounts of SSB protein from 1-100 μg. DNA-protein complexes were bound for 20 minutes at 37°C, then fractionated by electrophoresis through a 0.8% agarose gel run with imidazole running buffer, stained with Sybr Safe and visualized using ultraviolet light. A) VacI3₁₋₂₇₀(H6). B) VacI3₁₅₋₂₄₄(H6).

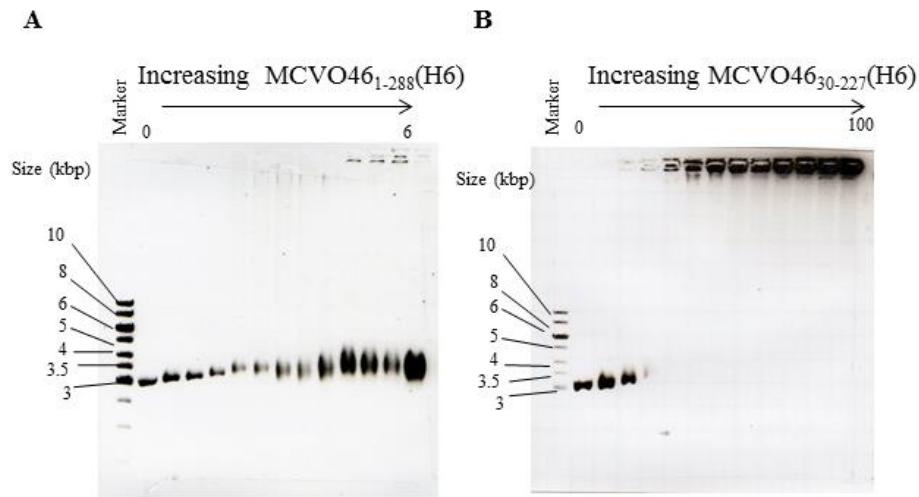


Figure 4-2: Electrophoretic mobility shift assay for MCVO46₁₋₂₈₈(H6) and MCVO46₃₀₋₂₂₇(H6).
 A) Reactions contained 1 μg single stranded M13mp19 and an increasing amount of MCVO46₁₋₂₈₈(H6) from 0.5-6 μg. B) Reactions contained 1 μg single stranded M13mp19 and an increasing amount of MCVO46₃₀₋₂₂₇(H6) protein from 1-100 μg. DNA-protein complexes were bound for 20 minutes at 37°C, then fractionated by electrophoresis through a 0.8% agarose gel run with imidazole running buffer, stained with Sybr Safe and visualized using ultraviolet light. A) MCVO46₁₋₂₈₈(H6) SSB. B) MCVO46₃₀₋₂₂₇(H6) SSB.

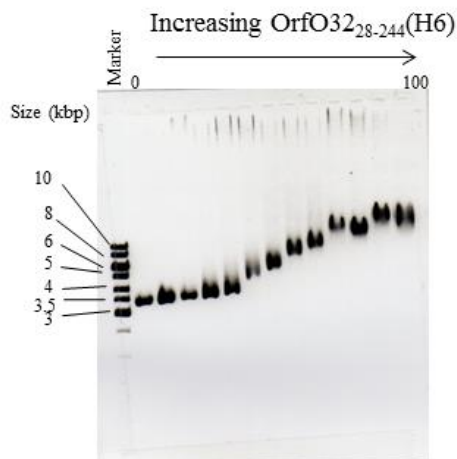


Figure 4-3: Electrophoretic mobility shift assay for OrfO32₂₈₋₂₄₄(H6).

Reactions contained 1 μ g single stranded M13mp19 and an increasing amount of protein from 1-100 μ g. DNA-protein complexes were bound for 20 minutes at 37°C, then fractionated by electrophoresis through a 0.8% agarose gel run with imidazole running buffer, stained with Sybr Safe and visualized using ultraviolet light.

4.2.2 ssDNA Affinity Measured for His6 Tagged Poxviral SSBs.

To test the ssDNA binding affinity of the different poxvirus SSBs, we used an ssDNA cellulose binding assay. 20nmol of each SSB protein were bound to 500 μ L of 50% single stranded calf thymus DNA cellulose (Sigma) slurry. Proteins were bound to the ssDNA cellulose for 1 hour at room temperature and eluted with Buffer A (Tris, EDTA, β -mercaptoethanol, glycerol) with varying concentrations of NaCl ranging from 300mM-3M in steps of 300mM. The eluted fractions were separated by denaturing PAGE gels, and stained with Blue Silver Coomassie dye. Gels were photographed using a GelDoc (BioRad) system and the intensity of the bands relative to unbound protein was measured using ImageLab software (BioRad). The percent protein eluted was calculated based on the band

intensities and graphed against NaCl concentration (Figure 4-4). EC₅₀ values, or the concentration of NaCl where 50% of the SSB was eluted from the cellulose, are indicated on the graphs as solid and dotted lines (Figure 4-4). VacI3₁₋₂₇₀(H6) exhibited a lower EC₅₀ value of 0.55M NaCl (R²=0.99) than VacI3₁₅₋₂₄₄(H6) at 0.64M NaCl (R²=0.99) (Figure 4-4 A). This same pattern was observed for the SSBs from MCV, where full length MCVO46₁₋₂₈₈(H6) protein had a lower EC₅₀ value (0.14M NaCl, R²=0.99) than the truncated MCVO46₃₀₋₂₂₇(H6) protein (1.3M, R²=0.97) (Figure 4-4 B). For both the Vaccinia and MCV SSB proteins, the N and C-terminal truncated proteins had a higher affinity for ssDNA than the full length proteins. A summary of the EC₅₀ values for the proteins tested is found in Table 7.

Table 7: EC₅₀ values from ssDNA elution of His6 tagged SSBs

Protein	Mutations	EC ₅₀ from ssDNA Cellulose Column (M NaCl)
VacI3 ₁₋₂₇₀ (H6)	-----	0.55
VacI3 ₁₅₋₂₄₄ (H6)	N and C Terminal Truncation	0.64
MCVO46 ₁₋₂₈₈ (H6)	-----	0.14
MCVO46 ₃₀₋₂₂₇ (H6)	N and C Terminal Truncation	1.3

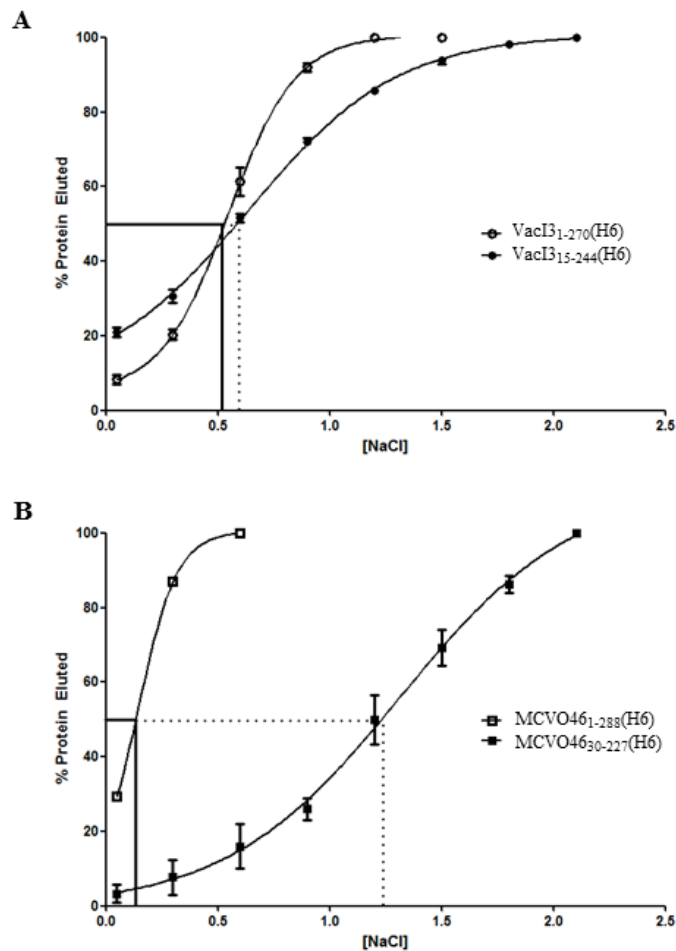


Figure 4-4: ssDNA cellulose elution curves for His6 tagged poxvirus SSBs.

20 nmol of each SSB was bound to single stranded calf thymus DNA cellulose and eluted with buffer containing an increasing concentration of NaCl. Fractions were run on 10% SDS PAGE blue silver stained gels. Protein bands were quantitated and percent protein eluted was calculated. EC_{50} values are marked. A) VacI3₁₋₂₇₀(H6), EC_{50} value of 0.55M NaCl (solid line), $R^2=0.99$. VacI3₁₅₋₂₄₄(H6), EC_{50} value of 0.64M NaCl (dotted line), $R^2=0.99$. B) MCVO46₁₋₂₈₈(H6), EC_{50} value of 0.14M NaCl (solid line), $R^2=0.99$. MCVO46₃₀₋₂₂₇(H6), EC_{50} value of 1.3M NaCl (dotted line), $R^2=0.97$.

4.2.3 Cloning and Purification of Untagged Poxvirus SSBs.

Electrophoretic mobility shift assays and the ssDNA cellulose experiments with the His6 tagged proteins suggested that the truncated poxvirus SSBs were better able to bind ssDNA than the full length proteins. However, we were concerned that the His6 tag might be affecting these studies. To test this we created untagged Vaccinia and MCV proteins that were only truncated at the C terminus, VacI3₁₋₂₄₄ and MCVO46₁₋₂₆₅. We created untagged proteins to ensure that the effects that we were seeing were not influenced by the properties of the amino acids in the tags. We also created three full length Vaccinia mutant proteins, using site-directed mutagenesis, which had point mutations in some of the negative charges in the C terminal tail. 3 Neutral Charges contains mutations at E241A, D251A, and E264A. 6 Neutral Charges contains mutations at E240A, E241A, D251A, E255A, D260A, and E264A. 3 Positive Charges contains mutations at E241K, D251K, and E264K. All of these proteins were cloned into DHE 142 *E. coli* for expression and were purified using heparin and ssDNA cellulose columns. The purified proteins were run on 10% SDS PAGE Coomassie stained gels to determine purity (Figure 4-5). The charge mutant I3 proteins contained amounts of C-terminal truncated I3, indicating that mutations to the C terminus destabilized the C terminus, resulting in the removal of this region (Figure 4-5).

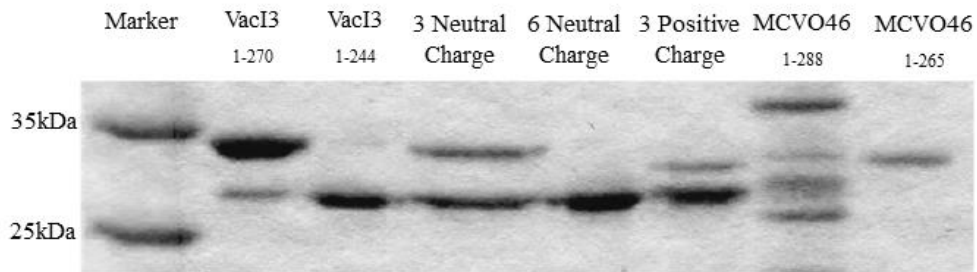


Figure 4-5: Purified untagged poxvirus SSBs. Affinity purified proteins were fractionated on a 10% SDS PAGE gel and visualized using Coomassie stain.

4.2.4 Electrophoretic Mobility Shift Assays for Untagged Vaccinia and MCV SSBs.

To measure ssDNA affinity, all of the untagged proteins were subjected to electrophoretic mobility shift assays as described above. Briefly, 1-100 μ g of each SSB was bound to 1 μ g of ϕ X 174 ssDNA for 20 minutes at 37 $^{\circ}$ C. The protein-ssDNA complexes were separated on 0.8% agarose gels, stained with Sybr Safe (Invitrogen) and visualized with ultraviolet light. We observed that the full length proteins were able to retard the mobility of the ssDNA better than the C terminal truncated proteins (Figure 4-6, 4-7). The VacI3₁₋₂₇₀ protein showed a laddering of the ssDNA within the gel (Figure 4-6 A), while the VacI3₁₋₂₄₄ protein at equivalent protein amounts barely shifted the ssDNA at all (Figure 4-6 B). This was again observed with the MCV proteins; MCVO46₁₋₂₈₈ produced a laddering of the ssDNA in the gel and MCVO46₁₋₂₆₅ at equivalent protein amounts barely shifted the ssDNA (Figure 4-7). These experiments were also repeated with the full length Vaccinia charge mutants. Three Neutral Charge mutant produced a

laddering shift of the ssDNA similar to VacI3₁₋₂₇₀, at equivalent protein amounts (Figure 4-8 A). Both 6 Neutral Charge and 3 Positive Charge mutants did not shift the ssDNA in the gel as much as I3₁₋₂₇₀, but they did shift the ssDNA in the gel more than VacI3₁₋₂₄₄ at equivalent amounts of protein (Figure 4-8 B-C).

4.2.5 ssDNA Affinity Measured for Untagged Poxvirus SSBs.

To test if the negatively charged C terminal tail affected ssDNA binding affinity, we repeated the ssDNA cellulose binding experiment described above with the untagged proteins. 20nmol of each VacI3₁₋₂₇₀, VacI3₁₋₂₄₄, MCVO46₁₋₂₈₈, MCVO46₁₋₂₆₅ and the three Vaccinia charge mutants were bound to 500 μ L of a 50% slurry of single stranded calf thymus DNA cellulose for 1 hour at room temperature. Proteins were eluted with Buffer A (Tris, EDTA, β -mercaptoethanol, glycerol) with increasing concentrations of NaCl (300mM-3M in 300mM increments). The eluted fractions were separated by denaturing PAGE, and stained with Blue Silver Coomassie dye. The gels were photographed using a GelDoc (BioRad) system and the band intensity relative to unbound protein was measured using ImageLab software (BioRad). Percent protein eluted was calculated from the band intensities and graphed against NaCl concentration. EC₅₀ values, or the concentration of NaCl where 50% of the SSB protein was eluted from the cellulose, are indicated on the graphs as solid, dashed and dotted lines (Figure 4-9, 4-10, 4-11). Of the Vaccinia proteins, the EC₅₀ value for VacI3₁₋₂₇₀ was the lowest at 0.44M NaCl ($R^2=1.0$) (Figure 4-9). The EC₅₀ value for VacI3₁₋₂₄₄ was higher at 0.71M NaCl ($R^2=1.0$) (Figure 4-9). The EC₅₀ values for the three Vaccinia C terminal tail charge mutants were higher than both VacI3₁₋₂₇₀ and

VacI3₁₋₂₄₄, and ranged from 0.68M-0.84M NaCl (Figure 4-10). The SSBs from MCV exhibited a similar pattern of EC₅₀ values as the Vaccinia proteins. MCVO46₁₋₂₈₈ had an EC₅₀ value of 0.21M NaCl (R²=1.0), while MCVO46₁₋₂₆₅ had a much higher EC₅₀ value of 0.79M NaCl (R²=1.0) (Figure 4-11). These data suggest that deleting the C-terminal tail enhances the affinity of SSB for ssDNA. A summary of the EC₅₀ values for the untagged proteins is found in Table 8.

Table 8: EC₅₀ values from ssDNA elution of untagged SSBs

Protein	Mutations	EC ₅₀ from ssDNA Cellulose Column (M NaCl)
VacI3 ₁₋₂₇₀	-----	0.44
VacI3 ₁₋₂₄₄	C Terminal Truncation	0.71
MCVO46 ₁₋₂₈₈	-----	0.21
MCVO46 ₁₋₂₆₅	C Terminal Truncation	0.79
6 Neutral Charge	E240A, E241A, D251A, E255A, D260A, E264A	0.84
3 Neutral Charge	E241A, D251A, E264A	0.75
3 Positive Charge	E241K, D251K, E264K	0.68

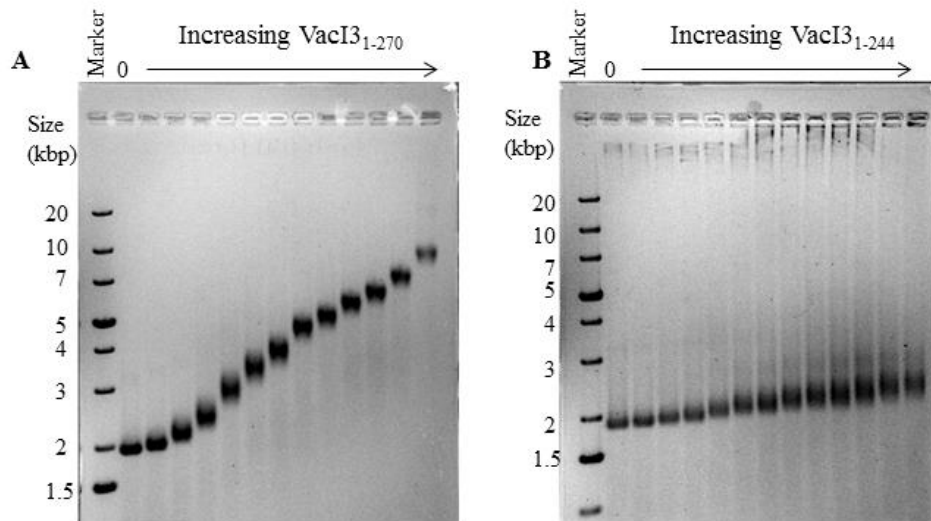


Figure 4-6: Electrophoretic mobility shift assay for VacI3₁₋₂₇₀ and VacI3₁₋₂₄₄.

Reactions contained 1 μg single stranded ΦX 174 and an increasing amount of SSB from 1-100 μg. DNA-protein complexes were bound for 20 minutes at 37°C, fractionated by electrophoresis through a 0.8% agarose gel, stained with Sybr Safe and visualized using ultraviolet light. A) VacI3₁₋₂₇₀. B) VacI3₁₋₂₄₄.

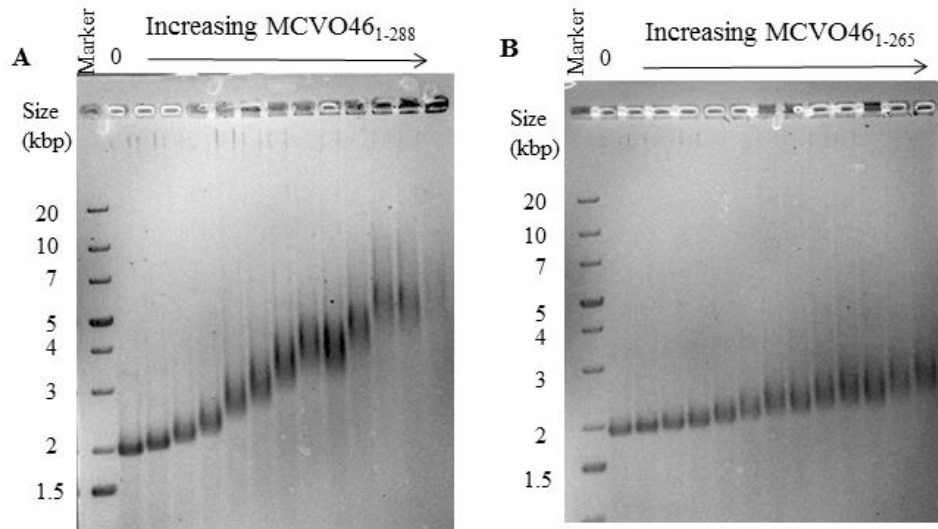


Figure 4-7: Electrophoretic mobility shift assay for MCVO46₁₋₂₈₈ and MCVO46₁₋₂₆₅.

Reactions contained 1 μ g single stranded Φ X 174 and an increasing amount of SSB from 1-100 μ g. DNA-protein complexes were bound for 20 minutes at 37°C, fractionated by electrophoresis through a 0.8% agarose gel, stained with Sybr Safe and visualized using ultraviolet light. A) MCVO46₁₋₂₈₈. B) MCVO46₁₋₂₆₅.

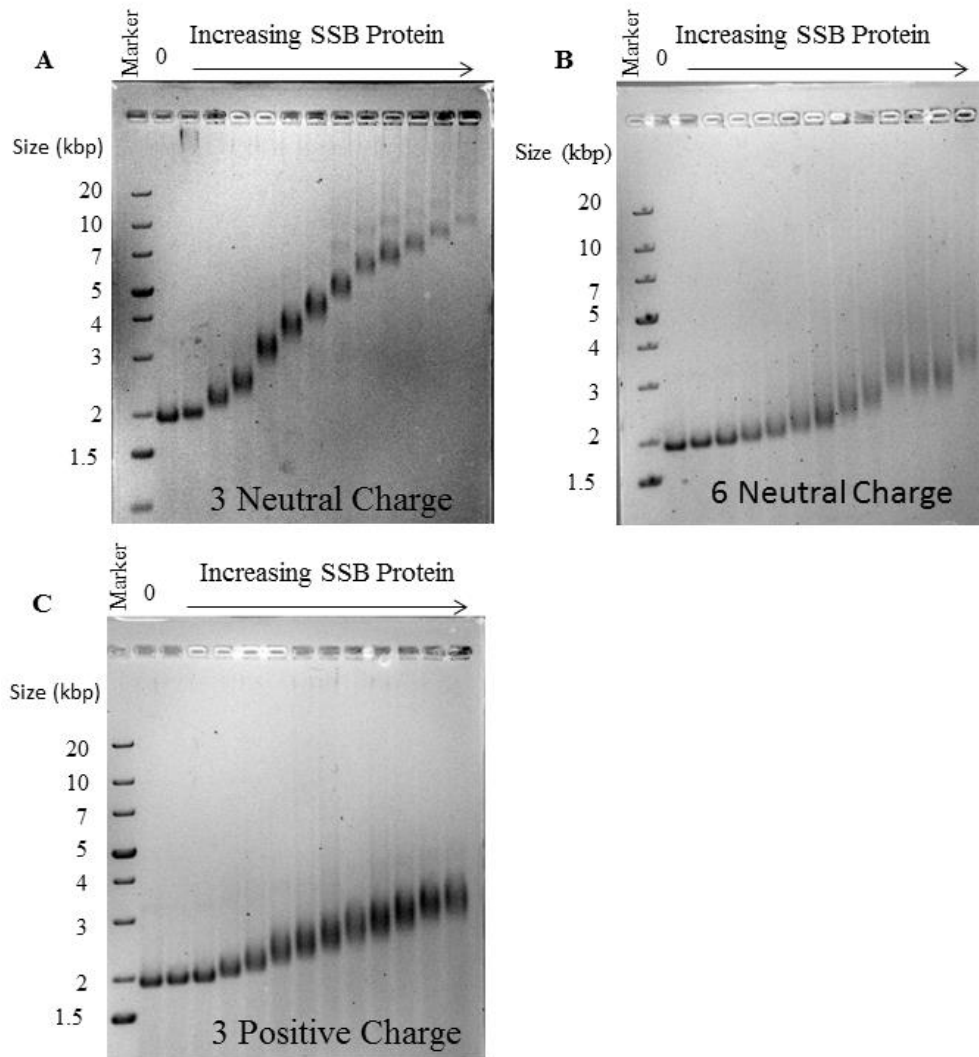


Figure 4-8: Electrophoretic mobility shift assay of I3 charge mutant proteins.

Reactions contained 1 μg single stranded ΦX 174 and an increasing amount of SSB from 1-100 μg . DNA-protein complexes were bound for 20 minutes at 37°C, fractionated by electrophoresis through a 0.8% agarose gel, stained with Sybr Safe and visualized using ultraviolet light. A) 3 Neutral Charge Mutant. B) 6 Neutral Charge Mutant. C) 3 Positive Charge Mutant.

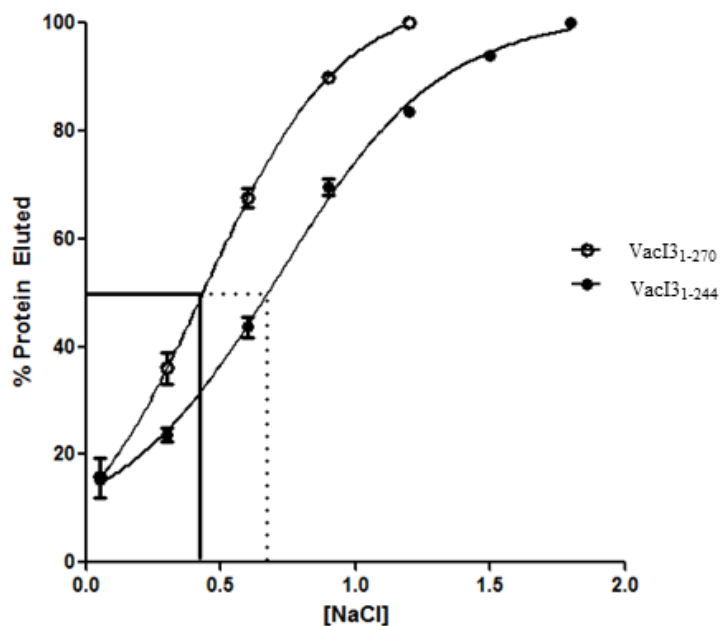


Figure 4-9: ssDNA cellulose elution curves for VacI3₁₋₂₇₀ and VacI3₁₋₂₄₄.

20nmol of each SSB was bound to single stranded calf thymus DNA cellulose and eluted with buffers containing an increasing concentration of NaCl. Fractions were run on 10% SDS PAGE blue silver stained gels. Protein bands were quantitated and percent protein eluted was calculated. EC₅₀ values are marked.

VacI3₁₋₂₇₀, EC₅₀ value of 0.44M NaCl (solid line), R² =1.0.

VacI3₁₋₂₄₄, EC₅₀ value of 0.71M NaCl (dotted line), R² =1.0.

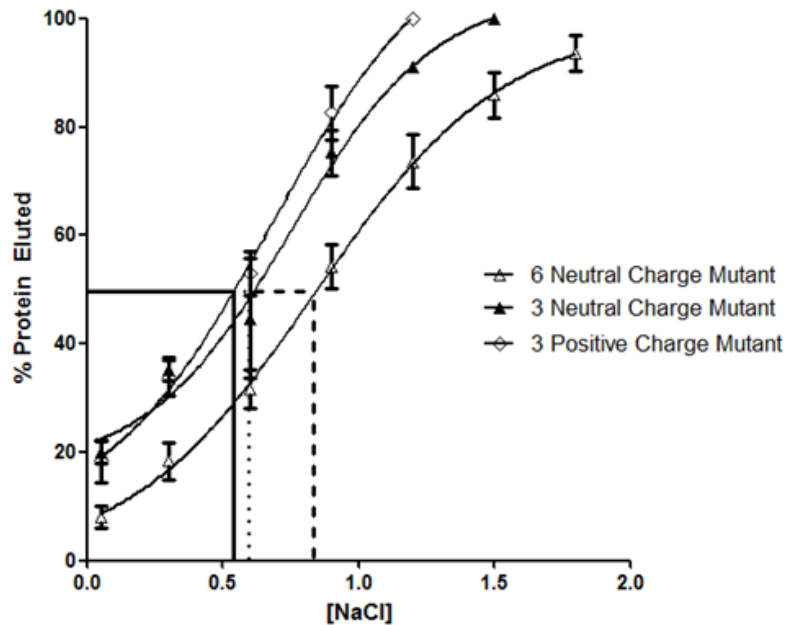


Figure 4-10: ssDNA cellulose elution curves for I3 charge mutant proteins.

20nmol of each SSB was bound to single stranded calf thymus DNA cellulose and eluted with buffers containing an increasing concentration of NaCl. Fractions were run on 10% SDS PAGE blue silver stained gels. Protein bands were quantitated and percent protein eluted was calculated. EC₅₀ values are marked. 6 Neutral Charge Mutant, EC₅₀ value of 0.84M NaCl (dashed line), R²=0.97. 3 Neutral Charge Mutant, EC₅₀ value of 0.75M NaCl (dotted line), R²=0.94. 3 Positive Charge Mutant, EC₅₀ value of 0.68M NaCl (solid line), R²=0.97.

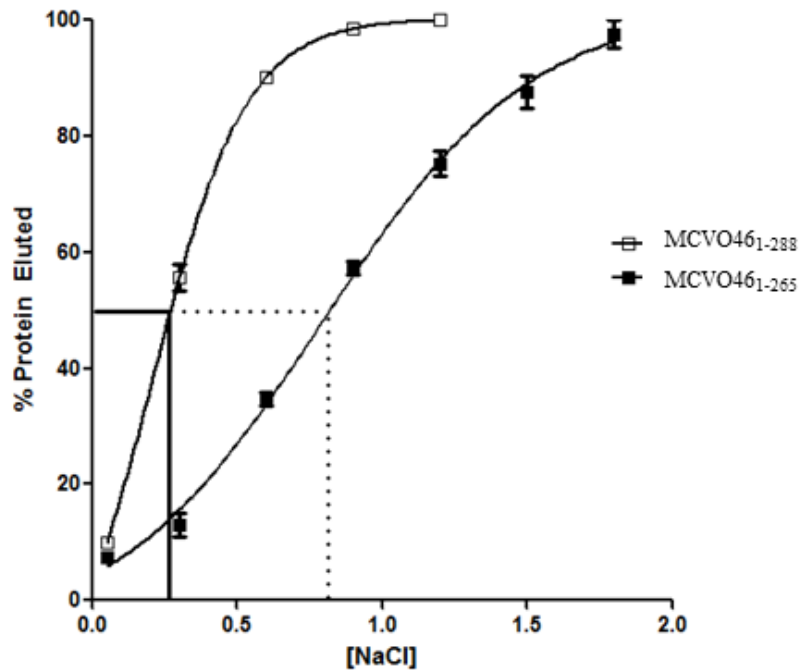


Figure 4-11: ssDNA cellulose elution curves for MCVO46₁₋₂₈₈ and MCVO46₁₋₂₆₅.

20nmol of each SSB was bound to single stranded calf thymus DNA cellulose and eluted with buffers containing an increasing concentration of NaCl. Fractions were run on 10% SDS PAGE blue silver stained gels. Protein bands were quantitated and percent protein eluted was calculated. EC₅₀ values are marked.

MCVO46₁₋₂₈₈, EC₅₀ value of 0.21M NaCl (solid line), R² =1.0.

MCVO46₁₋₂₆₅, EC₅₀ value of 0.79M NaCl (dotted line), R² =1.0.

4.2.6 Electrophoretic Mobility Shift Assays with Peptide Competition for ssDNA Binding.

The last thirty amino acids of the Vaccinia I3 protein contain thirteen negatively charged residues. These negative charges could serve as a direct competitor to ssDNA for SSB binding. To test this hypothesis we synthesized two 30-mer peptides. The first, a native 30-mer (N30mer) corresponded exactly to the sequence of the last thirty amino acids of Vaccinia I3. The second comprised a peptide encoding a scrambled version of the last thirty amino acids of Vaccinia I3 (S30mer). These peptides were used in electrophoretic mobility shift experiments in competition assays. 30 μ g of untagged VacI3₁₋₂₇₀ was bound to either N30mer or S30mer peptides in 1:1, 5:1, 10:1, 20:1 or 30:1 molar ratios of peptide:I3 for 20 minutes at 37°C. 1 μ g of ϕ X 174 ssDNA was added to the peptide-protein complexes and incubated for another 20 minutes at 37°C. The complexes were then fractionated on 0.8% agarose gels, stained with Sybr Safe dye (Invitrogen) and visualized using ultraviolet light. When the N30mer peptide was added, the ssDNA exhibited an increased mobility in the gel when compared to I3 protein with no peptide (Figure 4-12 A). At 30:1 peptide:I3, the highest ratio used in this experiment, the ssDNA recovered almost all of the mobility, migrating at a position similar to what is seen with ssDNA alone (Figure 4-12 A). When the S30mer peptide was added, it also caused an increase in ssDNA mobility (Figure 4-12 B). This increased mobility required less of the S30mer peptide than was seen with the N30mer peptide (Figure 4-12). These experiments suggest that the N30mer peptide can compete with ssDNA for SSB binding. It also suggests that

the effect is mostly related to charge composition as the S30mer is a more effective competitor.

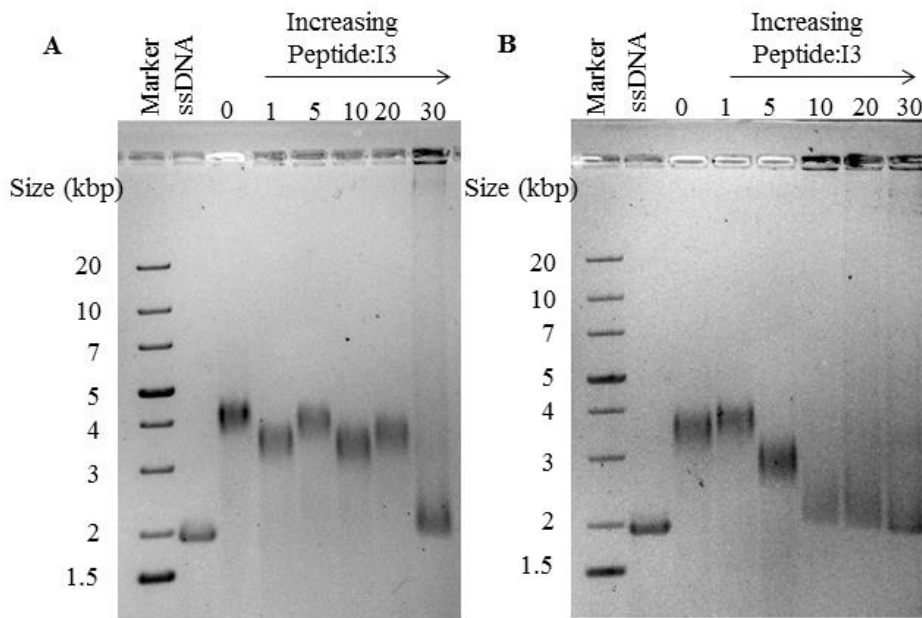


Figure 4-12: Electrophoretic mobility shift assay of C-terminal tail peptides competition with ssDNA.

Reactions contained 1 μg single stranded ΦX 174, 30 μg of VacI3₁₋₂₇₀ and an increasing molar ratio of peptide to I3₁₋₂₇₀. Peptide-protein complexes were bound for 20 minutes at 37°C, ssDNA was added and incubated for a further 20 minutes at 37°C. Complexes were fractionated by electrophoresis through a 0.8% agarose gel, stained with Sybr Safe and visualized using ultraviolet light.

A) N30mer B) S30mer

4.2.7 Anti-I3 Antibody Epitope Mapping.

In the previous immunoprecipitation experiments, the His6 tagged poxvirus SSBs were tested in Western blots to see if they would be recognized by the 10D11 anti-I3 antibody (Figure 3-6, 3-7). Only the VacI3₁₋₂₇₀(H6) protein was recognized by the 10D11 anti-I3 antibody (Figure 3-6). As the antibody did not recognize VacI3₁₅₋₂₄₄(H6), the epitope for this antibody can be narrowed down to either 15 N terminal amino acids or 26 C terminal amino acids. In order to determine which region of I3 is bound by this antibody, additional Western blots were performed. Untagged VacI3₁₋₂₇₀ and VacI3₁₋₂₄₄ were fractionated on two identical 10% SDS PAGE gels. One gel was Coomassie stained and the other was Western blotted with the 10D11 anti-I3 antibody. The Coomassie gel detected essentially identical quantities of both proteins (Figure 4-13 A). However, only VacI3₁₋₂₇₀ is detected by the 10D11 anti-I3 antibody in the Western blot (Figure 4-13 B). This shows that the epitope for this antibody is the C-terminal tail.

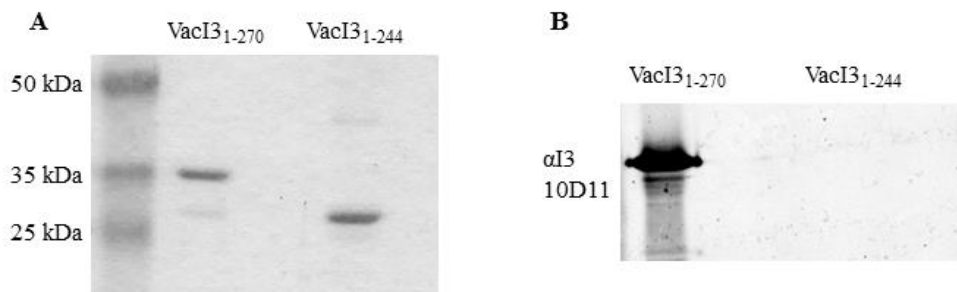


Figure 4-13: 10D11 anti-I3 antibody epitope determination. 10% SDS PAGE gels were prepared and 1 mg of VacI3₁₋₂₇₀ and VacI3₁₋₂₄₄ proteins was electrophoresed on two identical gels. A) Proteins were visualized using Coomassie stain. B) Western blot using 10D11 anti-I3 antibody to detect either full length or C terminal truncated Vaccinia proteins. The antibody was only able to detect the VacI3₁₋₂₇₀ full length protein.

4.2.8 Using the 10D11 Anti-I3 Antibody to Supershift the ssDNA in EMSA.

Previous experiments showed that the epitope recognized by the 10D11 anti-I3 antibody is the C-terminal tail (Figure 4-13). This raises the question whether the C-terminal tail is exposed in DNA-protein complexes. To test whether the C-terminal tail is surface exposed, we performed electrophoretic mobility shift assays and used the 10D11 anti-I3 antibody to see if we could supershift the ssDNA-protein complexes. Different quantities of untagged VacI3₁₋₂₇₀ or VacI3₁₋₂₄₄ proteins were bound at different molar ratios to the anti-I3 10D11 antibody for 20 minutes at 37°C. 1 µg of φX 174 ssDNA was added and the complex was incubated for another 20 minutes at 37°C. The complexes were fractionated on 0.8% agarose gels, stained and visualized. φX 174 ssDNA bound to the highest amount of 10D11 anti-I3 antibody used in these experiments, and I3-ssDNA complexes without antibody were also fractionated on the gels as controls. The antibody did not shift ssDNA by itself, (Figure 4-14 A-D lane 1) and I3 alone shifted the ssDNA as described previously (Figure 4-14 A-D lanes 2, 6, 10). When increasing amounts of 10D11 anti-I3 antibody was added to ssDNA-protein complexes, an additional shift in the mobility of the complexes can be observed that is greater than the shift of protein and ssDNA with no antibody (Figure 4-14 A lanes 3, 7, 11). This supershift increases with increasing amounts of antibody (Figure 4-14 A lanes 3-5, 7-9, 11-13). When this experiment was repeated with VacI3₁₋₂₄₄, there is a shift in the ssDNA seen with increasing amounts of antibody, but not to the extent seen with VacI3₁₋₂₇₀ (Figure 4-14 B lanes 3-5, 7-9, 11-

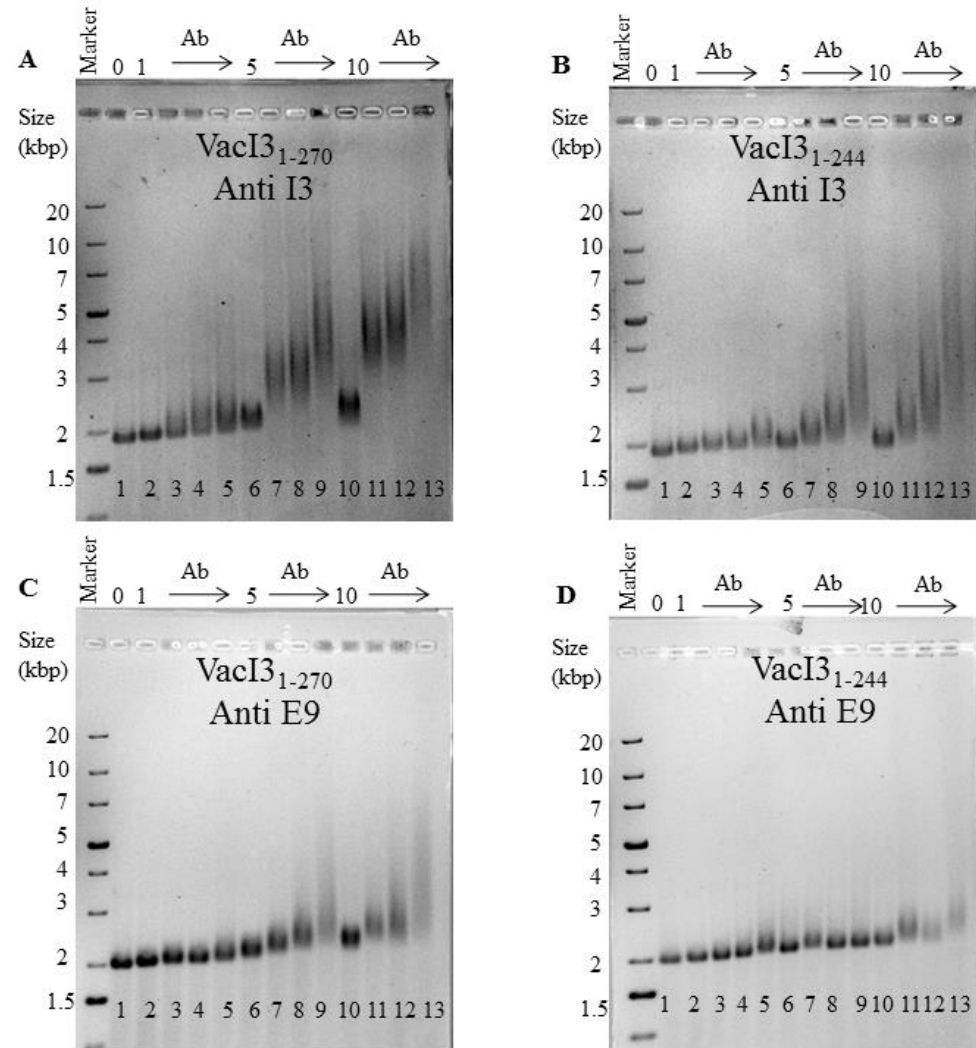


Figure 4-14: Electrophoretic mobility shift assay of antibody supershift.

Reactions contained 1 μg single stranded ΦX 174, 1, 5 or 10 μg of SSB and an increasing molar ratio of antibody. Lane 0 contains ΦX 174 ssDNA and antibody but no SSB. Antibody-protein complexes were bound for 20 minutes at 37°C, ssDNA was added and incubated for a further 20 minutes at 37°C, fractionated by electrophoresis through a 0.8% agarose gel, stained with Sybr Safe and visualized using ultraviolet light. A) VacI3_{1-270} bound to 10D11 anti-I3 antibody B) VacI3_{1-244} bound to 10D11 anti-I3 antibody C) VacI3_{1-270} bound to anti-E9 antibody D) VacI3_{1-244} bound to anti-E9 antibody. Lane numbers are indicated at the bottom of each gel.

13). These experiments were repeated using an anti-E9 antibody (against Vaccinia DNA polymerase) as an isotype control (Figure 4-14 C-D). For both VacI3₁₋₂₇₀ and VacI3₁₋₂₄₄, there was a slight supershift of the complex in the gel, but it was far less than what was seen for VacI3₁₋₂₇₀ with the 10D11 anti-I3 antibody (Figure 4-14 C and D lanes 3-5, 7-9, 11-13). These experiments showed that the C-terminal tail is exposed and accessible to other proteins in the complexes, and is recognized by the 10D11 anti-I3 antibody.

4.2.9 Microinjection of 10D11 Anti-I3 Antibody into BSC40 Cells to Disrupt Virus Factories.

Previous experiments demonstrated that the epitope recognized by the anti-I3 antibody 10D11 is the I3 C-terminal tail (Figure 4-13). Previous work on other SSB proteins have shown that the negatively charged C-terminal tail binds to many proteins involved in DNA repair, recombination and replication (Breschkin and Mosig 1977a, 1977b, Kim et al. 1992a, Kim and Richardson 1994, He et al. 2003, Hyland et al. 2003, Hamdan et al. 2005, Lohman and Ferrari 1994, Shereda et al. 2008). Based on our data, we wanted to test if blocking access to the C-terminal tail will have an effect on Vaccinia virus replication, perhaps by disrupting protein-protein interactions. To test this hypothesis we microinjected BSC40 cells with 10D11 anti-I3 antibodies, infected these cells for 6 hours and measured the size of DAPI-stained virus factories using immunofluorescence microscopy. Cells were microinjected with either 10D11 anti-I3 or isotype control anti-His6 antibodies at 5mg/mL, then infected with A5L-YFP Vaccinia virus (Katsafanas and Moss 2007) for 6 hours. The cells were then fixed and stained

with DAPI for DNA, rhodamine phalloidin for actin and a Cy-5 secondary antibody to detect the microinjected antibodies. Cells were imaged using a spinning disc confocal microscope and the virus factory size was measured using the ROI tools by drawing around the virus factories. Virus factories were observed in infected cells (Figure 4-15) and there was no secondary antibody staining in cells that were not microinjected, but seen in the same slides (Figure 4-15). In cells that were microinjected with the anti-His6 isotype control antibody, the antibodies stained throughout the cell (Figure 4-15). In cells that were microinjected with 10D11 anti-I3 antibody, the antibody staining was limited to the virus factories (Figure 4-15). Student's t tests were performed and it was determined that there was no significant difference in the size of virus factories in non-microinjected cells on both the anti-I3 and the anti-His6 slides (Figure 4-16, clusters 1 and 3). The factories from cells that were microinjected with the anti-His6 antibody were significantly smaller than the factories in non-microinjected cells (Figure 4-16). The virus factories in cells microinjected with 10D11 anti-I3 antibody were also significantly smaller than factories from non-microinjected cells (Figure 4-16). Most importantly, the factories from cells microinjected with 10D11 anti-I3 antibody were significantly smaller than the factories from cells microinjected with anti-His6 antibodies (Figure 4-16). This suggests that by binding to the I3 C terminal tail, the antibody has negative effects on virus replication.

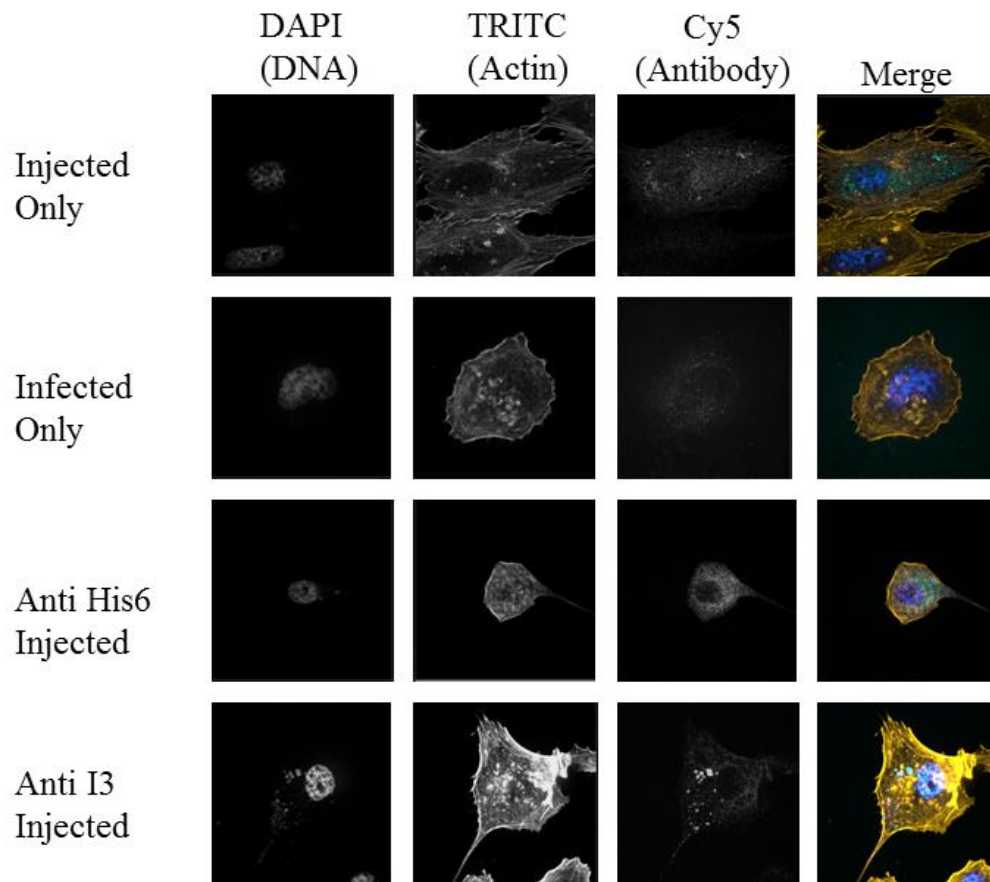


Figure 4-15: Microinjection of 10D11 anti-I3 antibodies into Vaccinia infected cells. BSC40 cells were injected with anti-I3 or anti-His6 antibodies (5mg/ml) and infected with A5L-YPF Vaccinia virus for 6 hours. The cells were stained for DNA (DAPI), actin (TRITC) and antibodies (Cy5) and imaged using a spinning disc confocal microscope.

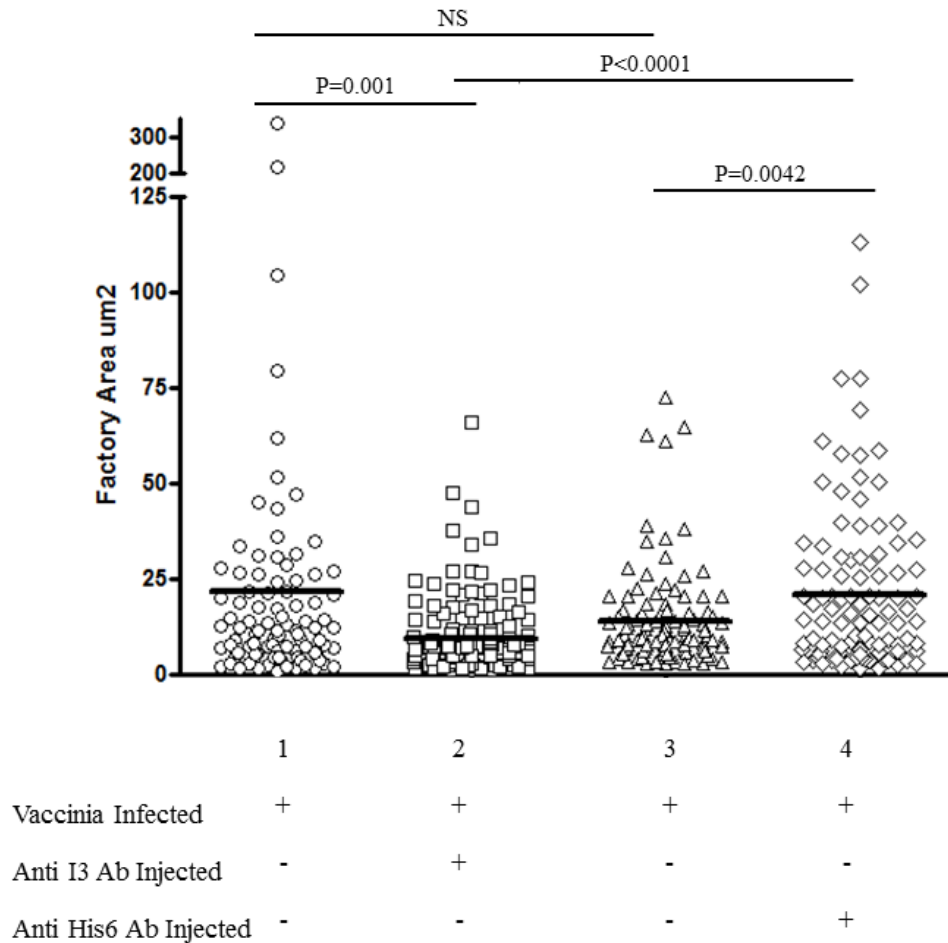


Figure 4-16: Quantification of virus factory area from antibody microinjected cells. BSC40 cells were injected with antibodies (5 mg/ml) and infected with A5L-YPF Vaccinia virus for 6 hours. Cells were stained for DNA, actin and antibodies. Virus factory size was quantitated using Volocity version 6.0.1. Student's t tests were performed to determine significant changes in virus factory sizes. There was no significant difference between the factory sizes in infected only cells. Antibody injected factories were significantly smaller than non-injected cells. The cells injected with 10D11 anti-I3 antibody had the smallest factories.

4.2.10 Microinjection of C Terminal Tail Peptide into BSC40 Cells to Compete for ssDNA Binding.

The experiments described above showed that a 30 amino acid peptide corresponding to either the sequence of the C-terminal tail (N30mer) or a scrambled version of the C-terminal tail (S30mer) can interfere with ssDNA binding to I3 (Figure 4-12). Based on this experiment, and the previous microinjection experiment, we wanted to see if microinjecting these peptides into virus infected cells could interfere with ssDNA binding *in vivo* and have any effect on the virus replication. To test this, BSC40 cells were microinjected with N30mer or S30mer peptides. To control for the effects of microinjection, we also injected cells with unrelated JunB or c-Jun peptides (a gift from Dr. R. Ingham), and to identify injected cells, we included Texas-red labelled dextran. The cells were infected with A5L-YFP Vaccinia virus for 6 hours, and then fixed and stained with DAPI, and Alexa647 phalloidin. The cells were imaged using a spinning disc confocal microscope and the amount of virus replication was determined from the size of the DAPI-stained factories (Figure 4-17). Student's t tests were performed and showed that there was no significant difference between factories in the non-microinjected cells on all the slides (Figure 4-18). The factories in cells microinjected with either the N30mer or S30mer peptide were significantly smaller than the factories in non-microinjected cells, $P=0.0422$ and $P=0.0206$ respectively (Figure 4-18), but there were no significant differences between cells microinjected with the N30mer and S30mer peptides (Figure 4-18). Virus factories in cells microinjected with S30mer peptide were significantly

smaller than factories in cells microinjected with JunB peptide, $P=0.006$ (Figure 4-18). There was no significant difference in virus factory size between the JunB peptide microinjected cells and any of the other treatments (Figure 4-18). There was no significant difference in virus factory size between cells microinjected with c-Jun peptide and any of the other treatments (Figure 4-18). P values are summarized in Table 8.

Table 9: P values from student's t tests of quantification of virus factory size from peptide microinjections

		N30mer		S30mer		c-Jun		JunB	
		-	+	-	+	-	+	-	+
N30mer	-		0.04	NS	NS	NS	NS	NS	NS
	+			NS	NS	NS	NS	NS	NS
S30mer	-				0.02	NS	NS	NS	0.006
	+					NS	NS	NS	NS
c-Jun	-						NS	NS	NS
	+							NS	NS
JunB	-								NS
	+								

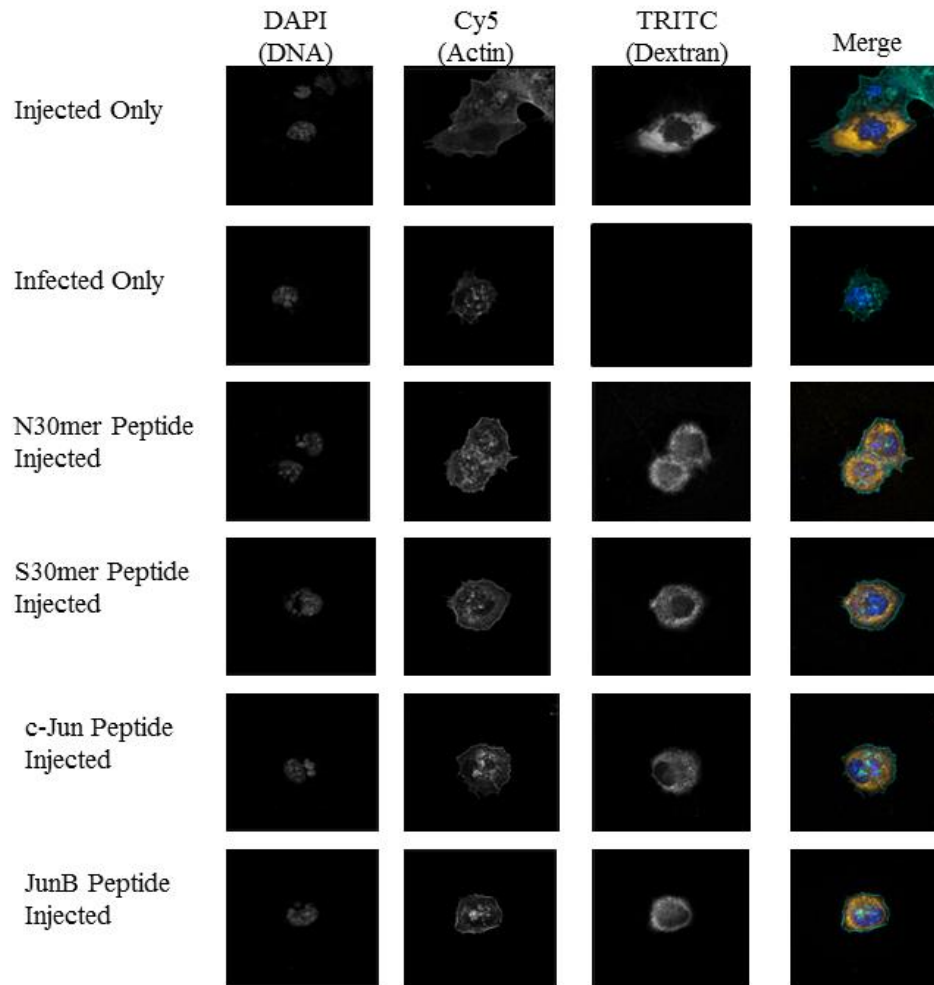


Figure 4-17: Microinjection of C-terminal tail peptides into Vaccinia infected cells.

BSC40 cells were injected with N30mer, S30mer, c-Jun or JunB peptides (5 mg/ml) mixed with Texas Red Dextran (TRITC) and infected with A5L-YPF Vaccinia virus for 6 hours. The cells were stained for DNA (DAPI) and actin (Cy5) and imaged using a spinning disc confocal microscope.

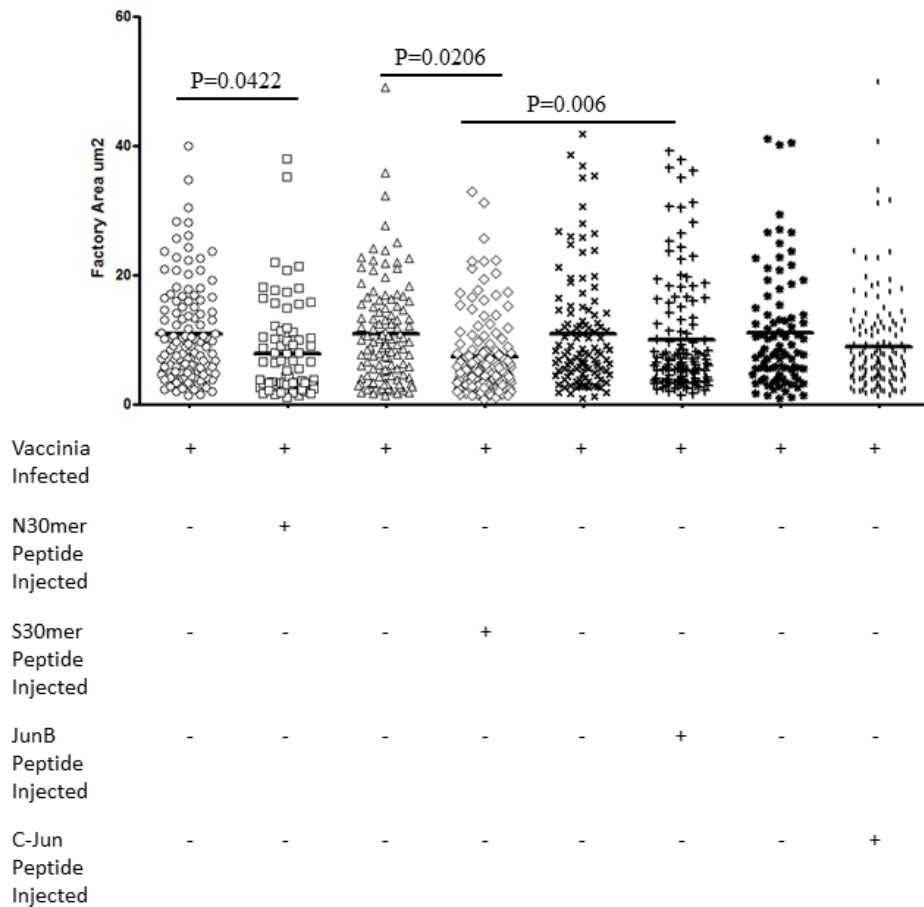


Figure 4-18: Quantification of virus factory area after microinjection with peptides.

BSC40 cells were injected with N30mer, S30mer, c-Jun or JunB peptides (5 mg/ml) and infected with A5L-YPF Vaccinia virus for 6 hours. The cells were stained for DNA and actin. Injected cells were detected by co-injecting a Texas Red labelled dextran. Virus factory size was quantitated using Volocity software. Student's t tests were performed to determine significant changes in virus factory sizes. The cells injected with either the N30mer or S30mer peptides had significantly smaller factories than non-injected cells. Factories in cells injected with S30mer were significantly smaller than factories in cells injected with JunB peptide. All other groups showed no significant differences in virus factory size.

4.2.11 Determining the Amount of I3 in a Vaccinia Infected Cell

The microinjection experiments described above suggest that the I3 protein is made in excess of what is required for a virus infection. To confirm this hypothesis, we wanted to determine how much I3 is produced per cell in a virus infection. We infected BSC40 cells with Vaccinia strain WR at an MOI of 5 for 6 hours, and electrophoresed known numbers of infected cells with several standards of I3 at known concentrations. I3 was detected in a Western blot using the 10D11 anti-I3 monoclonal antibody, and a standard curve was created from the I3 samples of known concentrations (Figure 4-19). From the curve, the amount of I3 per infected cell was calculated to be roughly 3×10^{-15} mol/cell, or 2×10^9 molecules per cell. This corresponds to 2×10^5 I3 per Vaccinia genome, and there are 6 million binding sites (30 nucleotides per binding site) for I3 present in an infected cell.

4.2.12 Immunoprecipitations to Search for Binding Partners

SSBs from other organisms have been described to bind to many proteins involved in DNA replication, recombination and repair, and this interaction is often mediated through the negatively-charged C-terminal tail of the SSB. This pattern of negative charges in the C-terminal tail is also present in Vaccinia I3, so we hypothesize that there may be protein-protein interactions between I3 and either viral or cellular proteins. There have been a few reports in the literature of potential binding partners for I3, such as ribonucleotide reductase and the cellular translation initiation factor eIF4G, but these are not definitive (Davis and Mathews 1993, Zaborowska *et al.* 2012).

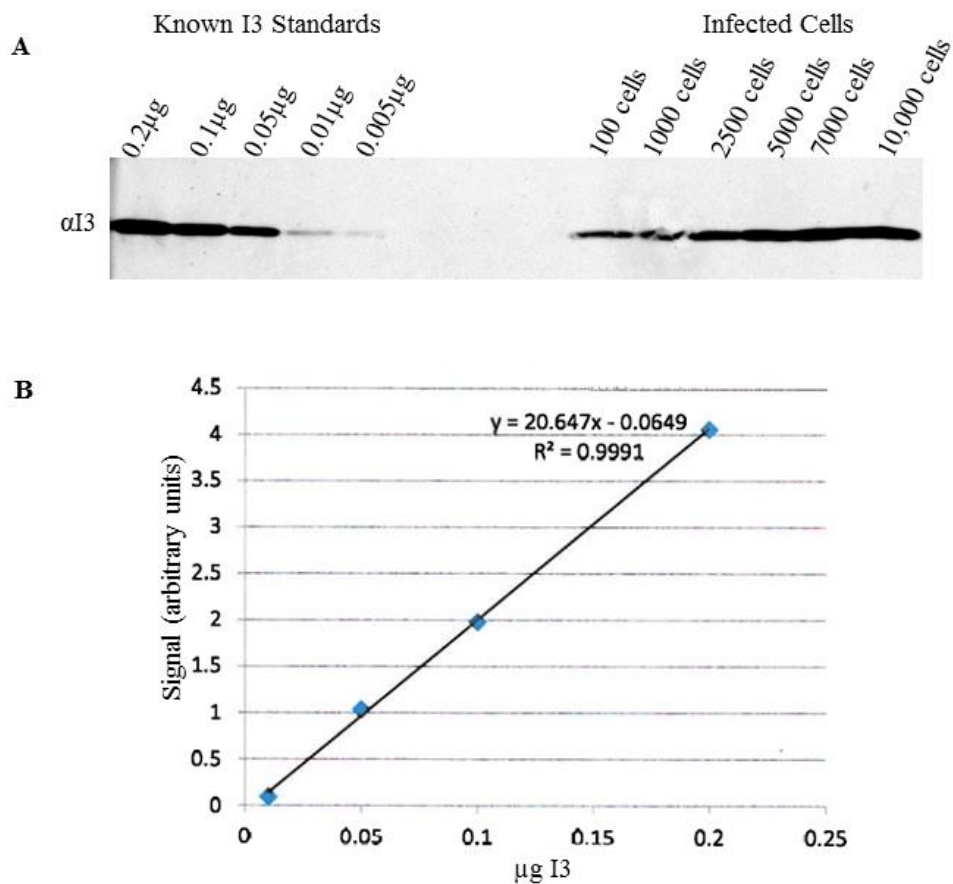


Figure 4-19: Determination of how much I3 is in an infected cell. BSC40 cells were infected with Vaccinia virus strain WR for 6 hours before harvesting. Cells were counted and electrophoresed with I3 standards of known concentrations. Samples were transferred to Western blot and stained for I3 using the 10D11 anti-I3 mouse monoclonal antibody. The band intensities were measured with the Odyssey software (Version 3.0), and a standard curve was created. Solving for x in the equation of the line calculates how much I3 is in an infected cell.

To test whether Vaccinia I3 has any binding partners, we made an N-terminal Flag tagged I3 (N Flag I3) for expression in virus infected cells. The N-terminal Flag tag will allow us to use an anti-Flag antibody to immunoprecipitate I3 and any other proteins complexed to it, while leaving the C terminus free to bind other proteins. By expressing this protein in Vaccinia infected cells, we can determine if there are both cellular and/or viral proteins that bind I3.

We expressed the N Flag I3 protein in BSC40 cells infected with Vaccinia WR strain overnight. After cell lysis, we added a 30-mer polyT oligonucleotide and monoclonal anti-Flag magnet beads to the lysates overnight to immunoprecipitate N Flag I3 and any other proteins complexed to it. These samples were electrophoresed for silver staining and Western blotting to detect cellular and viral ribonucleotide reductase. We added ssDNA to expose the C-terminal tail, thereby making it accessible for binding to other proteins. There were no bands present on the silver stained gel in the N Flag I3 expressing cells that were not also present in mock transfected (plasmid without N-terminal Flag I3) and mock infected (no virus infection) cells (Figure 4-20 A). This suggests that there are no proteins that bind to I3.

There is a report in the literature that used anti-idiotypic antibodies to show that the small subunit of ribonucleotide reductase interacts with I3 (Davis and Mathews 1993). Our lab has also done immunoprecipitations showing that purified recombinant ribonucleotide reductase and I3 can interact (Evans Lab, unpublished data). To test if I3 can interact with either subunit of ribonucleotide reductase, we performed a Western blot on the samples, staining with antibodies

for cellular and viral R1 and R2. The Western blot showed that the N Flag I3 protein was expressed (Figure 4-20). We detected bands corresponding to cellular and viral R1 and R2 in the control Vaccinia infected cells, indicating that the Western blot was working correctly (Figure 4-20). However, we were unable to detect cellular or viral R1 or R2 in the N Flag I3 expressing cells (Figure 4-20). This experiment suggests that I3 does not interact with cellular or viral R1 or R2.

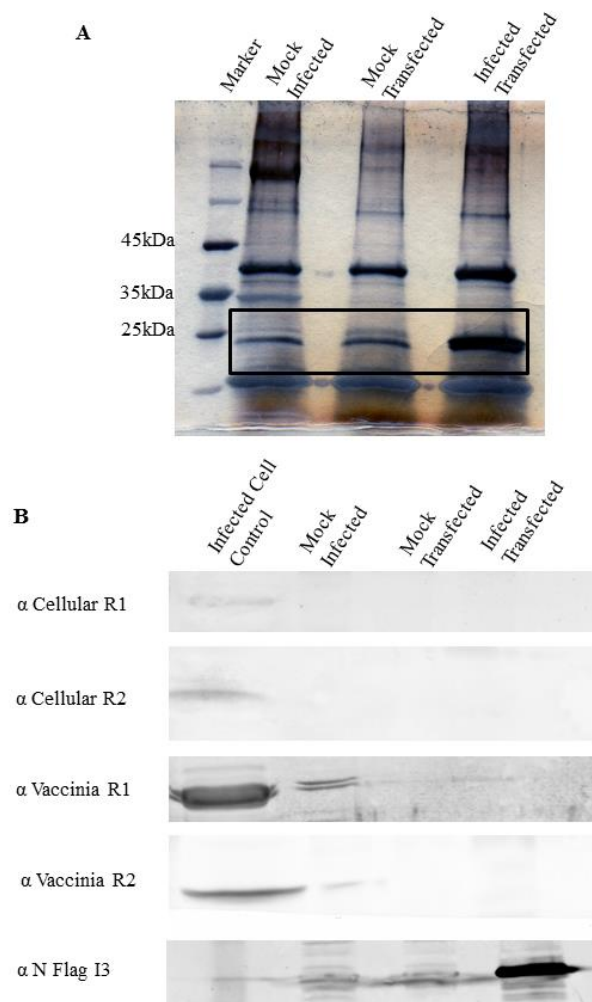


Figure 4-20: Immunoprecipitation to determine if I3 can form a complex with cellular or viral proteins.

BSC40 cells were infected with Vaccinia strain WR and transfected with a plasmid containing an N-terminal Flag tagged I3. Cells were harvested and anti-Flag magnet beads were used to immunoprecipitate the Flag tagged I3 and any other proteins in complex. Samples were run on a silver stained gel or Western blotted for cellular and viral R1 and R2. A) Silver stained gel showing that N-terminal Flag tagged I3 is expressed in infected/transfected cells (black box). B) Western blots to detect cellular and viral R1 and R2. Cellular and viral R1 and R2 was only detected in control infected cells and not in cells where N Flag I3 was expressed. N Flag I3 was expressed only in cells that were transfected with the plasmid containing this gene.

4.3 DISCUSSION

The C termini of many of the single stranded DNA binding proteins has no defined structure, therefore making it very flexible. This flexibility leaves the C terminus free to interact with other proteins, as well as creating the potential to form associations with the ssDNA binding domain in cis or in trans (Breschkin and Mosig 1977a, 1977b, Kim *et al.* 1992a, Kim and Richardson 1994, Lohman and Ferrari 1994, He *et al.* 2003, Hyland *et al.* 2003, Hamdan *et al.* 2005, Shokri *et al.* 2006, Shereda *et al.* 2008, Marintcheva *et al.* 2008). Although the sequences of the SSB proteins are not well conserved, there is a pattern of acidic amino acids in the C terminus that is conserved across the SSB proteins from different organisms. This region of C-terminal negative charges is also conserved in the poxvirus SSB proteins. Our objective was to determine if the C terminus of the poxvirus SSB proteins might exhibit some of the same properties of other SSBs.

Firstly, we used C-terminal His6 tagged proteins in electrophoretic mobility shift assays and in an ssDNA cellulose binding assay. However, these studies led us to the conclusion that positioning the His6 tag on the C terminus was a flaw, and that the properties of the His6 tag itself could confuse the results about the C terminus. Therefore, we created untagged full length and C-terminal truncated SSBs from Vaccinia and MCV.

We also created three mutant full length I3 proteins that had several of the negative charges in the C-terminal tail mutated to either neutral or positive charges. However, these mutations made the mutant proteins unstable and the C-terminal tail was quickly degraded (Figure 4-5).

The untagged SSB proteins were used in electrophoretic mobility shift assays. We hypothesized that the C-terminal truncated proteins would produce a greater shift of the ssDNA in the gel than the full length proteins, because the C-terminal tail would interfere with the ssDNA binding to the SSB. We observed that VacI3₁₋₂₄₄ produced a very small mobility shift in the gel, where with VacI3₁₋₂₇₀ there was an increase in the shift with an increased amount of protein (Figure 4-6). This was also observed with the MCV proteins, MCVO46₁₋₂₆₅ was barely able to produce a shift in the gel and MCVO46₁₋₂₈₈ produced an increased ssDNA shift with an increased amount of protein (Figure 4-7). One possible explanation for these results is that the C-terminal tail influences how the SSB is binding to the ssDNA. The C-terminal truncated proteins could be binding ssDNA in a tight complex, due to the SSB randomly binding along the ssDNA and interacting with other SSBs throughout the ssDNA. This complex would have a small size and would migrate quickly through the gel, appearing as if there is little protein bound. The presence of the C-terminal tail would prevent this from occurring. The SSB would be recruited to the ssDNA sequentially, forming an open circle of SSB bound to ssDNA. This complex would have a large size and migrate slowly in the gel, producing an increasing shift of the ssDNA when increasing amounts of SSB is bound. These data may also be showing the cooperativity of the SSB binding to ssDNA. The full length SSBs are showing a laddering effect when more of the SSB is added. The shift seen with the truncated SSBs is more indicative of each SSB binding independently to the ssDNA. More experiments, such as electron

microscopy would be needed to confirm this hypothesis and to look at the structures that these proteins make on the ssDNA.

To test whether the removal of the C-terminal tail from the poxvirus SSBs has any effect on the affinity for ssDNA, we used an ssDNA cellulose binding assay. The EC_{50} values showed that VacI3₁₋₂₄₄ had a higher EC_{50} value than VacI3₁₋₂₇₀ (Figure 4-9). This pattern was also reflected in the MCV SSB proteins, where MCVO46₁₋₂₆₅ had a much higher EC_{50} value than MCVO46₁₋₂₈₈ (Figure 4-11). These data suggest that the negative charges present in the C-terminal tail are interfering with ssDNA binding to the SSB. The negatively-charged C terminus could bind into the positively charged ssDNA binding pocket and prevent the ssDNA from binding, mimicking ssDNA. The absence of the C terminus would allow the ssDNA to bind the SSB more readily, which is what we observed for the truncated proteins.

This interaction between the C terminus and the ssDNA binding pocket could lead to a competition with ssDNA for binding to the SSB. This competition could act as a regulatory mechanism, similar to what is seen with T7 GP2.5 where the C terminus has been shown to bind the same region on GP2.5 as ssDNA (Marintcheva *et al.* 2008). To test if the poxvirus SSB C terminus can compete with ssDNA for binding, we performed a competition assay using peptides corresponding to the native amino acid sequence of the C-terminal tail (N30mer), as well as a scrambled version of the same sequence (S30mer), in an electrophoretic mobility shift assay to see if we could prevent the shift of the ssDNA when VacI3₁₋₂₇₀ was bound to the peptide. With both the N30mer and

S30mer peptides, the shift of the ssDNA was decreased with increasing amounts of peptide, and nearly returned to the mobility observed when VacI3₁₋₂₇₀ is not present (Figure 4-12). These data demonstrate that the C-terminal tail can potentially bind to the ssDNA binding pocket and prevent ssDNA from binding. The S30mer peptide competed better for ssDNA binding than the N30mer peptide, as it required less peptide to create a similar mobility of the ssDNA in the gel as the lane with no VacI3₁₋₂₄₄ present (Figure 4-12). This is an interesting observation which will require follow up experiments. These data also suggest that the sequence order of the charges is not necessarily important, but the presence of the negative charges that has an effect on the ssDNA binding ability. Further experiments are needed to determine if the C terminus and ssDNA can bind to the same region of I3.

Our lab has created an anti-I3 antibody (clone 10D11) that can be used in a wide range of applications (Evans Lab unpublished data). This work has shown that the epitope for this antibody is the C-terminal tail (Figure 4-13). We hypothesize that the C terminus is exposed on the surface of I3 and could be available to bind itself or other proteins. To test this, we performed a series of electrophoretic mobility shift assays using the anti-I3 antibody to supershift the ssDNA in the gel (Figure 4-14). We were able to supershift the ssDNA when increasing amounts of anti-I3 antibody was added to VacI3₁₋₂₇₀ (Figure 4-14). This supershift was not seen when antibody was added to VacI3₁₋₂₄₄, nor was it seen when the anti-E9 isotype control antibody was added to either VacI3₁₋₂₇₀ or VacI3₁₋₂₄₄ (Figure 4-14). The supershift of the ssDNA suggests that the C terminal

tail is freely exposed to solution and is accessible to the antibody. This would allow other proteins or I3 monomers to bind to the exposed C-terminal tail and to be recruited to the ssDNA.

There have been a couple of reports in the literature of potential binding partners for I3. The first identified Vaccinia encoded ribonucleotide reductase (RR) as a potential binding partner for I3 using anti-idiotypic antibodies against the RR small subunit R2 to search for binding partners (Davis and Mathews 1993). The second report identified the host translation initiation factor eIF4G as a binding partner for I3 (Zaborowska *et al.* 2012). Our lab has tried to identify any protein-protein interactions using immunoprecipitations with the 10D11 anti-I3 antibody (Evans Lab unpublished data). These studies were flawed, as they were using the 10D11 anti-I3 antibody that binds the C terminus, they were blocking the potential protein binding site on I3.

We created an N-terminal Flag tagged I3 protein to identify any potential proteins that bind to I3. However, we were unable to find any proteins that complex with I3 (Figure 4-20). We also were unable to detect cellular or viral R1 or R2 subunits of RR binding to I3 (Figure 4-20). These data suggest that I3 might not bind to any other proteins, but only self-recruits other I3 molecules to the ssDNA. Further work is needed to confirm this hypothesis.

We have been unable to identify any binding partners for I3, and the role of the C-terminal tail in the context of a virus infection remains unclear. To try to determine what this role may be, we sought to attempt to block the C terminus of the I3 protein in virus infected cells. To accomplish this, we microinjected BSC40

cells with the 10D11 anti-I3 antibody and infected the cells with Vaccinia virus. Virus factory size was measured and compared between non-microinjected cells, infected and microinjected cells and cells that were microinjected with an anti-His6 antibody as an isotype control (Figures 4-15, 4-16). These data show that the 10D11 anti-I3 antibody localizes to the virus factories and that the cells microinjected with 10D11 anti-I3 antibody had the smallest virus factories (Figure 4-16). This suggests that blocking the C terminus of I3 inhibits viral DNA synthesis.

The fact that there virus factories were present at all, even though I3 is an essential protein, indicates that I3 is most likely present in excess of what is required during a virus infection. This reflects what has been shown in the literature, where I3 was knocked down using siRNAs (Gammon and Evans 2009, Greseth *et al.* 2012). When I3 was knocked down, the virus was still able to replicate, but at drastically lower levels to the control siRNA treated virus (Gammon and Evans 2009, Greseth *et al.* 2012). Our experiments determined that there are 3×10^{15} moles of I3 per infected cell, or 2×10^9 I3 protein monomers per infected cell. This corresponds to 2×10^5 I3 proteins per genome, or six million 30 nucleotide binding sites that are present in an infected cell. This suggests that I3 present is great excess to what is needed in an infection, however the reasons for such a high production is unclear.

We demonstrated that a peptide of the C-terminal tail can compete with ssDNA for binding to VacI3₁₋₂₇₀ (Figure 4-12). In order to see if we could reproduce this competition in a virus infection, we microinjected BSC40 cells

with N30mer peptide, S30mer peptide, and peptides containing sequences of JunB and c-Jun, which are unrelated to the sequence of Vaccinia I3. Virus factory size was measured and compared between all peptides (Figures 4-17, 4-18). Virus factories in cells microinjected with N30mer peptide and S30mer peptides were significantly smaller than non-microinjected cells (Figure 4-18). This tells us that the peptides can decrease the amount of virus DNA replication. As a control we microinjected cells with JunB and c-Jun peptides and found that the factories in cells microinjected with S30mer peptide were significantly smaller than cells microinjected with JunB peptide (Figure 4-18). There was no significant differences found between any of the other peptides tested (Figure 4-18). Both the JunB and c-Jun peptides contained some negative charges but both peptides had fewer negative charges than either the N30mer or S30mer peptides. The JunB and c-Jun peptides were also phosphorylated on two residues and contained a biotin at their N terminus. We also are assuming that the peptides are localizing to the virus factories, as we do not have a method for detecting the peptides in the microinjected cells. Together, this experiment and the gel shift competition experiment suggest that the presence of the negative charges within the C terminus of I3 can compete with ssDNA for binding to the SSB and this competition can have a detrimental effect on virus replication. However, further experimentation to determine if the C-terminal tail and ssDNA bind to the same region of I3 is required.

CHAPTER 5 CONCLUSIONS AND FUTURE WORK

5.1 CONCLUSIONS

5.1.1 Multimerization Model

The data from the multi-angle laser light scattering provides insights into how Vaccinia I3 forms oligomeric complexes on the ssDNA. In the absence of ssDNA, full length VacI3₁₋₂₇₀ forms a monomer that is in rapid exchange with a dimer (Figure 3-11). The C terminus of I3 contains many negative charges; therefore it has the potential to bind into the expected positively charged ssDNA binding pocket. When ssDNA is present, the negatively-charged C-terminal tail is displaced and the ssDNA binds I3. The ssDNA binding results in a free C-terminal tail that is now available to bind to other I3 monomers, resulting in the recruitment of more I3 monomers to form higher ordered structures (Figure 3-11). We observed dimeric and tetrameric structures, but this model also allows for larger structures, including octameric structures that have been reported in the literature (Tseng *et al.* 1999).

VacI3₁₋₂₄₄ also forms monomers in solution (Figure 3-11). The VacI3₁₋₂₄₄ monomer is more stable than the VacI3₁₋₂₇₀ monomer because there is no C-terminal tail available to bind a second VacI3₁₋₂₄₄ monomer, so a rapid exchange between VacI3₁₋₂₄₄ monomers and dimers does not occur. With the addition of ssDNA, we only observed tetramers and not any of the dimeric structures that were observed with full length VacI3₁₋₂₇₀ (Figure 3-11). This suggests that the presence of the C-terminal tail makes the ssDNA:I3 complex unstable resulting in

a dynamic exchange between the monomers and dimers formed by full length VacI3₁₋₂₇₀. Removal of the C terminus stabilizes the VacI3₁₋₂₄₄ monomer in the absence of ssDNA, and stabilizes the interactions between VacI3₁₋₂₄₄ and ssDNA, resulting in a stable tetrameric complex. This stabilization is likely due to the removal of electrostatic charge interactions between the negatively charged C-terminal tail and the predicted positively charged ssDNA binding pocket.

These data reflect what has been shown in the literature. Recently, a report has been published describing the oligomeric state of I3 (Greseth *et al.* 2012). These authors found that full length I3 can form monomers and tetramers, which was surprising because they used recombinant proteins (Greseth *et al.* 2012). This could be due to self-recruitment of I3 to form tetramers. However, it is more likely that the samples from these experiments were contaminated with ssDNA. If the local concentration of I3 was high enough, then I3 monomers could have the potential to contact and bind other I3 monomers, forming higher ordered structures. This is unlikely unless ssDNA is present to bring the I3 monomers into close proximity.

5.1.2 ssDNA Binding Model

Our model for multimerization suggests a self-recruitment model that would be important to the virus *in vivo*. Full length I3₁₋₂₇₀ would bind to ssDNA and the negatively-charged C-terminal tail would be displaced. This exposed C-terminal tail is now available to bind to a second VacI3₁₋₂₇₀ monomer, recruiting it to the ssDNA (Figure 5-1). As the ssDNA binding site in I3 has a higher affinity for ssDNA than the C terminus, the second VacI3₁₋₂₇₀ monomer is able to bind the

ssDNA (Figure 5-1). This method of self-recruitment causes I3 to evenly coat the ssDNA molecule, leaving it accessible to bind to other enzymes will act on the ssDNA. It is also possible that the C-terminal tail is creating a collectively stronger complex of I3 on the ssDNA, allowing for more cooperative recruitment of I3 to the ssDNA.

C-terminal truncated VacI3₁₋₂₄₄ lacks this negatively-charged C-terminal tail so when it binds to ssDNA, it binds randomly and is not recruited to the location where other VacI3₁₋₂₄₄ proteins are bound. If VacI3₁₋₂₄₄ still retains some ability to self-interact, this will pose a problem for the ssDNA and any enzymes that will be acting on it. If two VacI3₁₋₂₄₄ bind to regions of ssDNA some distance from each other, and are still able to dimerize, the region of ssDNA in between the two proteins will form a hairpin (Figure 5-1). This will become more pronounced when more VacI3₁₋₂₄₄ bind, eventually leaving the ssDNA tangled (Figure 5-1). This would prevent other enzymes from accessing the ssDNA, and prevent them from acting on the ssDNA. If this occurred at a replication fork, this would prevent the polymerase from replicating the DNA.

5.1.3 C-Terminal Tail of I3 in Protein-Protein Interactions

There are reports in the literature that I3 can form protein-protein interactions with the small subunit of ribonucleotide reductase and the host translation initiation factor eIF4G (Davis and Mathews 1993, Zaborowska *et al.* 2012). However, these reports do not provide definitive evidence that I3 binds to either of these proteins. We attempted to determine if I3 binds to any cellular or viral proteins and were unsuccessful. We had assumed that since other SSBs have

been shown to interact with a wide variety of other proteins, that I3 would also have similar protein binding partners. However, we were able to show that only the full length I3 protein could form higher order structures when ssDNA was present. These data suggest that the C-terminal tail may not interact with other proteins, but is important for binding to other I3 molecules instead. This hypothesis would explain why it has been so difficult to identify proteins that interact with I3.

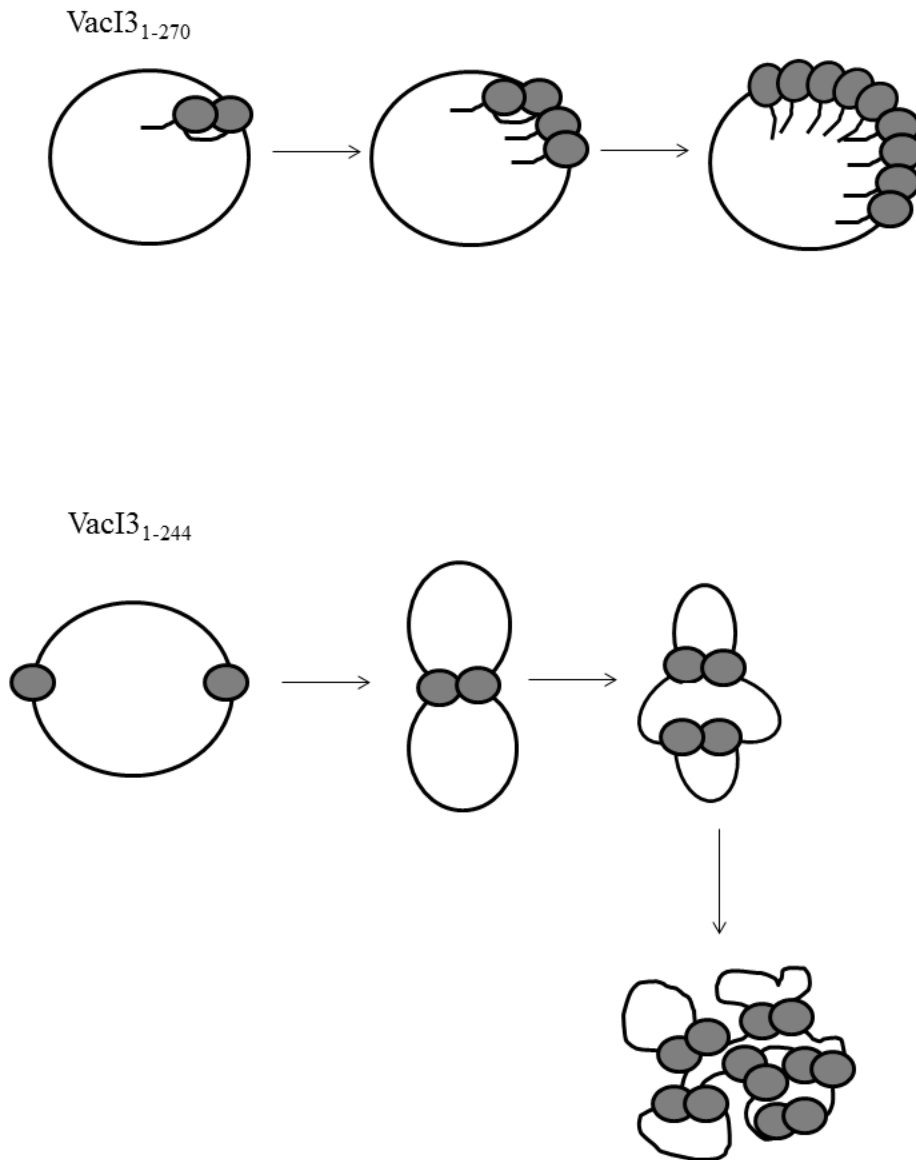


Figure 5-1: Model of I3 in complex with ssDNA.

VacI3₁₋₂₇₀ can self-recruit other I3 molecules to the exposed ssDNA. As more VacI3₁₋₂₇₀ is recruited, the ssDNA becomes evenly coated with I3 and remains accessible to proteins involved in DNA replication, recombination and repair.

VacI3₁₋₂₄₄ monomers bind to ssDNA randomly due to lack of self-recruitment. When VacI3₁₋₂₄₄ forms dimers, the ssDNA is pulled into hairpin structures. With the addition of more VacI3₁₋₂₄₄, the ssDNA becomes knotted and inaccessible to other enzymes.

5.2 FUTURE WORK

5.2.1 Crystal Structure

The crystal structures of many of the SSBs from several organisms have been solved. These structures show that although there is divergence in the sequence, most of the SSBs use a conserved structure to bind to ssDNA (Murzin 1993). The SSBs also form different oligomeric structures to bring together several OB folds for optimal ssDNA binding.

The preceding experiments attempted to crystallize the poxvirus SSBs to determine the protein structure. Although our attempts were unsuccessful, we were able to show a multimerization similar to what is seen with other SSBs. However, the solved crystal structure would be of great benefit in determining the organization of the protein and if poxvirus SSBs utilize this conserved OB fold for ssDNA binding. The crystal structure would also provide insight into the number of OB folds present on each monomer, as well as the multimeric organization of the protein.

5.2.2 I3-ssDNA Complexes

Our model for ssDNA binding at replication forks is based on the model for multimerization and what would occur during a virus infection. It would be interesting to observe the structures depicted in Figure 5-1 using electron microscopy. This would allow us to confirm our model, and provide insights into the role of the C-terminal tail during a virus infection. We were unable to show that I3 has any protein-protein interactions with any viral or cellular proteins.

However, we were able to show that I3 can self-interact, and it would be interesting to observe I3-ssDNA complexes using both the full length and C-terminal truncated I3 proteins, to look more closely at the role the C-terminal tail plays in self-recruitment and ssDNA binding.

5.2.3 Location of ssDNA and C-Terminal Tail Binding to the SSB

We have demonstrated that a peptide corresponding to the C-terminal tail of I3 can prevent ssDNA from binding to the SSB. We hypothesize that the C-terminal tail and the ssDNA are binding to the same region on I3, but further work is needed to confirm this hypothesis. Work with T7 GP2.5 used NMR to show that the C-terminal tail of GP2.5 binds to the same place as ssDNA (Marintcheva *et al.* 2008). Similar experiments should be conducted with Vaccinia I3 to help elucidate how the ssDNA and the C terminus are binding to I3 and how the binding of the C-terminal tail is mediating ssDNA binding.

BIBLIOGRAPHY

- Alberts, B.M., Amodio, F.J., Jenkins, M., Gutman, E.D., and F.L. Ferris. 1968. Studies with DNA-cellulose chromatography. I. DNA-binding proteins from *Escherichia coli*. Cold Spring Harbor Symposia on Quantitative Biology. 33: 289-305.
- Alberts, B.M. 1970. Function of gene 32-protein, a new protein essential for the genetic recombination and replication of T4 bacteriophage DNA. Federation Proceedings. 29: 1154-1163.
- Alberts, B.M., and L. Frey. 1970. T4 bacteriophage gene 32: a structural protein in the replication and recombination of DNA. Nature. 227: 1313-1318.
- Araki, H., and H. Ogawa. 1981. A T7 amber mutant defective in DNA-binding protein. Molecular and General Genetics. 183: 66-73.
- Baroudy, B.M., Venkatesan, S., and B. Moss. 1982. Incompletely base-paired flip-flop terminal loops link the two DNA strands of the vaccinia virus genome into one uninterrupted polynucleotide chain. Cell. 28: 315-324.
- Berns, K.I., Silverman, C., and A. Weissbach. 1969. Separation of a new deoxyribonucleic acid polymerase from vaccinia-infected HeLa cells. Journal of Virology. 4: 15-23.
- Bernstein, D.A., Eggington, J.M., Killoran, M.P., Mistic A.M., Cox, M.M., and J.L. Keck. 2004. Crystal structure of the *Deinococcus radiodurans* single-stranded DNA-binding protein suggests a mechanism for coping with DNA damage. Proceedings of the National Academy of Sciences. 10: 8575-8580.

- Birthsitle, K., and D. Carrington. 1997. Molluscum contagiosum virus. *Journal of Infection*. 34: 21-28.
- Black, M.E., and D.E. Hruby. 1990. Quaternary structure of vaccinia virus thymidine kinase. *Biochemical and Biophysical Research Communications*. 169: 1080-1086.
- Blackwell, L.J., and J.A. Borowiec. 1994. Human replication protein A binds single-stranded DNA in two distinct complexes. *Molecular and Cellular Biology*. 14: 3993-4001.
- Bochkarev, A., Pfuetzner, R.A., Edwards, A.M., and L. Frappier. 1997. Structure of the single-stranded-DNA-binding domain of replication protein A bound to DNA. *Nature*. 385: 176-181.
- Bochkareva, E., Korolev, S., Lees-Miller, S.P., and A., Bochkarev. 2002. Structure of the RPA trimerization core and its role in the multistep DNA-binding mechanism of RPA. *EMBO Journal*. 21: 1855-1863.
- Boyle, D.B. Genus *Avipoxvirus*. In *Poxviruses*. 2007. Birkhäuser Verlag. Basel.
- Breschkin, A.M., and G. Mosig. 1977a. Multiple interactions of a DNA-binding protein *in vivo*: I. Gene 32 mutations of phage T4 inactivate different steps in DNA replication and recombination. *Journal of Molecular Biology*. 112: 279-294.
- Breschkin, A.M., and G. Mosig. 1977b. Multiple interactions of a DNA-binding protein *in vivo*: II. Effects of host mutations on DNA replication of phage T4 gene 32 mutants. *Journal of Molecular Biology*. 112: 295-308.

- Brill, S.J., and B. Stillman. 1991. Replication factor-A from *Saccharomyces cerevisiae* is encoded by three essential genes coordinately expressed at S phase. *Genes and Development*. 5: 1589-1600.
- Bugert, J.J. Genus *Molluscipoxvirus*. In *Poxviruses*. 2007. Birkhäuser Verlag. Basel.
- Bujalowski, W., and T.M. Lohman. 1986. *Escherichia coli* single-strand binding protein forms multiple, distinct complexes with single-stranded DNA. *Biochemistry*. 25: 7799-7802.
- Bujalowski, W., and T.M. Lohman. 1987. Limited co-operativity in protein-nucleic acid interactions: A thermodynamic model for the interactions of *Escherichia coli* single strand binding protein with single-stranded nucleic acids in the “beaded”, (SSB)₆₅ mode. *Journal of Molecular Biology*. 195: 897-907.
- Bujalowski, W., and T.M. Lohman. 1989a. Negative co-operativity in *Escherichia coli* single strand binding protein-oligonucleotide interactions. I. Evidence and a quantitative model. *Journal of Molecular Biology*. 207: 249-268.
- Bujalowski, W., and T.M. Lohman. 1989b. Negative co-operativity in *Escherichia coli* single strand binding protein-oligonucleotide interactions. II. Salt, temperature and oligonucleotide length effects. *Journal of Molecular Biology*. 207: 269-288.
- Burke, R.L., Alberts, B.M., and J. Hosoda. 1980. Proteolytic removal of the COOH terminus of the T4 gene 32 helix-destabilizing protein alters the T4

- in Vitro* replication complex. Journal of Biological Chemistry. 255: 11484-11493.
- Calista, D., Boschini, A., and G. Landi. 1999. Resolution of disseminated molluscum contagiosum with Highly Active Anti-Retroviral Therapy (HAART) in patients with aids. European Journal of Dermatology. 9: 211-213.
- Carlini, L.E., Porter, R.D., Curth, U., and C. Urbanke. 1993. Viability and preliminary *in vivo* characterization of site-directed mutants of *Escherichia coli* single-stranded DNA-binding protein. Molecular Microbiology. 10: 1067-1075.
- Challberg, M.D., and P.T. Englund. 1979. Purification and properties of the deoxyribonucleic acid polymerase induced by vaccinia virus. Journal of Biological Chemistry. 254: 7812-7819.
- Chase, J.W., and K.R. Williams. 1986. Single-stranded DNA binding proteins required for DNA replication. Annual Review of Biochemistry. 55: 103-136.
- Chrysogelos, S., and J. Griffith. 1982. *Escherichia coli* single-strand binding protein organizes single-stranded DNA into nucleosome-like units. Proceedings of the National Academy of Sciences. 79: 5803-5807.
- Citarella, R.V., Muller, R., Schlabach, A., and A. Weissach. 1972. Studies on vaccinia virus-directed deoxyribonucleic acid polymerase. Journal of Virology. 10: 721-729.

- Coverley, D., Kenny, M.K., Munn, M., Rupp, W.D., Lane, D.P., and R.D. Wood. 1991. Requirement for the replication protein SSB in human DNA excision repair. *Nature*. 349: 538-541.
- Curth, U., Genschel, J., Urbanke, C., and J. Greipel. 1996. *In vitro* and *in vivo* function of the C-terminus of *Escherichia coli* single-stranded DNA binding protein. *Nucleic Acids Research*. 24: 2706-2711.
- Cyrklaff, M., Risco, C., Fernández, J.J., Jiménez, M.V, Estéban, M., Baumeister, W., and J.L. Carrascosa. 2005. Cryo-electron tomography of vaccinia virus. *Proceedings of the National Academy of Sciences*. 102: 2772-2777.
- Dales, S. 1963. The uptake and development of vaccinia virus in strain L cells followed with labeled viral deoxyribonucleic acid. *Journal of Cell Biology*. 18: 51-72.
- Dales, S, and L. Siminovitch. 1961. The development of vaccinia virus in Earle's L strain cells as examined by electron microscopy. *Journal of Biophysical and Biochemical Cytology*. 10: 475-503.
- Damon, I.K. Chapter 75: Poxviruses. In *Fields Virology*, 5th Edition. 2007. Wolter Kluwer Lippincott Williams and Wilkins. Philadelphia, USA.
- Davis, R.E., and C.K. Mathews. 1993. Acidic C terminus of vaccinia virus DNA-binding protein interacts with ribonucleotide reductase. *Proceedings of the National Academy of Sciences*. 90: 745-749.
- DeSilva, F.S., Lewis, W., Berglund, P., Koonin, E.V., and B. Moss. 2007. Poxvirus DNA primase. *Proceedings of the National Academy of Science*. 104: 18724-18729.

- Dong, A., Xu, X., and A.M. Edwards. 2007. *In situ* proteolysis for protein crystallization and structure determination. *Nature Methods*. 4: 1019-1021.
- Dong, G., Nowakowski, J., and D.W. Hoffman. 2002. Structure of small protein B: the protein component of the tmRNA-SmpB system for ribosome rescue. *EMBO Journal*. 21:1845-1854.
- Easterbrook, K.B. 1966. Controlled degradation of vaccinia virions *in vitro*: an electron microscopic study. *Journal of Ultrastructure Research*. 14: 484-496.
- Eggington, J.M., Haruta, N., Wood, E.A., and M.M. Cox. 2004. The single-stranded DNA-binding protein of *Deinococcus radiodurans*. *BMC Microbiology*. 4: 2-14.
- Epstein, R.H., Bolle, A., and C.M. Steinberg. 2012. Amber mutants of bacteriophage T4D: Their isolation and genetic characterization. *Genetics*. 190: 833-840.
- Erdile, L.F., Heyer, W., Kolodner, R., and T.J. Kelly. 1991. Characterization of a cDNA encoding the 70-kDa single-stranded DNA-binding subunit of human replication protein A and the role of the protein in DNA replication. *Journal of Biological Chemistry*. 266: 12090-12098.
- Esteban, M., Flores, L., and J.A. Holowczak. 1977. Model for vaccinia virus DNA replication. *Virology*. 83: 467-473.
- Fairman, M.P., and B. Stillman. 1988. Cellular factors required for multiple stages of SV40 DNA replication *in vitro*. *The EMBO Journal*. 7: 1211-1218.

- Fan, J., and N.P. Pavletich. 2012. Structure and conformational change of a replication protein A heterotrimer bound to ssDNA. *Genes and Development*. 26: 2337-2347.
- Fenner, F., Henderson, D.A., Arita, I., Ježek, Z., and I.D. Ladnyi. Smallpox and its Eradication. 1988. World Health Organization. Geneva.
- Fleming, S.B., and A.A. Mercer. Genus *Parapoxvirus*. In *Poxviruses*. 2007. Birkhäuser Verlag. Basel.
- Gammon, D.B., and D.H. Evans. 2009. The 3'-to5' exonuclease activity of vaccinia virus DNA polymerase is essential and plays a role in promoting virus genetic recombination. *Journal of Virology*. 83: 4236-4250.
- Gammon, D.B., Gowrishankar, B., Duraffour, S., Andrei, G., Upton, C., and D.H. Evans. 2010. Vaccinia virus-encoded ribonucleotide reductase subunits are differentially required for replication and pathogenesis. *PLoS Pathogens*. 6: e1000984.
- Garon, C.F., Barbosa, E., and B. Moss. 1978. Visualization of an inverted terminal repetition in vaccinia virus DNA. *Proceedings of the National Academy of Sciences*. 75: 4863-4867.
- George, N.P., Ngo, K.V., Chitteni-Pattu, S., Norais, C.A., Battista, J.R., Cox, M.M., and J.L. Keck. 2012. Structure and cellular dynamics of *Deinococcus radiodurans* single-stranded DNA (ssDNA)-binding protein (SSB)-DNA complexes. *Journal of Biological Chemistry*. 287: 22123-22132.

- Goebel, S.J., Johnson, G.P., Perkus, M., Davis, S.W., Winslow, J.P., and E. Paoletti. 1990. The complete DNA sequence of vaccinia virus. *Virology*. 179: 247-266.
- Gomes, X.V., and M.S. Wold. 1995: Structural analysis of human replication protein A: mapping functional domains of the 70-kDa subunit. *Journal of Biological Chemistry*. 270: 4534-4543.
- Gomes, X.V., and M.S. Wold. 1996. Functional domains of the 70-kilodalton subunit of human replication protein A. *Biochemistry*. 35: 10558-10568.
- Gottlieb, S.L., and P.L. Myskowski. 1994. Molluscum contagiosum. *International Journal of Dermatology*. 33: 453-461.
- Greseth, M.D., Boyle, K.A., Bluma, M.S., Unger, B., Wiebe, M.S., Soares-Martins, J.A., Wickramasekera, N.T., Wahlberg, J., and P. Traktman. 2012. Molecular genetic and biochemical characterization of the vaccinia virus I3 protein, the replicative single-stranded DNA binding protein. *Journal of Virology*. 86: 6197-6209.
- Griffith, J.D., Harris, L.D., and J. Register III. 1984. Visualization of SSB-ssDNA complexes active in the assembly of stable RecA-DNA filaments. *Cold Spring Harbor Symposia on Quantitative Biology*. 49: 553-559.
- Gubser, C. Hué, S., Kellam, P., and G.L. Smith. 2004. Poxvirus genomes: a phylogenetic analysis. *Journal of General Virology*. 85: 105-117.
- Hamdan, S.M., Marintcheva, B., Cook, T., Lee, S.J., Tabor, S., and C.C. Richardson. 2005. A unique loop in T7 DNA polymerase mediates the

- binding of helicase-primase, DNA binding protein, and processivity factor. Proceedings of the National Academy of Sciences. 102: 5096-5101.
- He, Z.G., Rezende, L.F., Willcox, S., Griffith, J.D., and C.C. Richardson. 2003. The carboxyl-terminal domain of bacteriophage T7 single-stranded DNA-binding protein modulates DNA binding and interaction with T7 DNA polymerase. Journal of Biological Chemistry. 32: 29538-29545.
- Henricksen, L.A., Umbricht, C.B., and M.S. Wold. 1994. Recombinant replication protein A: expression, complex formation, and functional characterization. Journal of Biological Chemistry. 269:11121-11132.
- Hertig, C., Coupar, B.E.H., Gould, A.R., and D.B. Boyle. 1997. Field and vaccine strains of fowlpox virus carry integrated sequences from the avian retrovirus, reticuloendotheliosis virus. Virology. 235: 367-376.
- Hiramatsu, Y., Uno, F., Yoshida, M., Hatano, Y., and S. Nii. 1999. Poxvirus virions: their surface ultrastructure and interaction with the surface membrane of host cells. Journal of Electron Microscopy. 48: 937-946.
- Hollis, T., Stattel, J.M., Walther, D.S., Richardson, C.C., and T. Ellenberger. 2001. Structure of the gene 2.5 protein, a single-stranded DNA binding protein encoded by bacteriophage T7. Proceedings of the National Academy of Sciences. 98: 9557-9562.
- Hosoda, J., and H. Moise. 1978. Purification and physicochemical properties of limited proteolysis products of T4 helix destabilizing protein (gene 32 protein). Journal of Biological Chemistry. 253: 7547-7555.

- Hruby, D.E. 1985. Inhibition of vaccinia virus thymidine kinase by the distal products of its own metabolic pathway. *Virus Research*. 2: 151-156.
- Hruby, D.E., and L.A. Ball. 1982. Mapping and identification of the vaccinia virus thymidine kinase gene. *Journal of Virology*. 43: 403-409.
- Hruby, D.E., Maki, R.A., Miller, D.B., and L.A. Ball. 1983. Fine structure analysis and nucleotide sequence of the vaccinia virus thymidine kinase gene. *Proceedings of the National Academy of Sciences*. 80: 3411-3415.
- Huberman, J.A., Kornberg, A., and B.M. Alberts. 1971. Stimulation of T4 bacteriophage DNA polymerase by the protein product of T4 gene 32. *Journal of Molecular Biology*. 62: 39-52.
- Hyland, E.M., Rezende, L.F., and C.C. Richardson. 2003. The DNA binding domain of the gene 2.5 single-stranded DNA-binding protein of bacteriophage T7. *Journal of Biological Chemistry*. 278: 7247-7236.
- Jensen, D.E., Kelly, R.C., and P.H. von Hippel. 1976. DNA "melting" proteins II. Effects of bacteriophage T4 gene 32-protein binding on the conformation and stability of nucleic acid structures. *Journal of Biological Chemistry*. 251: 7215-7228.
- Joklik, W.R., and Y. Becker. 1964. The replication and coating of vaccinia DNA. *Journal of Molecular Biology*. 10: 452-474.
- Karzai, A.W., Susskind, M.M., and R.T. Sauer. 1999. SmpB, a unique RNA-binding protein essential for the peptide-tagging activity of SsrA (tmRNA). *EMBO Journal*. 18: 3793-3799.

- Katsafanas, G.C., and B. Moss. 2007. Colocalization of transcription and translation within cytoplasmic poxvirus factories coordinates viral expression and subjugates host functions. *Cell Host and Microbe*. 2: 221-228.
- Kazlauskas, D., and C. Venclovas. 2012. Two distinct SSB protein families in nucleo-cytoplasmic large DNA viruses. *Bioinformatics*. 28: 3186-3190.
- Keck, J.G., C.J. Baldick Jr., and B. Moss. 1990. Role of DNA replication in vaccinia virus gene expression: a naked template is required for transcription of three late *trans*-activator genes. *Cell*. 61: 801-809.
- Kim, C., Snyder, R.O., and M.S. Wold. 1992. Binding properties of replication protein A from human and yeast cells. *Molecular and Cellular Biology*. 12: 3050-3059.
- Kim, Y.T., Tabor, S., Bortners, C., Griffith, J.D., and C.C. Richardson. 1992a. Purification and characterization of the bacteriophage 7 gene 2.5 protein: a single-stranded DNA-binding protein. *Journal of Biological Chemistry*. 267: 15022-15031.
- Kim, Y.T., Tabor, S., Churchuch J.E., and C.C. Richardson. 1992b. Interactions of gene 2.5 protein and DNA polymerase of bacteriophage T7. *Journal of Biological Chemistry*. 267: 15032-15040.
- Kim, Y.T., and C.C. Richardson. 1993. Bacteriophage T7 gene 2.5 protein: an essential protein for DNA replication. *Proceedings of the National Academy of Sciences*. 90: 10173-10177.

- Kim, Y.T., and C.C. Richardson. 1994. Acidic carboxyl-terminal domain of gene 2.5 protein of bacteriophage T7 is essential for protein-protein interactions. *Journal of Biological Chemistry*. 269: 5270-5278.
- Kim, T-J., and D.N. Tripathy. 2001. Reticuloendotheliosis virus integration in the fowl poxvirus genome: not a recent event. *Avian Diseases*. 45: 663-669.
- Kimura, M. 1980. A simple method for estimating evolutionary rates of base substitutions through comparative studies of nucleotide sequences. *Journal of Molecular Evolution*. 16: 111-120.
- Kong, D., and C.C. Richardson. 1996. Single-stranded DNA binding protein and DNA helicase of bacteriophage T7 mediate homologous DNA strand exchange. *The EMBO Journal*. 15: 2010-2019.
- Kowalczykowski, S.C., Lonberg, N., Newport, J.W., Paul, L.S., and P.H. von Hippel. 1980. On the thermodynamics and kinetics of the cooperative binding of bacteriophage T4-coded gene 32 (helix destabilizing) protein to nucleic acid lattices. *Biophysical Journal*. 32: 403-418.
- Kowalczykowski, S.C., Lonberg, N., Newport, J.W., and P.H. von Hippel. 1981. Interactions of bacteriophage T4-coded gene 32 protein with nucleic acids I. Characterization of the binding interactions. *Journal of Molecular Biology*. 145: 75-104.
- Krassa, K.B., Green, L.S., and L. Gold. 1991. Protein-protein interactions with the acidic COOH terminus of the single-stranded DNA-binding protein of the bacteriophage T4. *Proceedings of the National Academy of Sciences*. 88: 4010-4014.

- Krauss, G., Sindermann, H., Schomburg, U., and G., Maass. 1981. *Escherichia coli* single-strand deoxyribonucleic acid binding protein: stability, specificity, and kinetics of complexes with oligonucleotides and deoxyribonucleic acid. *Biochemistry*. 20: 5346-5352.
- Liu, C.C., Burke, R.L., Hibner, U., Barry, J., and B. Alberts. 1978. Probing DNA replication mechanisms with the T4 bacteriophage in vitro system. *Cold Spring Harbor Symposia on Quantitative Biology*. 43: 469-487.
- Lodish, H., Berk, A., Zipursky, S.L., Matsudaira, P., Baltimore, D., and J. Darnell. 2000. 12.3: The role of topoisomerases in DNA replication. In *Molecular Cell Biology*. 4th Edition. W.H. Freeman, New York,
- Lohman, T.M., and W. Bujalowski. 1988. Negative cooperativity within individual tetramers of *Escherichia coli* single strand binding protein is responsible for the transition between the (SSB)₃₅ and (SSB)₅₆ DNA binding modes. *Biochemistry*. 27: 2260-2265.
- Lohman, T.M., Bujalowski, W., Overman, L.B., and T.F. Wei. 1988. Interactions of the *E. coli* single strand binding (SSB) protein with ss nucleic acids. Binding mode transitions and equilibrium binding studies. *Biochemical Pharmacology*. 37: 1781-1782.
- Lohman, T.M. and M.E. Ferrari. 1994. *Escherichia coli* single-stranded DNA-binding protein: multiple DNA-binding modes and cooperativities. *Annual Review of Biochemistry*. 63: 527-570.

- Lohman, T.M., and L.B. Overman. 1985. Two binding modes in *Escherichia coli* single strand binding protein-single stranded DNA complexes: modulation by NaCl concentration. *Journal of Biological Chemistry*. 260: 3594-3603.
- Lohman, T.M., Overman, L.B., and S. Datta. 1986. Salt-dependent changes in the DNA binding co-operativity of *Escherichia coli* single strand binding protein. *Journal of Molecular Biology*. 187: 603-615.
- Longhese, M.P., Plevani, P., and G. Lucchini. 1994. Replication factor A is required in vivo for DNA replication, repair, and recombination. *Molecular and Cellular Biology*. 14: 7884-7890.
- Marintcheva, B., Hamdan, S.M., Lee, S.J., and C.C. Richardson. 2006. Essential residues in the C terminus of the bacteriophage T7 gene 2.5 single-stranded DNA-binding protein. *Journal of Biological Chemistry*. 281: 25831-25840.
- Marintcheva, B., Marintchev, A., Wagner, G., and C.C. Richardson. 2008. Acidic C-terminal tail of the ssDNA-binding protein of bacteriophage T7 and ssDNA compete for the same binding surface. *Proceedings of the National Academy of Sciences*. 105: 1855-1860.
- McCraith, S., Holtzman, T., Moss, B., and S. Fields. 2000. Genome-wide analysis of vaccinia virus protein-protein interactions. *Proceedings of the National Academy of Sciences*. 97: 4879-4884.
- McFadden, G. 2005. Poxvirus tropism. *Nature Reviews Microbiology*. 3: 201-213.

- Meadows, K.P., Tyring, S.K., Pavia, A.T., and T.M. Rallis. 1997. Resolution of recalcitrant molluscum contagiosum virus lesions in human immunodeficiency virus-infected patients treated with cidofovir. *Archives of Dermatology*. 133: 987-990.
- Mo, M., Fleming, S.B., and A.A. Mercer. 2009. Cell cycle deregulation by a poxvirus partial mimic of anaphase-promoting complex subunit 11. *Proceedings of the National Academy of Sciences*. 106: 19527-19532.
- Mo, M., Fleming, S.B., and A.A. Mercer. 2010. Orf virus cell cycle regulator, PACR, competes with subunit 11 of the anaphase promoting complex for incorporation into the complex. *Journal of General Virology*. 91: 3010-3015.
- Moise, H., and J. Hosoda. 1976. T4 gene 32 protein model for control of activity at replication fork. *Nature*. 259: 455-458.
- Molineux, I.J., Friedman, S., and M.L. Gefter. 1974. Purification and properties of the *Escherichia coli* deoxyribonucleic acid-unwinding protein. *Journal of Biological Chemistry*. 249: 6090-6098.
- Molineux, I.J., and M.L. Gefter. 1974. Properties of the *Escherichia coli* DNA binding (unwinding) protein: interaction with DNA polymerase and DNA. *Proceedings of the National Academy of Science*. 71: 3858-3862.
- Molineux, I.J., and M.L. Gefter. 1975. Properties of the *Escherichia coli* DNA-binding (unwinding) protein interaction with nucleolytic enzymes and DNA. *Journal of Molecular Biology*. 98: 811-825.

- Molineux, I.J., Pauli, A., and M.L. Gefter. 1975. Physical studies of the interaction between the *Escherichia coli* DNA binding protein and nucleic acids. *Nucleic Acids Research*. 2: 1821-1837.
- Mosig, G., Berquist, W. and S. Bock. 1977. Multiple interactions of a DNA-binding protein *in vivo*. III. Phage T4 gene-32 mutations differentially affect insertion-type recombination and membrane properties. *Genetics*. 86: 5-23.
- Mosig, G., Luder, A., Dannenberg, G.R., and S. Bock. 1978. *In vivo* interactions of genes and proteins in DNA replication and recombination of phage T4. *Cold Spring Harbor Symposia on Quantitative Biology*. 43: 501-515.
- Moss, B. 1990. Regulation of vaccinia virus transcription. *Annual Review of Biochemistry*. 59: 661-688.
- Moss, B. Chapter 74: *Poxviridae*: The viruses and their replication. In *Fields Virology*. 5th Edition. 2007. Wolters Kluwer Lippincott Williams and Wilkins. Philadelphia, USA.
- Moyer, R.W., and R.L. Graves. 1981. The mechanism of cytoplasmic orthopoxvirus DNA replication. *Cell*. 27: 391-401.
- Murzin, A.G. 1993. OB (oligonucleotide/oligosaccharide binding) –fold: common structural and functional solution for non-homologous sequences. *EMBO Journal*. 12: 861-867.
- Nakai, H., and C.C. Richardson. 1988. The effect of the T7 and *Escherichia coli* DNA-binding proteins at the replication fork of bacteriophage T7. *Journal of Biological Chemistry*. 263: 9831-9839.

- Ohta, T., Michel, J.J., and Y. Xiong. 1999. Association with cullin partners protects ROC proteins from proteasome-dependent degradation. *Oncogene*. 18: 6758-6766.
- Olgati, F.S., Pogo, B.G.T., and S. Dales. 1976. Evidence for RNA linked to nascent DNA in HeLa cells. *Journal of Cell Biology*. 68: 557-566.
- Palaniyar, N. 1997. Biochemical and molecular biological studies on poxviral recombination and telomere resolution. Doctor of Philosophy Thesis. University of Guelph.
- Pestryakov, P.E., and O.I. Lavrik. 2008. Mechanisms of single-stranded DNA-binding protein functioning in cellular DNA metabolism. *Biochemistry (Moscow)*. 73: 1388-1404.
- Peters, D. and G. Müller. 1963. The fine structure of the DNA-containing core of vaccinia virus. *Virology*. 21: 266-269.
- Pfuetzner, R.A., Bochkarev, A., Frappier, L., and A.M. Edwards. 1997. Replication protein A: Characterization and crystallization of the DNA binding domain. *Journal of Biological Chemistry*. 272: 430-434.
- Raghunathan, S., Ricard, C.S., Lohman, T.M., and G. Waksman. 1997. Crystal structure of the homo-tetrameric DNA binding domain of *Escherichia coli* single-stranded DNA-binding protein determined by multiwavelength x-ray diffraction on the selenomethionyl protein at 2.9-Å resolution. *Proceedings of the National Academy of Sciences*. 94: 6652-6657.

- Raghunathan, S., Kozlov, A.G., Lohman, T.M., and G. Waksman. 2000. Structure of the DNA binding domain of *E. coli* SSB bound to ssDNA. *Nature Structural Biology*. 7: 648-652.
- Reuben, R.C., and M.L. Gefter. 1973. A DNA-binding protein induced by bacteriophage T7. *Proceedings of the National Academy of Sciences*. 70: 1846-1850.
- Reuben, R.C., and M.L. Gefter. 1974. A deoxyribonucleic acid-binding protein induced by bacteriophage T7: Purification and properties of the protein. *Journal of Biological Chemistry*. 249: 3843-3850.
- Rezende, L.F., Hollis, T., Ellenberger, T., and C.C. Richardson. 2002. Essential amino acid residues in the single-stranded DNA-binding protein of bacteriophage T7: identification of the dimer interface. *Journal of Biological Chemistry*. 277: 50643-50653.
- Rochester, S.C., and P. Traktman. 1998. Characterization of the single-stranded DNA binding protein encoded by the vaccinia virus I3 gene. *Journal of Virology*. 72: 2917-2926.
- Roy, R., Kozlov, A.G., Lohman, T.M., and T. Ha. 2007. Dynamic structural rearrangements between DNA binding modes of *E. coli* SSB protein. *Journal of Molecular Biology*. 369: 1244-1257.
- Ruyechan, W.T., and J.G. Wetmur. 1975. Studies on the cooperative binding of the *Escherichia coli* DNA unwinding protein to single-stranded DNA. *Biochemistry*. 14: 5529-5534.

- Sancar, A., Williams, K.R., Chase, J.W., and W.D. Rupp. 1981. Sequences of the *ssb* gene and protein. Proceedings of the National Academy of Sciences. 78: 4274-4278.
- Scherzinger, E., Litfin, F., and E. Jost. 1973. Stimulation of T7 DNA polymerase by a new phage-coded protein. Molecular and General Genetics. 123: 247-262.
- Schmelz, M., Sodeik, B., Ericsson, M., Wolffe, E.J., Shida, H., Hiller, G., and G. Griffiths. 1994. Assembly of vaccinia virus: the second wrapping cisterna is derived from the trans Golgi network. Journal of Virology. 68: 130-147.
- Senkevich, T.G., Bugert, J.J., Sisler, J.R., Koonin, E.V., Darai, G., and B. Moss. 1996. Genome sequence of a human tumorigenic poxvirus: prediction of specific host response-evasion genes. Science. 273: 813-816.
- Senkevich, T.G., Koonin, E.V., Bugert, J.J., Darai, G., and B. Moss. 1997. The genome of molluscum contagiosum virus: analysis and comparison with other poxviruses. Virology. 233: 19-42.
- Senkevich, T.G., Koonin, E.V., and B. Moss. 2009. Predicted poxvirus FEN1-like nuclease required for homologous recombination, double-strand break repair and full-size genome formation. Proceedings of the National Academy of Science. 106: 17921-17926.
- Shaffer, R. and P. Traktman. 1987. Vaccinia virus encapsidates a novel topoisomerase with the properties of a eucaryotic type I enzyme. Journal of Biological Chemistry. 262: 9309-9315.

- Shamoo, Y., Friedman, A.M., Parsons, M.R., Konigsberg, W.H., and T.A. Steitz. 1995. Crystal structure of a replication fork single-stranded DNA binding protein (T4 gp32) complexed to DNA. *Nature*. 375: 362-366.
- Shereda, R.D., Kozlov, A.G., Lohman, T.M., Cox, M.M., and J.L. Keck. 2008. SSB as an organizer/mobilizer of genome maintenance complexes. *Critical Reviews in Biochemistry and Molecular Biology*. 43: 289-318.
- Shokri, L., Marintcheva, B., Richardson, C.C., Rouzina, I., and M.C. Williams. 2006. Single molecule force spectroscopy of salt-dependent bacteriophage T7 gene 2.5 protein binding to single-stranded DNA. *Journal of Biological Chemistry*. 281: 38689-38696.
- Shores, Teri. 2009. Chapter 14: Poxviruses. 376-400. *Understanding Viruses*. Jones and Bartlett Publishers. Sudbury, Massachusetts.
- Shuman, S. 1992. Vaccinia virus RNA helicase: an essential enzyme related to the DE-H family of RNA-dependent NTPases. *Proceedings of the National Academy of Sciences*. 89: 10935-10939.
- Shuman, S., and B. Moss. 1987. Identification of a vaccinia virus gene encoding a type I DNA topoisomerase. *Proceedings of the National Academy of Sciences*. 84: 7478-7482.
- Sigal, N., Delius, H., Kornberg, T., Gefter, M.L., and B. Alberts. 1972. A DNA-unwinding protein isolated from *Escherichia coli*: its interaction with DNA and with DNA polymerase. *Proceedings of the National Academy of Science*. 69: 3537-3541.

- Slabaugh, M., Roseman, N., Davis, R. and C. Mathews. 1988. Vaccinia virus-encoded ribonucleotide reductase: sequence conservation of the gene for the small subunit and its amplification in hydroxyurea-resistant mutants. *Journal of Virology*. 62: 519-527.
- Smith, G.L., Genus *Orthopoxvirus: Vaccinia Virus*. In Poxviruses. 2007. Birkhäuser Verlag. Basel.
- Snustad, D.P. 1968. Dominance interactions in *Escherichia coli* cells mixedly infected with bacteriophage T4D wild-type and amber mutants and their possible implications as to type of gene-product function: catalytic vs. stoichiometric. *Virology*. 35: 550-563.
- Sodeik, B., Doms, R.W., Ericsson, M., Hiller, G., Machamer, C.E., van't Hof, W., van Meer, G., Moss, B., and G. Griffiths. 1993. Assembly of vaccinia virus: role of the intermediate compartment between the endoplasmic reticulum and the Golgi stacks. *Journal of Cell Biology*. 121: 521-541.
- Sonenberg, N., and A.G. Hinnebusch. 2009. Regulation of translation initiation in eukaryotes: mechanisms and biological targets. *Cell*. 136: 731-745.
- Suck, D. 1997. Common fold, common function, common origin? *Nature Structural Biology*. 4: 161-165.
- Tengelsen, L.A., Slabaugh, M.B., Bibler, J.K., and D.E. Hraby. 1988. Nucleotide sequence and molecular genetic analysis of the large subunit of ribonucleotide reductase encoded by vaccinia virus. *Virology*. 164: 121-131.

- Tseng, M., 1999. Characterization of the vaccinia virus I3L gene product. Master of Science Thesis. University of Guelph.
- Tseng, M., Palaniyar, N., Zhang, W., and D.H. Evans. 1999. DNA binding and aggregation properties of the vaccinia virus I3L gene product. *Journal of Biological Chemistry*. 274: 21637-21644.
- Traktman, P. Poxvirus DNA Replication. In *DNA Replication in Eukaryotic Cells*. 1996. Cold Spring Harbor Laboratory. Cold Spring Harbor NY.
- Traktman, P., Sridhar, P., Condit, R.C., and B.E. Roberts. 1984. Transcriptional mapping of the DNA polymerase gene of vaccinia virus. 49: 125-131.
- Tyring, S.K. 2003. Molluscum contagiosum: the importance of early diagnosis and treatment. *American Journal of Obstetrics and Gynecology*. 189 (3 Suppl): S12-S16.
- Vos, J.C., and H.G. Stunnenberg. 1988. Derepression of a novel class of vaccinia virus genes upon DNA replication. *EMBO Journal*. 7: 3487-3492.
- Weiner, J.H., Bertsch, L.L., and A. Kornberg. 1975. The deoxyribonucleic acid unwinding protein of *Escherichia coli*. *Journal of Biological Chemistry*. 250: 1972-1980.
- Weir, J.P., Bajszár, G., and B. Moss. 1982. Mapping of the vaccinia virus thymidine kinase gene by marker rescue and by cell-free translation of selected mRNA. *Proceedings of the National Academy of Sciences*. 79: 1210-1214.
- Wetzel, S., and A. Wollenberg. 2004. Eczema molluscatum in tacrolimus treated atopic dermatitis. *European Journal of Dermatology*. 14: 73-74.

- Wheeler, L.J., Ray, N.B., Ungermann, C., Hendricks, S.P., Bernard, M.A., Hanson, E.S., and C.K. Mathews. 1996. T4 phage gene 32 protein as a candidate organizing factor for the deoxyribonucleoside triphosphate synthetase complex. *Journal of Biological Chemistry*. 271: 11156-11162.
- Williams, K.R., and W. Konigsberg. 1978. Structural changes in the T4 gene 32 protein induced by DNA and polynucleotides. *Journal of Biological Chemistry*. 253: 2463-2470.
- Williams, K.R., LoPresti, M.B., and M. Setoguchi. 1981. Primary structure of the bacteriophage T4 DNA helix-destabilizing protein. *Journal of Biological Chemistry*. 256: 1754-1762.
- Williams, K.R., Spicer, E.K., LoPresti, M.B., Guggenheimer, R.A., and J.W. Chase. 1983. Limited proteolysis studies on the *Escherichia coli* single-stranded DNA binding protein: Evidence for a functionally homologous domain in both the *Escherichia coli* and T4 DNA binding protein. *Journal of Biological Chemistry*. 258: 3346-3355.
- Wittek, R., Kuenzle, C.C., and R. Wyler. 1979. High C + G content in parapoxvirus DNA. *Journal of General Virology*. 43: 231-234.
- Wobbe, C.R., Weissbach, L., Borowiec, J.A., Dean, F.B., Murakmi, Y., Bullock, P., and J. Hurwitz. 1987. Replication of simian virus 40 origin-containing DNA *in vitro* with purified proteins. *Proceedings of the National Academy of Sciences*. 84: 1834-1838.
- Wold, M.S., and T. Kelly. 1988. Purification and characterization of replication protein A, a cellular protein required for *in vitro* replication of simian virus

- 40 DNA. Proceedings of the National Academy of Sciences. 85: 2523-2527.
- Wold, M.S., Weinberg, D.H., Virshup, D.M., Li, J.J., and T.J. Kelly. 1989. Identification of cellular proteins required for simian virus 40 DNA replication. Journal of Biological Chemistry. 264: 2801-2809.
- Wu, M., Flynn, E.K., and R.L. Karpel. 1999. Details of the nucleic acid binding site of T4 gene 32 protein revealed by proteolysis and DNA T_m depression methods. Journal of Molecular Biology. 286: 1107-1121.
- Zaborowska, I., Kellner, K., Henry, M., Meleady, P., and D. Walsh. 2012. Recruitment of host translation initiation factor eIF4G by the vaccinia virus ssDNA-binding protein I3. Virology. 425: 11-22.
- Zhang, W., and D.H. Evans. 1995. DNA strand transfer catalyzed by the 5'-3' exonuclease domain of *Escherichia coli* DNA polymerase 1. Nucleic Acids Research. 23: 4620-4637.

APPENDIX 1: BUFFER COMPOSITIONS

A1.1 Bacterial Culture Media

Luria Broth (LB): 1% Bacto-Tryptone, 0.5% Bacto Yeast Extract, 1% NaCl

NZY⁺ Media: 1% NZ Amine, 0.5% Bacto Yeast Extract, 0.5% NaCl, 0.0125M MgCl₂, 0.0125M MgSO₄, 0.4% (w/v) glucose

SOC Media: 2% tryptone, 0.5% yeast extract, 10mM NaCl, 2.5mM KCl, 10mM MgCl₂, 10mM MgSO₄, 20mM glucose

Ampicillin: 1g ampicillin sodium salt in 10mL ddH₂O

Chloramphenicol: 0.3g chloramphenicol in 10mL 95% ethanol

Rifampicin: 0.5g rifampicin in 20mL methanol

Salt Solution for Electroporation: 1.2M NaCl, 0.06M MgCl₂

A1.2 Cell Culture Media

MEM: MEM, 1% non- essential amino acids, 1% antibiotic/antimycotic, 1% L-glutamine, 5% fetal bovine serum

Versene: 16g NaCl, 0.4g KCl, 2.3g Na₂HPO₄, 0.4g KH₂PO₄, 2.36mL 0.5M

EDTA, 1.5mL 1% phenol red, in 2L ddH₂O, autoclave in 400mL aliquots, store 4°C, add 40mL trypsin for use

A1.3 Protein Purification

Nickel Binding Buffer: 500mM NaCl, 20mM NaPO₄ pH 7.4, 60mM imidazole pH 7.4

Nickel Elution Buffer: 500mM NaCl, 20mM NaPO₄ pH 7.4, 800mM imidazole pH 7.4

Heparin Binding Buffer: 200mM Tris pH 7.8, 0.1mM EDTA pH 8.0, 10mM β-mercaptoethanol, 10% glycerol, 50mM NaCl

Heparin Elution Buffer: 200mM Tris pH 7.8, 0.1mM EDTA pH 8.0, 10mM β-mercaptoethanol, 10% glycerol, 1M NaCl

1X Buffer A: 200mM Tris pH 7.8, 0.1mM EDTA pH 8.0, 10mM β -mercaptoethanol, 10% glycerol, XmM NaCl

*can change the concentration of NaCl depending on the experiment

A1.4 DNA Cloning

10X *Taq* Buffer + KCl: 100mM Tris HCl (pH 8.8), 500mM KCl, 0.8% Nonidet P40

dNTP mix: 10mM each dATP, dTTP, dCTP and dGTP

10X Polymerase Buffer (Infusion Cloning): 300mM Tris pH 7.9, 50mM MgCl₂, 700mM NaCl, 18mM DTT, 800 μ g/mL acetylated BSA

10X Buffer O: 500mM Tris HCl (pH 7.5), 100mM MgCl₂, 1M NaCl, 1mg/ml BSA

10X Fast Digest Green Buffer: 100mM Tris HCl (pH 7.5), 100mM MgCl₂, 500mM NaCl, 1mg/ml BSA

A1.5 Gel Electrophoresis

10X EMSA Buffer: 120mM Tris HCl, 24% glycerol, 10mM EDTA, 25mM β -mercaptoethanol

10X TAE Running Buffer: 242g Tris OH, 57.1mL glacial acetic acid, 100mL 0.5M EDTA in 1L ddH₂O

5X IBE Running Buffer: 74mL 6M imidazole pH 8.3, 27.5g boric acid, 10mL EDTA in 1L ddH₂O

10X GLB Loading Dye: 0.05mL 1M Tris pH 7.5, 0.6mL glycerol, 0.350mL ddH₂O

Blue Silver Coomassie Stain: 10% phosphoric acid, 100g ammonium sulphate, 1.2g Coomassie Blue G-250, 200mM methanol in 1L ddH₂O

Separating Gel Buffer: 90.8g Tris OH in 500mL ddH₂O, pH to 8.8

Stacking Gel Buffer: 60.57g Tris OH in 500mL ddH₂O, pH to 6.8

10% SDS: 12.5g sodium dodecyl sulphate in 125mL ddH₂O

Western Blot Blocking Buffer: 5mL Odyssey Blocking Buffer (Li-cor), 5mL PBS

10X PBS: 0.1M KPO₄ pH 7.4, 1.5M NaCl

10X PBS-T: 0.1M KPO₄ pH 7.4, 1.5M NaCl, 1% Tween-20

4X SDS PAGE Loading Dye: 9.2mL 10% SDS, 1mL β-mercaptoethanol, 10mL glycerol, 1.25mL 1M Tris pH 6.8, 25mg bromophenol blue in 25mL ddH₂O

10X Western Blot Transfer Buffer: 250mM Tris, 1920mM glycine pH 8.3

10X SDS PAGE Running Buffer: 576g glycine, 120g Tris, 200mL 20% SDS in 4L ddH₂O

A1.6 Microinjections

Microinjection Buffer: 100mM glutamic acid, 140mM KOH, 1mM MgSO₄, 1mM DTT, pH to 7.2 using citric acid

1M Citric Acid: 96.1g citric acid in 500mL ddH₂O

Texas Red Dextran: 10mg Texas Red Dextran MW 70,000 (Invitrogen) in 10mL microinjection buffer

4% Paraformaldehyde: 0.4g paraformaldehyde in 10mL PBS

0.1M Glycine: 0.4g glycine in 50mL PBS-T

3% BSA: 0.3g bovine serum albumin in 10mL PBS-T

10X PBS: 40g NaCl, 1g KCl, 13.4g Na₂HPO₄•7H₂O, 1.2g KH₂PO₄

Mowoil: 6g glycerol, 2.4g Mowoil, 6ml ddH₂O, incubate overnight at room temperature, 12mL 0.2M Tris pH 6.8, incubate 50°C 10 minutes, centrifuge 5000xg 15 minutes at 4°C

A1.7 Immunoprecipitations

TBS: 50mM Tris pH 7.4, 150mM NaCl

Lysis Buffer: 150mM NaCl, 20mM Tris, 1mM EDTA, 0.5% NP-40, 1 cOmplete

Mini, EDTA free protease inhibitor cocktail tablet (Roche)

10X PBS A: 50g NaCl, 1.25g KCl, 7.2g Na₂HPO₄, 1.25g KH₂PO₄